TESIS DE LA UNIVERSIDAD DE ZARAGOZA

2017

91

Pedro José Fernández Concellón

Development, analysis and validation of a passive system compensator of accelerations applicable to transport delicate loads

Departamento

Ingeniería Mecánica

Director/es

Baselga Ariño, Santiago
Clavero Gracia, Carmelo

ISSN 2254-7606

Prensas de la Universidad
Universidad Zaragoza

ISSN 2254-7606

Universidad Zaragoza
1542

Tesis Doctoral

DEVELOPMENT, ANALYSIS AND VALIDATION OF A PASSIVE SYSTEM COMPENSATOR OF ACCELERATIONS APPLICABLE TO TRANSPORT DELICATE LOADS

Autor

Pedro José Fernández Concellón

Director/es

Baselga Ariño, Santiago
Clavero Gracia, Carmelo

UNIVERSIDAD DE ZARAGOZA

Ingeniería Mecánica

2017

Universidad Zaragoza
1542

DEVELOPMENT, ANALYSIS AND VALIDATION OF A PASSIVE SYSTEM COMPENSATOR OF ACCELERATIONS APPLICABLE TO TRANSPORT DELICATE LOADS

Doctoral Program in Mechanical Engineering

by
Pedro José Fernández Concellón

Advisors
Dr. Santiago Baselga Ariño
Dr. Carmelo Clavero Gracia

University of Zaragoza

27 *February*, 2017

Declaration of Authorship

D. Santiago Baselga Ariño, profesor titular del Departamento de Ingeniería Mecánica de la Escuela de Ingeniería y Arquitectura de la Universidad de Zaragoza y **D. Carmelo Clavero Gracia**, profesor titular del Departamento de Matemática Aplicada de la Escuela de Ingeniería y Arquitectura de la Universidad de Zaragoza,

CERTIFICAN:

Que la memoria de Tesis Doctoral presentada por **D. Pedro José Fernández Concellón** con el título *Development, Analysis and Validation of a Passive System Compensator of Accelerations Applicable to Transport Delicate Loads* ha sido realizada bajo su dirección en el programa de Doctorado en Ingeniería Mecánica, en la Universidad de Zaragoza, y se corresponde con el Proyecto de Tesis aprobado por la Comisión de Doctorado en 2013, por lo que autorizan su presentación en la modalidad de tesis por capítulos y con la Mención de **Doctor Internacional** cumpliendo por lo tanto las condiciones requeridas para que su autor pueda optar al grado de Doctor por la Escuela de Doctorado de la Universidad de Zaragoza.

Y para que así conste, firmado en Zaragoza a 1 de febrero de 2017

Fdo.: D. Santiago Baselga Ariño

Fdo.: D. Carmelo Clavero Gracia

Resumen

Esta tesis aborda el campo de la compensación pasiva de aceleraciones horizontales e introduce un nuevo enfoque sobre el transporte de cargas delicadas y pacientes en vehículos. La compensación pasiva de aceleraciones ha sido ampliamente estudiada y algunas de sus aplicaciones se encuentran en vehículos, aparatos y edificios. Aquí se introduce y analiza el diseño de un sistema multicuerpo 3D utilizado para transportar cargas delicadas o personas, capaz de compensar aceleraciones de forma pasiva en un porcentaje específico (no necesariamente al 100%, se define de acuerdo a las exigencias de la carga que se transporta en él).

En primer lugar, se ha llevado a cabo una revisión de la literatura en el campo de la compensación pasiva de aceleraciones durante la que se han encontrado diferentes sistemas aplicados al transporte ferroviario, al transporte por carretera, en edificios y otros aparatos, tales como equipamiento médico. Aunque estos sistemas comparten el objetivo de compensar aceleraciones de forma pasiva con el sistema analizado en esta tesis, difieren de dicho sistema en el modo en que alcanzan la compensación, en las direcciones en que se consigue, y/o en su capacidad para compensar aceleraciones. Esto es por lo que tras revisar el estado del arte en este campo, el diseño de este nuevo sistema ha seguido adelante. En esta revisión, algunos problemas que pueden aparecer durante el transporte por carretera de cargas delicadas y/o personas se han tenido en consideración durante el diseño del sistema.

Teniendo un diseño general del sistema, sin limitar su aplicación a un uso específico, se ha llevado a cabo su parametrización para plantear un modelo matemático de sus ecuaciones de movimiento. En su parametrización se han teniendo en cuenta las dimensiones de sus componentes, sus masas, inercias y los coeficientes de amortiguamiento de los amortiguadores. Los sólidos que lo integran tienen un comportamiento como sólido rígido, pueden moverse en un espacio tridimensional, tienen su masa concentrada en su centro geométrico, sus tensores de inercia sólo tienen valores en la diagonal principal y los amortiguadores han sido modelados caracterizando únicamente su comportamiento viscoso, sin tener en cuenta el fenómeno de fricción en estos ni en las uniones entre los sólidos.

Las ecuaciones de movimiento del sistema han formado un sistema no lineal de ecuaciones diferenciales algebráicas de segundo orden que ha sido resuelto mediante un método de integración numérica (programado manualmente por completo) basado en el método de Newton-Raphson, sobre el que se han llevado a cabo una serie de modificaciones para hacer que el método resolviese el sistema de la manera más eficiente posible. Se ha actuado sobre el tamaño de paso, el tipo de selección del mismo (fijo o variable) y la fórmula empleada para aproximar las derivadas. Los resultados obtenidos con el método de integración propuesto han sido contrastados con los resultados que se obtienen al simular el movimiento del sistema en un programa de análisis dinámico de sistemas multicuerpo, MSc Adams.

Tras validar computacionalmente el modelo matemático general, se ha particularizado el análisis del sistema multicuerpo 3D para su aplicación en el transporte de pacientes en ambulancias. Para esta aplicación, la configuración del sistema que se ha analizado se comporta cinemáticamente como un mecanismo de cuadrilátero articulado, por tratarse de un ejemplo significativo que facilita el análisis del movimiento del sistema.

Las dimensiones del sistema y las características de sus amortiguadores necesarias para adaptar el diseño del sistema a esta aplicación específica han sido obtenidas tras realizar dos tipos de análisis. En ellos no se ha tenido en cuenta el fenómeno de fricción entre las partes del sistema ni la transmisión de vibraciones entre ellas ni entre éstas y el vehículo. Esto requiere un modelado del sistema más complejo y realista y una caracterización específica del vehículo en el que se va a instalar.

El primer análisis, basado en la aplicación de la teoría del Diseño de Experimentos, ha analizado la influencia que dos paramétros dimensionales y las masas del sistema (por ser los parámetros más fácilmente modificables en la fase experimental) tienen sobre el movimiento de la base del sistema (los dos parámetros dimensionales) y sobre su modo natural de vibración (los dos parámetros dimensionales y las masas).

En el segundo análisis, en base a los resultados obtenidos con el primero y teniendo en cuenta las limitaciones dimensionales impuestas por la aplicación específica a la que se pretende destinar, se han determinado las dimensiones que debería poseer el sistema para poder alcanzar en su movimiento un porcentaje de compensación de aceleraciones específico y su factor de amortiguamiento para que su respuesta vibracional fuese apropiada para el transporte de personas en una posición tumbada. En este punto se han tenido en cuenta lo que anteriores investigaciones han encontrado con respecto al mareo y al malestar cuando las personas que mantienen una postura sentada están expuestas a diferentes tipos de oscilaciones (lateral pura, giro puro y lateral compensada al 100% con el giro).

La parte experimental de esta investigación está dividida en dos partes que se detallan a continuación.

La primera parte está centrada en el movimiento del sistema. Para ello, se han construido dos prototipos con los que se ha llevado a cabo una parte experimental en la Universidad de Zaragoza, que ha permitido validar la teoría sobre la que se ha basado la obtención del diseño del sistema y en la que se han detectado algunos problemas y limitaciones durante su diseño y montaje.

La segunda parte ha estado centrada en el efecto que diferentes tipos de oscilaciones tienen sobre el malestar de las personas. Como no se había llevado a cabo todavía un estudio del malestar, teniendo en cuenta oscilaciones en las que diferentes porcentajes de la aceleración lateral eran compensados con el giro ni considerando adoptar una postura tumbada, se realizó una estancia de investigación en el Instituto de Investigación de Sonido y Vibraciones de la Universidad de Southampton para ello. Dando continuidad a los estudios realizados anteriormente para personas que mantienen una postura sentada, el experimento incluyó, además de las oscilaciones anteriormente consideradas (lateral pura, giro puro y lateral compensada al 100% con el giro), un tipo de oscilación adicional (oscilaciones laterales compensadas en un 25% a través del giro) para personas en una posición tumbada, como si estuvieran tumbados en una camilla. Los resultados de este experimento han servido para determinar el intervalo de frecuencias y el tipo de oscilaciones bajo los que las personas son más sensibles a las aceleraciones horizontales laterales cuando mantienen una postura de decúbito supino. Mejoras

en la percepción del malestar se han encontrado sólo en un intervalo limitado de frecuencias de todo el intervalo considerado en el experimento.

Esta investigación deja varias líneas abiertas. El modelo general parametrizado del sistema puede incorporar más parámetros que puedan ser de interés (materiales o fricción, entre ellos), así como considerar para los sólidos un comportamiento distinto al de sólido rígido. Si se cuenta con los medios adecuados, su validación puede llevarse a cabo experimentalmente y no sólo computacionalmente. La experimentación con personas puede contemplar además de la problemática del malestar, la del mareo y en ambas, más porcentajes de compensación de aceleraciones que los contemplados hasta ahora. Aparte de una aplicación para el transporte de pacientes, este sistema puede ser de interés para los fabricantes de productos delicados (como el vidrio o la cerámica), pero es necesario realizar un análisis particularizado del diseño del sistema para cada aplicación específica.

Abstract

This thesis deals with the field of passive compensation of horizontal accelerations and introduces a new approach to transport delicate loads or patients in vehicles. Passive compensation of accelerations has been studied largely and some of its applications are found in vehicles, devices and buildings. However, here it is introduced and analysed a 3D multibody system used to transport loads capable of compensating accelerations passively at a specific rate (no necessarily at 100%, it is defined according to the requirements of the load transported in it).

Firstly, a literature review has been carried out during which different systems applied to railway transport, road transport, buildings and other devices, such as medical equipment, have been found. Although these systems share the aim of compensating accelerations passively with the system analysed in this thesis, they differ from it in the way of achieving this compensation and/or in the capabilities for compensating accelerations. This is why after reviewing the state of the art in this field, the design of this new approach has continued. In this review some problems that may arise during the road transportation of delicate loads and people have been considered for the design of the system.

Having a general design of the system, without limiting its use for a specific purpose, the system has been parameterized in order to pose a mathematical model of its equations of motion. In this stage, the dimensions of its components, their masses, inertias and the damping coefficient of its dampers have been considered. The solids that form the 3D multibody system are considered to behave as rigid solids, can move in the tri-dimensional space, have their mass concentrated in their geometrical centre, their inertia tensors have values only in their principal axes and the dampers have been modelled characterizing only their viscous behaviour, without considering the phenomena of friction neither between them nor in the links between the solids.

The equations of motion of the system have formed a nonlinear system of second order differential algebraic equations which has been solved through the Newton-Raphson numerical integration method. On it, several modifications have been carried out in order to make that the method solved the system as efficiently as possible. It has been acted on the size of the step, on the type of selection of the step (fixed or variable) and on the formulae used to approximate the derivatives. The results obtained with the proposed integration method have been compared against the results obtained after simulating the motion of the system in a software of dynamic analysis for multibody systems, MSc Adams.

After being validated computationally the general mathematical model, it has been particularized the analysis of the 3D multibody system for its application for transporting patients in ambulances. For this application, the configuration of the system that has been analysed behaves kinematically like the articulated

quadrilateral mechanism, because it is a significative example that eases the analysis of the motion of the system.

The dimensions of the system and the characteristics of its dampers needed for this particular application have been obtained after applying two types of analysis. They have not considered the phenomena of friction between the parts of the system neither the transmission of vibrations among them nor among them and the vehicle. This requires a modelling of the system more complex and realistic and a specific characterization of the vehicle in which the system is going to be installed.

The first analysis, through applying the Design of Experiments theory approach, has analysed the influence that two dimensional parameters and the masses of the system (because they are the parameters that can be modified most easily during experimentation) have on the motion of the base of the system (the two dimensional parameters) and on its natural mode of vibration (the two dimensional parameters and the masses).

In the second analysis, based on the results obtained with the first analysis and having into account the dimensional limitations imposed by the specific application to which it is intended to be applied, the dimensions that the system should dispose in order to achieve a specific rate of compensation of accelerations during its motion have been determined and so its damping ratio in order to obtain a vibrational response appropriate for transporting patients in a recumbent supine posture. In this point, the results obtained in previous researches have been considered in what respect to discomfort and motion sickness for people who maintain a seated posture and are exposed to different types of oscillations (pure lateral, pure roll y and fully roll-compensated lateral oscillation).

The experimental part of this research is divided into two parts that are detailed below:

The first part is focused on the motion of the system. For it, two different prototypes of the 3D multibody system were built with which a experimental part has been carried out at the University of Zaragoza that has allowed to validate the theory on which the design of the system is based and on which some problems and limitations have been found during their assembly and design.

The second part has been focused on the effect that different types of oscillations have on the discomfort of people. As a study of the discomfort of people who maintain a recumbent supine posture and considering roll-compensation of lateral oscillations at different rates had not been carried out previously, a research stay was carried out at the Institute of Sound and Vibration Research at the University of Southampton for it. Continuing with the studies carried out previously for people who maintain a seated posture, additionally to consider the types of oscillations previously analysed (pure lateral, pure roll and fully roll-compensated lateral oscillation) the experiment include a type of oscillation in which the lateral acceleration was roll-compensated at a rate of 25%, all for people who maintain a recumbent supine posture, like if they were lying on a stretcher. The results of this experiment have served to determine the range of frequencies and the types of oscillations under which people are more sensitive to lateral accelerations when they maintain a recumbent supine posture. Improvements in the perception of discomfort have been found only in a limited range of frequencies over the range of frequencies studied in the experiment.

This research leaves open several future lines of research. The general model that has been parameterized can incorporate more parameters that can be of interest (materials or friction, among others) and also it can consider a behaviour for the solids that form part of the system different to the rigid solid behaviour. With

appropriate means, the validation of the model can be done experimentally and not only computationally. The experimentation with people may consider in addition to discomfort, the problematic of motion sickness and for both, oscillations with more rates of roll-compensation of lateral oscillation. Additionally to the application of transporting patients, this system may be of interest for the manufacturers of delicate loads (like glass or ceramic products), but a specific analysis of the design of the system for its particular application is needed.

Acknowledgements

I can do it. In line with the U.S. presidential campaign slogan of Barack Obama during the general elections in 2008, my life has always been prompted by these words. There is no obstacle that has avoided to follow my way, I have always found the way of achieving my goals. The big challenges are hardly achievable in solitary, they require support, advise and collaboration of other people, and in the particular case of this thesis also. This is why I want to thank here to every person who have helped me during these three years and a half to carry out this thesis.

First of all, I want to sincerely thank my thesis supervisors, D. Santiago Baselga Ariño and D. Carmelo Clavero Gracia, for the support and advice provided during the achievement of the thesis. Carmelo, thanks for helping me selflessly since the first time that I knocked to the door of your office in July of 2014, without your help this thesis would not be finished yet. Your advice, patient and support have cleared my mind in tough moments when I did not know how to continue. Santiago, you have followed my trajectory at work and at University since 2007. Thank you for your help, for believing in the idea behind this thesis and for the help that has come from the Automotive Laboratory that you successfully managed. Thanks to both for supporting my decision of doing a research stay of three months at the University of Southampton. It has contributed to this thesis very positively and to myself personally, meaning a change in my career towards a new promising and challenging future.

To the Emeritus Professor Michael J. Griffin of the Institute of Sound and Vibration Research of the University of Southampton. Mike, you have given to me the opportunity for exploring a new field of engineering. Your advice, your support and your kindness have supposed for me something special and very important, making my stay more comfortable and improving my research. Thank you very much Mike for putting me in contact with Dr. Giulia Patelli without whom the experiment carried out at the University of Southampton would not be done so easily.

To Dr. Giulia Patelli, the perfect colleague. Thanks for teaching me so patiently how to carry out the experiment and the theory needed for it, for your advices and for the moments shared having a drink and fun during our spare time. You have made my stay much more comfortable than that I could imagine.

To the members of the Human Factors Research Unit of the University of Southampton. Thanks to Francesco, Hui, Sean, Chi, Jun, James, Jamie, Baris, Suzan, Xu, Jiewei, Mark, Jack, Minglian, Peter, Gary, Miyuki and all others who, belonging or not to the unit, have made my stay more comfortable, thank you for your kindness and hospitality and for all your help given to me during my stay.

To Roberto, Nacho and Diego, for helping me during the experimentation stage carried out at the University of Zaragoza. I would not have been able to carry out the experiments without your help.

To Sara and Juan, for being unique. Your experience, advice, availability and your willingness to listen to me have been very valuable for me.

A mis padres, porque siempre habéis creído en mi, me habéis apoyado y habéis vivido junto a mi los momentos agradables y complicados derivados de mi trabajo y mis estudios. Gracias por vuestra paciencia, por vuestro apoyo y generosidad. Vosotros me habéis educado y enseñado a ser un luchador, un trabajador y a perseguir mis sueños.

To Bea and to my brother Luis, for your advice, support and help. It has been a good support to hear alternative ideas and clear my owns when I did not know how to move forward. Thank you for your laptop and for helping me with the trailer Luis.

To my wife, Laura, because you have been a first hand witness of how I have felt during the last three years and a half of my life. Your patient, support and love have helped my to overcome all obstacles that have appeared in my way. You have calmed and motivated me when I have felt stressed and under pressure, you have helped me to do a step ahead and progress, thank you for being like you are and making my life happier.

Thank you for everything to everybody. I am a very lucky person because I am surrounded by very good and kind people, extraordinary people.

Contents

List of Figures

List of Tables

List of Abbreviations

AQM	**A**rticulated **Q**uadrilateral **M**echanism
BDF	**B**ackward **D**ifferentiation **F**ormula
DAE	**D**ifferential **A**lgebraic **E**quations
DAQ	**D**ata **A**quisition **U**nit
DOE	**D**esign **O**f **E**xperiment**s**
IMU	**I**nertial **M**easurement **U**nit
ODE	**O**rdinary **D**ifferential **E**quations
RCA	**R**ate (of) **C**ompensation (of) **A**ccelerations

Dedicated to Laura

Chapter 1

General introduction

1.1 Introduction

1.1.1 Motivation

The motivation behind this research comes from the inventive activity focused on two mechanical systems whose common aim is to compensate the accelerations that act on passengers, animals and/or loads transported in vehicles during driving conditions.

The first mechanical system, a 3D pendular system compensator of horizontal accelerations [1] displayed in Figure 1.1, was developed and then patented in 2007. With this system, the compensation of accelerations was achieved through the passive oscillatory motion (it oscillates like a pendulum) due to the inertial forces that acted on it. The system, installable in any type of vehicle, could oscillate modifying the orientation that it and the load transported on it had in static conditions until they achieved a new dynamic equilibrium state. In this state, the acceleration measured in the plane of the system was less than the horizontal acceleration that acted on it. Because of the system shared its kinematic with the kinematic of the pendulum, the rate of compensation of accelerations achieved in every new dynamic equilibrium state coincided with 100% (supposing that the system had not beaten any object during its motion).

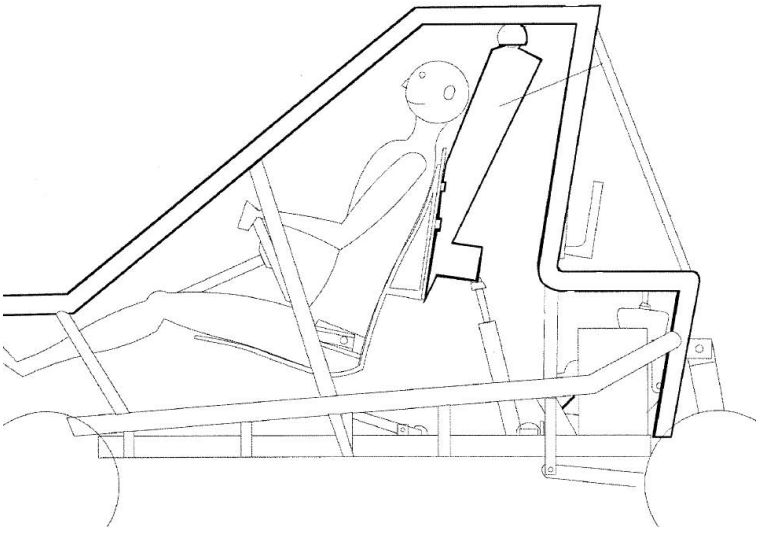

FIGURE 1.1: Previous 3D pendular system compensator of horizontal accelerations

This invention has resulted in the design of the second mechanical system, a new 3D multibody system installable into a vehicle (aerial, ground, or maritime) with the purpose of transporting delicate loads or people to which compensate, at a specific rate, the horizontal accelerations that act on them. The study of this new system is on the focus of this research, considering its particular application to transport patients. In this document is explained in detail the research carried out about this 3D multibody system.

1.1.2 Objectives of this research

The objectives of this research are:

- Develop a general 3D multibody system capable of compensating passively the horizontal accelerations that act on it at different rates.
- Pose and solve a mathematical model of the equations of motion of the system.
- Validate a mathematical model of the equations of motion of the system.
- Configure the system in order to make it applicable specifically to transport patients.
- Supplement the findings obtained from previous researches about the effect that different types of oscillations have on the discomfort of people who maintain a seated posture, through considering now a recumbent supine posture and different rates of roll-compensation of lateral oscillations (oscillatory motion experienced with this system), with the purpose of testing the applicability of this system to people.
- Supplement experimentally the analysis carried out previously with the model and the design of the system.

1.1.3 Methodology

This document is structured in seven chapters and one annex, being this introduction the first chapter. Chapters 2, 3 and 4 are currently submitted to different journals. Part of chapter 5 is intended to be submitted in a near future to another journal focused on Human Vibrations and chapters 6 and 7 contain the conclusions of the thesis in Spanish and English, respectively.

Chapter 2 is titled "Passive systems applied to compensate accelerations. Review of the literature and presentation of a new approach for transporting patients". In order to demonstrate that a passive system like the one presented in this thesis has not been developed, it has been reviewed both the existent academic papers and patents. The searches have been carried out in the databases WIPO (search engine of the World Intellectual Property Organization) [2] and Alcorze (search engine of scientific papers of the Universidad de Zaragoza) [3], which contain information about international patents and scientific papers, respectively. Therefore, in this chapter it is introduced the design of the new system focused on its application to transport patients.

Chapter 3 deals with the mathematical model of the equations of motion of the 3D multibody system and with its computational validation. It is titled "Efficiency of a BDF-Newton-Raphson numerical integration method applied to solve a system of nonlinear differential equations modeling a mechanical multibody system". There,

the system is parameterized and its equations of motion are introduced. The system to be solved is a nonlinear second order system of algebraic differential equations. Due to the complexity for handling the system numerically, the order of the system is reduced and its derivatives are approximated with a backward differentiation formula (BDF). After these operations, the system is solved through the Newton-Raphson numerical integration method and it is validated against the solution that the computational software MSc Adams provides.

Leaving aside the general model of the system, **chapter 4** is focused on a configuration of the system specifically focused on its application to transport patients.

In the first part of the chapter it is analysed how the variation of several parameters that form part of the 3D multibody system affect to the motion of its base and to its natural mode of vibration. It is carried out applying the Design of Experiments (DOEs) theory to these factors, in order to detect which are the ones that have a major effect on the tilting angle and the displacement of the base of the system and also on its natural mode of vibration.

In the second part of the chapter, the dimensions of the system and the damping coefficients of its dampers are determined with the purpose of that the system achieves a specific rate of compensation of horizontal accelerations during its motion, and that the system has an appropriate vibrational behaviour in order to be used for transporting patients. For these purposes there have been considered the results found previously and previous findings obtained in studies that have analysed the effect that different types of oscillations have on people who maintain a seated posture.

The experimental part of this research, that deals with the motion of the system, is explained in the **Annex A**. This annex contains the details of the experimentation stage of this research carried out at the University of Zaragoza. Two prototypes were built and tested in order to supplement the analysis carried out previously with the model and with the design of the system. The experimentation served to validate the theory behind the definition of the design of the system detailed in chapter 4 and to detect some limitations in its use and its assembly.

Chapter 5 is focused on the experimental part of this research that deals with Human Vibrations. A research stay of three months was carried out at the Institute of Sound and Vibration Research at the University of Southampton, in order to find out the effect that the motion conditions that can be experienced with the system may have on the discomfort of people who lay in a recumbent supine posture (posture maintained in a stretcher of an ambulance).

Previous researches have found that when people are exposed to oscillatory motions that try to compensate horizontal accelerations by combining roll and lateral oscillations, motion sickness or discomfort can be experienced. These researches are mainly focused on people who keep seated postures, however there are not studies about the effect that roll-compensation of lateral oscillations have on people who maintain a recumbent supine posture. If the system was applicable to transport patients in ambulances for example, patients would be exposed to these oscillatory motions while they lie in a stretcher. Therefore, for seated postures and at low frequencies [4, 5, 6], people who are exposed to roll-compensation of lateral accelerations have less sensitiveness to lateral accelerations when compensation of lateral accelerations occurs at a rate of 100%. However, at low frequencies and for seated postures also, the likelihood of suffering motion sickness increases if the rate of compensation of accelerations exceeds 50%[7]. This is why in this research it has been tested the effect that different rates of roll-compensation of lateral accelerations

(100% and 25%) have on people discomfort when they lie in a recumbent supine posture.

As the design of system can be modified to achieve a specific rate of compensation of accelerations, the results found with this experimentation may contribute to define which is the rate of compensation more appropriate for transporting patients with this system and whether this motion is appropriate for transporting people in a recumbent posture at least from the discomfort point of view.

Finally, in **chapters 6 and 7** the conclusions, scientific contributions, future lines of work and proofs of dissemination of the thesis are detailed (in Spanish and English, respectively).

Chapter 2

Passive systems applied to compensate accelerations. Review of the literature and presentation of a new approach to transport patients

Abstract

Passive compensation of accelerations has been used in vehicles, devices and buildings with different purposes. A review of these systems is presented here along with an introduction to a new system that represents a new approach for transporting both delicate loads and even patients in an ambulance. Here it is analysed the way in which compensation of accelerations is achieved and the rates of compensation that they can reach. Therefore, the disadvantages of applying compensation of accelerations to people are explained and considered in the new approach presented here.

2.1 Introduction

Compensation of accelerations has been used in vehicles, buildings and devices over time. Its aim has been to reduce the rate of acceleration that acts on a specific direction, in order to obtain an improvement in some particular property or capacity of the system in which it is applied. For example, when it is applied to railway vehicles the purpose of it is to increase the velocity of the train during negotiation of curves and as a consequence of it, improve passengers comfort [8] whereas in buildings it is applied to avoid the building to collapse in case of exposure to an earthquake [9].

Here different applications of these systems are reviewed and compared and so the design of a new system, which might be applied to transport delicate loads and even patients in ambulances. Therefore, some problems that appeared during the development of previous systems and that may affect also to the new one, are considered in this review. The systems presented here come from patents and journal articles and the new system introduced here is object of a research from which some preliminary results have been already obtained.

2.2 Review of the literature

2.2.1 Systems used in vehicles

The major development of passive systems focused on compensation of lateral accelerations appears in the railway sector. Persson et al. [8] reviewed several passive and semi-active systems used in trains and described their differences. Here some of their findings are mentioned and used for comparisons.

Compensation of lateral accelerations used in trains serves to increase the speed of the train during negotiation of curves maintaining the stability of the coach. In order to achieve this goal, the centrifugal acceleration that acts on the lateral direction of the coach while curving is decreased by modifying the orientation of the coach naturally, allowing the coach to oscillate laterally like a pendulum. As the centre of rotation of the coach is higher than its centre of mass, inertial forces (the centrifugal force that acts during negotiation of curves, mainly) acting on its centre of mass tilts the coach naturally. Although some train manufacturers based the motion of their systems on the kinematic of the pendulum (i.e. [10], [11] or [12]) others based their motion in the kinematic of an articulated quadrilateral mechanism (i.e. [13]). Figure 2.1 displays some of their designs.

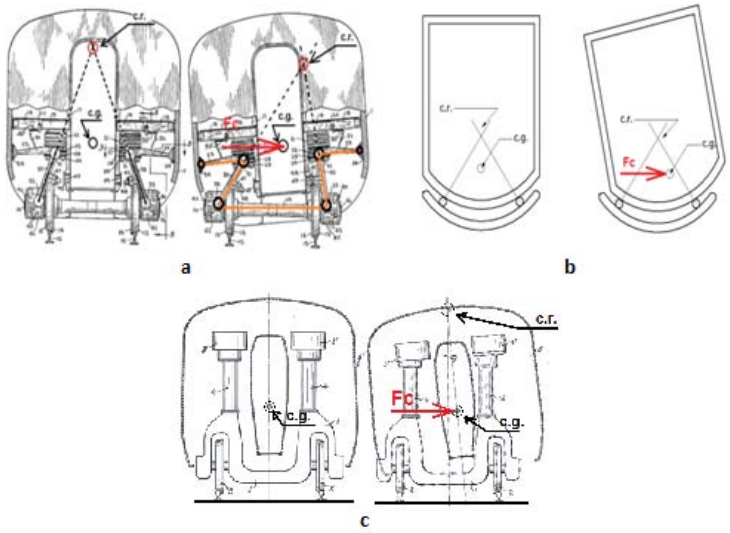

FIGURE 2.1: Systems used in trains

The main difference between systems that share their kinematic with the pendulum or with the articulated quadrilateral mechanism lies in the rate of compensation of accelerations that can be achieved with them. The rate of compensation refers to the percentage in which the acceleration that acts on a body in a specific direction can be reduced. Whereas with pendular systems compensation of accelerations can reach a rate of 100% as long as the motion of the system does not interfere with any obstacle, with articulated quadrilateral mechanisms such rate depends on the geometry of the mechanism. The capacity of the system for tilting the base of the mechanism (in the case of trains, the floor of the coach) influences the rate of compensation achieved freely. Other passive systems used in trains are inerters, mechanical devices which, along with springs and dampers, have demonstrated to be effective at improving ride comfort, by reducing the lateral displacement of the coach [14]. Systems presented here are focused on passive compensation of

accelerations, rather than on improvements of ride comfort through a reduction of vibrations.

Apart from the systems used in conventional trains, some suspended trains disposed also of passive systems that allowed them to oscillate (by roll) during negotiation of curves [15]. Both the systems used in conventional and the ones used in suspended trains allowed the vehicle to roll between $5 - 6$ degrees (for conventional trains) [8] and 10 degrees (in the case of suspended trains) [15]. In terms of compensation of accelerations, it means that the train entirely compensate accelerations up to $0.85 - 1.73\ m/s^2$, as long as there are not constraints to its oscillatory motion.

Leaving aside the railway context, passive systems were used for transporting delicate loads. Robertson designed a system to be installed in vehicles which transported delicate objects as for example glass [16]. Figure 2.2 displays his system. Its motion is based on the kinematic of the pendulum, like some systems used in trains were.

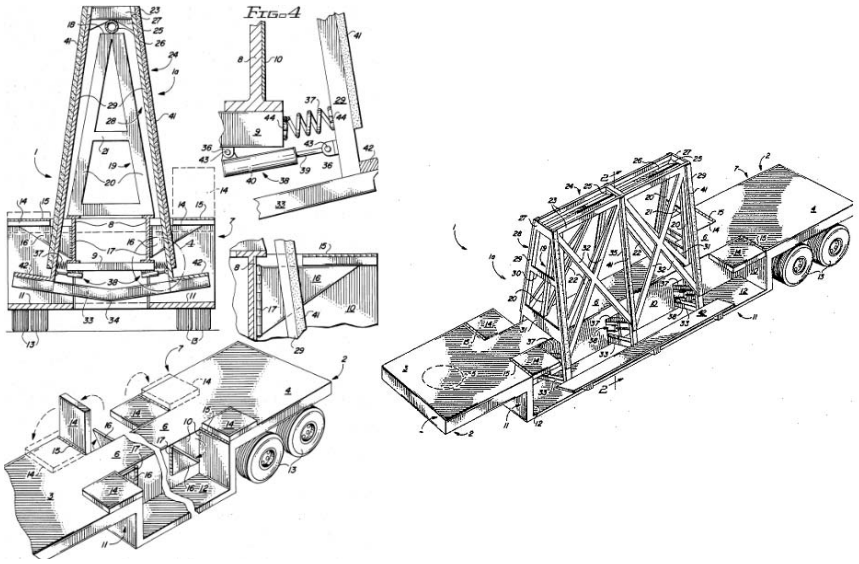

FIGURE 2.2: System applied to transport delicate loads

Robertson's system, more than improving the dynamic behaviour of the vehicle, aims to relieve some forces that acts on the load. Additionally to the oscillatory characteristic of the system, it includes some dampers that filter the motion of the load. According to Robertson, this system is estimated to allow the load to roll approximately 3 degrees, what is equivalent to a full compensation of a lateral acceleration of $0.51 m/s^2$.

Both the systems used in trains and the former system were designed with limitations in their tilting angle (roll), to avoid worsen the dynamic of the vehicle. However, other type of vehicles were equipped with systems which allowed them to oscillate with a wider range of their tilting angle. As it occurs in bikes and motorbikes, in some three wheeled vehicles the driver can experience compensation of accelerations unconsciously. Unlike previous systems, systems used in three wheeled vehicles own their centre of gravity higher than their centre of rotation as it is displayed in Figure 2.3 [17, 18, 19, 20]. It avoids that inertial forces (the centrifugal force that acts during negotiation of curves, mainly) tilt the vehicle by themselves

towards the direction where compensation of accelerations occurs, needing the help of the driver for it.

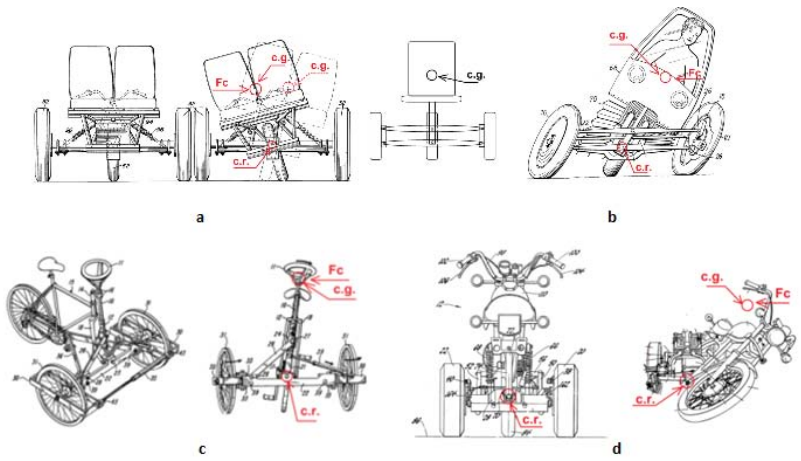

FIGURE 2.3: Systems used in three wheeled vehicles

Although passive systems discussed here are characterized by the absence of any active force in order to achieve the aimed movement, the action of the driver in these vehicles is considered to be a passive force, because the driver reacts against the inertial forces that act on him unconsciously, by instinct. The system contributes to maintain the dynamic equilibrium of the vehicle and therefore, it orientates the driver (he does by himself) in a more comfortable driving position. These systems make the driver to experience full compensation of accelerations.

Additionally to the systems introduced previously, the system used in the seat displayed in Figure 2.4 [21] can be installed and used in any kind of vehicle.

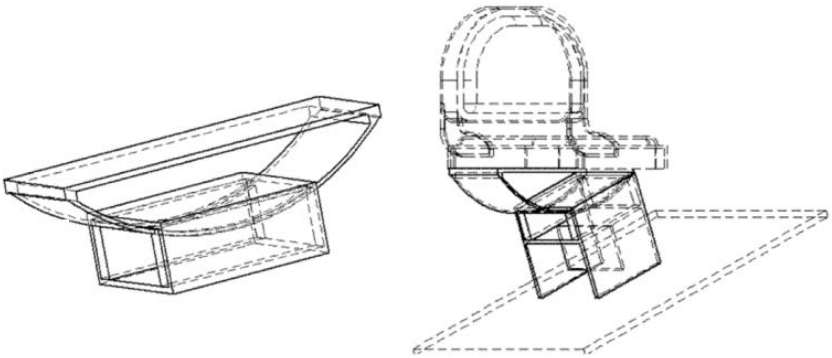

FIGURE 2.4: General applications seat

With an appropriate design of the circular rail that maintains the centre of rotation of the seat above the centre of mass of the seated person, it is guaranteed that under the action of external forces on the seated person, the seat will compensate passively the accelerations that act on its occupant. Depending on the geometry of the circular rail (shape and length of the circular arc), the rate of compensation achieved varies.

2.2.2 Systems used in buildings

Buildings do not move or translate as vehicles do, however they can oscillate and experience small displacements in some of their parts. Passive systems known as Tuned Mass Dampers (TMD) are used in order to mitigate the effects that vibrations can have on the structural integrity of buildings. TMD consist of a mass with a properly tuned spring and damper which absorb part of the energy that the building structure receives during exposure to an earthquake e.g., relieving it from the building structure. Such energy is transferred to the motion of the mass that belongs to the TMD and it decreases eventually [22]. Some examples of their applications are the Citicorp Center in New York, the John Hancock Building in Boston, Sydney Tower in Sydney and Taipei 101 Tower in Taiwan [23, 24]. Additionally to TMD systems, Tuned Liquid Dampers and Tuned Liquid Column Dampers are used with the same purposes. TLD and TLCD share their working principle, the flow of water through an orifice absorbs the energy that the building structure transfers to it [23].

2.2.3 Systems for patients

This section deals specifically with those systems that try to improve patient comfort. Independently whether they may or not be installed in vehicles, these systems are taken into account because they are directly related with the new approach to transport patients, which is introduced in the next section. Patients are exposed to undesirable motions that can affect their health, comfort and/or wellbeing during they receive medical treatment or while they are transported to receive it.

Figure 2.5 displays a stretcher that has been designed with rotational handholds in order to improve the transport conditions both for the patient and for the stretcher-bearers [25].

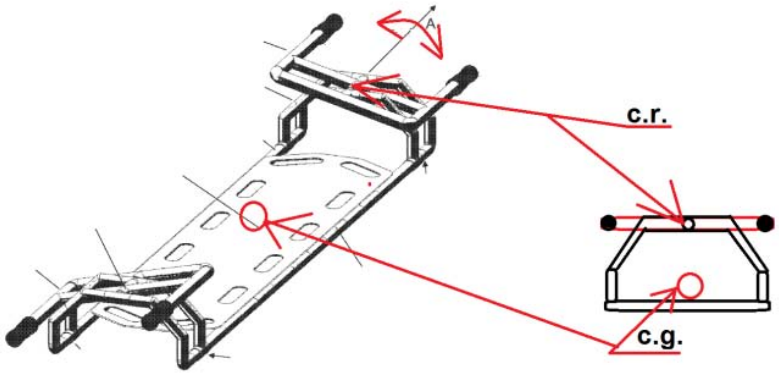

FIGURE 2.5: Stretcher with rotational hand-holds

The system displayed in Figure 2.6, more sophisticated than the former, is focused on isolating the patient from vibrations experienced during the motion of the vehicle in which it is installed. Although the system disposes of robotic parts that ease the access and egress of the stretcher into/from the vehicle, some joints between its parts, although in a limited range, allow the stretcher to oscillate freely longitudinally and transversally, what allows the system to achieve a reduced rate of compensation of accelerations.

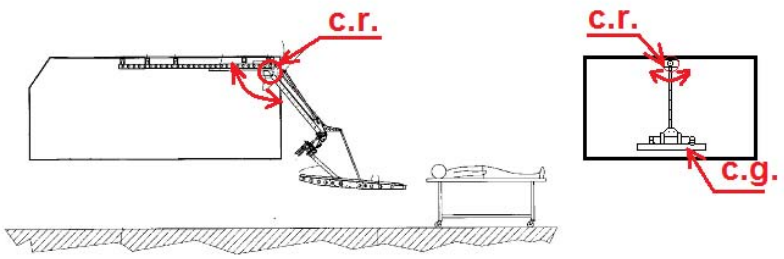

FIGURE 2.6: Low range oscillatory system

2.3 Effect of oscillations and passive compensation of accelerations on people

2.3.1 Effect on passengers

Some systems mentioned previously may have a negative effect on people due to the motion conditions to which they expose them. Oscillatory motions that are experienced during negotiation of curves can have a negative effect on passengers, increasing discomfort and also the likelihood of suffering motion sickness. This phenomena has been widely studied by researchers in the past and there is a clear relationship between low-frequency oscillations and motion sickness [26, 27].

Depending on the means of transport used, the direction in which oscillations can produce motion sickness varies (vertical oscillations in ships [28] and horizontal oscillations in road transport [26]). According to Turner and Griffin [26], motion sickness is influenced, among other factors, by the perception that a person has of the motion to which he/she is exposed, and the phase between the visual scene and the motion can also be important [27]. J. Joseph and M. Griffin studied the effect that variations in phase of combined lateral and roll oscillations had on people. The type of motion to which a person is exposed also affects both to the likelihood of suffering motion sickness and to passenger discomfort. Three factors have been analysed when compensation of acceleration is caused by oscillatory motions: the direction of oscillation, its phase, and the rate of compensation achieved. Joseph and Griffin [29] found that compensation of lateral accelerations by roll oscillation at rates lower than 50% was more appropriate to reduce motion sickness occurrence. Therefore, they found that for this combination of oscillations lower magnitudes reduced the likelihood of suffering motion sickness [7].

At the beginning of using passive systems in trains, an increase of the number of passengers reporting motion sickness caused that passive systems evolved to semi-active and active systems, trying to avoid some of the causes that contributed to the occurrence of motion sickness. Persson et al. covered in his study part of such evolution and they compared passive with semi-active systems [8].

2.3.2 Effect on patients

During transport in an ambulance to and from a hospital, patients are exposed to accelerations that affect negatively their health. The way the stretcher is restrained to the vehicle floor influences the transmission of vibrations and accelerations that occur during transport. Depending on the clinical state of the patient, vibrations can have a negative effect on his body, increasing discomfort or producing pain in parts

of his body which are especially sensitive as a consequence of having received a hit or being injured.

Recent studies about the effect of accelerations and velocity on patients suffering cardiac or chest medical problems have concluded that a reduction in the inertial forces experienced during transport benefits the patient and it reduces the risk of worsen his health [30, 31, 32, 33].

In order to reduce the magnitude of accelerations that affect the patient, apart from decreasing the speed of the vehicle, passive compensation of accelerations might be applied, considering the standards concerned with ambulances and the restraint systems of the stretcher (in Europe, EN 1789 and EN 1865 respectively [34, 35]).

2.4 New approach in patient or/and delicate loads transportation

2.4.1 Definition of the system

The new system introduced here is being object of a thorough study analysing its kinematic and dynamic, but here some preliminary results are included in order to compare it against some of the systems mentioned previously. It consists of a multibody mechanism formed by a supporting frame that is fixed to the vehicle, a base and one or several jointed bars that connect the supporting frame with the base. Figure 2.7 displays some general configurations that can be obtained by modifying the number of bars and the type of joints existing between its parts.

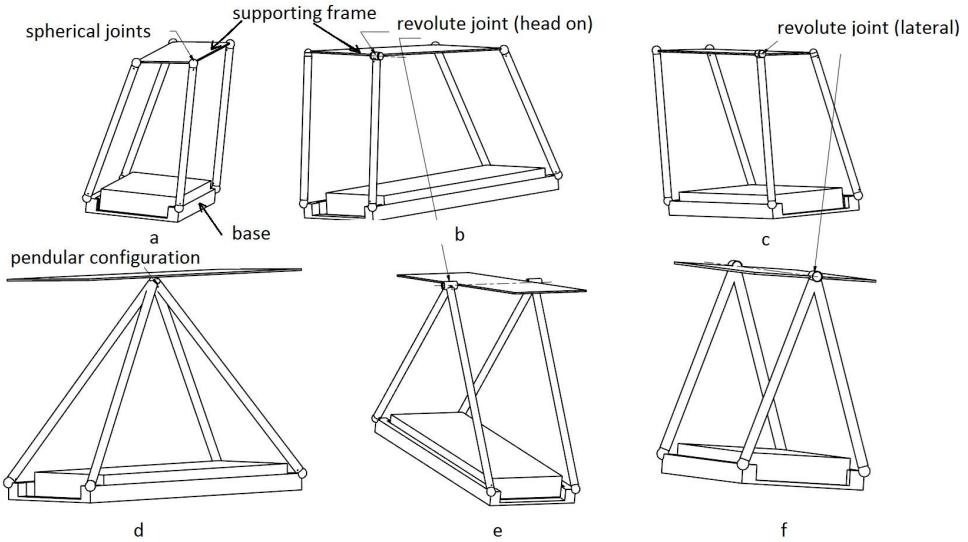

FIGURE 2.7: General designs

The connections between the supporting frame and the base employs joints that constrain partially or totally the motion of the base. Dampers of any type (i.e. linear, rotational) can be installed (they are not displayed in Figure 2.7) at any location, keeping in mind the purpose of the system and possible interferences with its use.

Independently of the type of joints installed, the distances between the joints that connect the supporting frame with the bars have to be smaller or equal than the dimensions of the base, both longitudinally and laterally. Such condition guarantees

that the motion of the base will keep its centre of rotation above the centre of mass of the load placed on the base.

2.4.2 Application to transport patients

Having in mind all the systems presented previously and considering the effects that oscillations and the rate of compensation of accelerations can have on patient comfort and motion sickness, the specific configuration, from all displayed in Figure 2.7, that the system should adopt so as to be applied to transport patients should correspond either with Figure 2.7b or 2.7c. It would allow the base, to which the stretcher is fixed, to tilt either longitudinally or laterally (yawing or rolling), respectively. In these configurations the system disposes of a revolute joint in one of its joints and of spherical joints in the others, what provides the system with only one degree of freedom (if the degrees of freedom corresponding to the spin of the bars are obviated), which corresponds with the oscillatory motion of its base (either pitch or roll).

When lateral and roll oscillations are combined so as to compensate lateral accelerations at low frequencies (close to 0.2 Hz, which are significant in road and rail transport) the rate of compensation of the lateral acceleration should not exceed 50%, in order to reduce the likelihood of experiencing motion sickness [29]. As the system is aimed to work under such conditions, the system should be configured in a way that not exceeds such rate of compensation. This may be achieved with a design of the system which provides the system with the kinematic of the articulated quadrilateral mechanism.

The system is intended to be installed into type A1 and A2 ambulances [34]. These types of ambulances are appropriate for transporting only one patient and at least one person in their medical compartment, but not for providing any treatment to the patient. Depending on the dimensions of the interior compartment of the ambulance, the system should be designed to compensate either lateral or longitudinal accelerations. Additionally, the system must dispose of limits to its free motion, avoiding that it hits any part of the interior compartment of the ambulance. Apart from these limits, in the direction in which the motion of the system is allowed, a mechanical emergency locking system accessible from either the driving seat or the seat beside the stretcher must exist.

Patients who would be able to take advantage of this system might be those who during driving conditions can experience some pain in their fractured or bruised limbs or/and hips. They should have received their treatment previously and they only would need to be transported in a vehicle. Although the system disposes of dampers, below its base for this application i.e., (in order to allow professionals walk around the stretcher when the vehicle is parked), the system should be used only when steady conditions are achieved during driving.

Figure 2.8 displays two examples of how this system could be fitted in the patient compartment of a type A1 or A2 ambulance.

The capacity of the system for compensating horizontal accelerations depends apart from its dimensions and the way its parts are linked each other, on the available space around it in the interior compartment of the ambulance. Although the details and results from the kinematic and dynamic analysis carried out for this system, are going to be described in detail in future publications, here it can be mentioned that this system can be designed for achieving rates of compensation of accelerations up to 50%, achieving its base an inclination of 8.83 degrees for what requires an available width of 1.02 m for a base of width of 0.6 m (results obtained

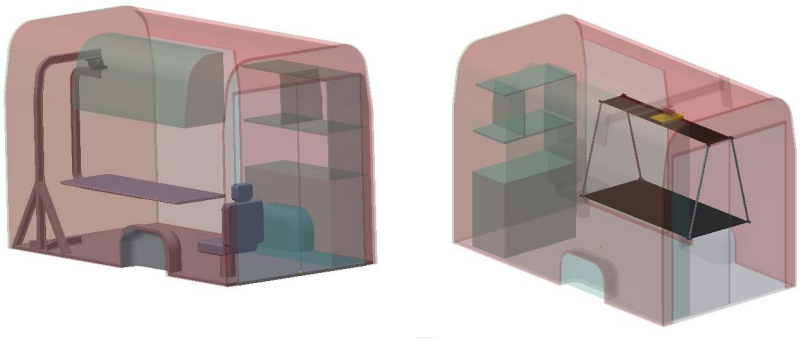

FIGURE 2.8: Application for patient transport

in computational simulations). As other passive systems, its vibrational response depends on the damping ratio with which the system is configured. The aim of its design is to be effective under steady and low frequency motions, but in the case of experiencing step-input lateral accelerations its damped motion can have a lag between the phase of the input and the response of the system, like it occurred with passive systems in trains [8]. For minimizing such lag effect the damping ratio along with its inertia should not be very high (below 0.6, attending to preliminary results obtained in computational simulations), but this is going to be discussed in detail in subsequent publications.

Although it is out of the scope of this work, this new approach shares its goal with an active system used in Japanese ambulances [36]. Unlike the passive system introduced here (in what respect to its application to transport patients), this system was designed to compensate at the same time longitudinal and lateral accelerations. The motion of the stretcher was controlled by a servo-system and it reached a pitch angle range between $2 - 12$ degrees and a roll angle range of 12 degrees. Due to limitations in its servo-system it could entirely compensate accelerations smaller than $2m/s^2$. With this passive system the magnitude of the accelerations expected to be compensated is higher, although in a rate smaller than 50%, following recommendations of previous researches.

2.4.3 Application to transport delicate loads

Although it has not been tested yet, transport of delicate loads such as fruit, glass or fragile materials might take advantage of using this system, being partially isolated from the vibrations that the motion of the vehicle transfers to them. Nevertheless, the size of the load, its weight and the available space in the compartment of the vehicle may influence the effectiveness of the system.

One of the most common problems that fruit experiences during transport is bruising [37, 38]. Damages in fruit and vegetables reduce their quality and therefore the prices to which they are sold, or even they can avoid that they reach the market [39]. Its effect on the economy cannot be underestimated, especially when these products come from undeveloped countries [40]. Although some measures already considered by other researchers are focused on improvements in their packaging to prevent loads to be damaged [37, 38, 39, 40], the use of this system could reduce the negative effects that vibrations have on them.

As the design of the system can be adjusted, the selection of the joints will be influenced by the direction in which vibration isolation wants to be achieved.

Therefore, damping must be adjusted in order to make the system to oscillate steadily and without affecting the stability of the vehicle.

2.5 Discussion

In the review of the state of the art in what refers to passive systems applied to compensate horizontal accelerations, it has not been found a passive system applicable to transport delicate loads or patients with the capabilities of the new system introduced previously. The systems found were designed specifically to be installed in a specific vehicle, constituted a part of its frame and/or had limited and influenced by its design the rate and the direction of compensation of horizontal accelerations.

The use of passive systems applied to compensate accelerations is spread and it has been proved to be effective. There are some problems intrinsically linked to them that have been solved through the addition of electronic and control systems, but in some cases it has not been needed (i.e. as mentioned before [17, 15, 21]).

Its use can be beneficial for the dynamic of the vehicle in which they are installed and also for people who use them, but also it can have negative effects on them which must be balanced and considered during the design stage of the system (i.e. a reduction of the load capacity, risk of overturning, discomfort, motion sickness). Some of these problems are intrinsic with the use of this system, like the reduction of the load capacity of the vehicle but others, like overturning, can be prevented with a limitation for the load capacity of the system along with a lower position of its centre of rotation with respect to the centre of mass of both the vehicle and the transported mass. Motion sickness and discomfort can be prevented following recommendations for the oscillatory motion of the system from previous research (based on the results obtained with experiments focused on seated postures, cited previously) and also extending the experiments carried out previously for seated postures to recumbent postures.

The new approach for transporting both delicate loads and patients in vehicles must keep in mind such considerations. The possibility of applying the system introduced here to such purposes requires experiment on both people and vehicles. In the case of people, it is required additional research to understand the effect that longitudinal and lateral oscillations have on people who maintain recumbent postures. This would bring feedback to the design stage of the system, allowing the system to be designed so as to move in a way appropriate for people.

Rates of compensation of acceleration will depend on the available space in the vehicle compartment, the dimensions and weight of the load and the stability of the vehicle, both to transport loads and patients. Further research and analysis is being carried out currently and the results will be object of consequent publication.

Chapter 3

Efficiency of a BDF-Newton-Raphson numerical integration method applied to solve a system of nonlinear differential equations modeling a mechanical multibody system

Abstract

A BDF-Newton-Raphson numerical integration method has been used to solve the equations of motion of a mechanical multibody system. The equations of motion of the system have been posed applying the Momentum and the Kinematic Momentum Theorems. The system of nonlinear second order algebraic differential equations has been reduced to a system of first order algebraic differential equations, increasing the number of equations and then transformed into a system of nonlinear equations by approximating its derivatives with a backward differentiation formula (BDF). Variations in the BDF formula, step size and step type approach (fixed or variable step) have been studied in order to optimize the solving process. The system has been validated against the solution provided by the computational software MSc Adams, whose solver uses the Lagrangian method.

3.1 Introduction

The equations of motion of multibody systems are nonlinear differential algebraic equations (DAE's) of index 3, see [41, 42, 43] for instance. In order to handle the system numerically, a reduction of order is convenient to obtain a first order system of algebraic differential equations, which increases the number of equations. Some implicit systems can be transformed into explicit systems of ordinary differential equations (ODE's) [44], but in this case that was not possible. For this reason, a backward differentiation formula (BDF) was used in order to approximate each derivative in the system and then solving the resulting nonlinear system through the Newton-Raphson numerical integration method [45, 46]. The multibody system considered here represents a mechanism that is going to be applied to compensate accelerations passively in delicate loads transportation. It is formed by 6 rigid solids (a base, four bars and a supporting solid). All of them

are connected to each other by mean of joints (ideally without friction and damping properties). The motion of one of them (its six degrees of freedom) is known and the others move as a consequence of the inertial forces that act on them, due to the motion of the first solid. Four dampers have been added and they are connected between the base and the supporting solid. Figure 3.1 displays the parameterized model.

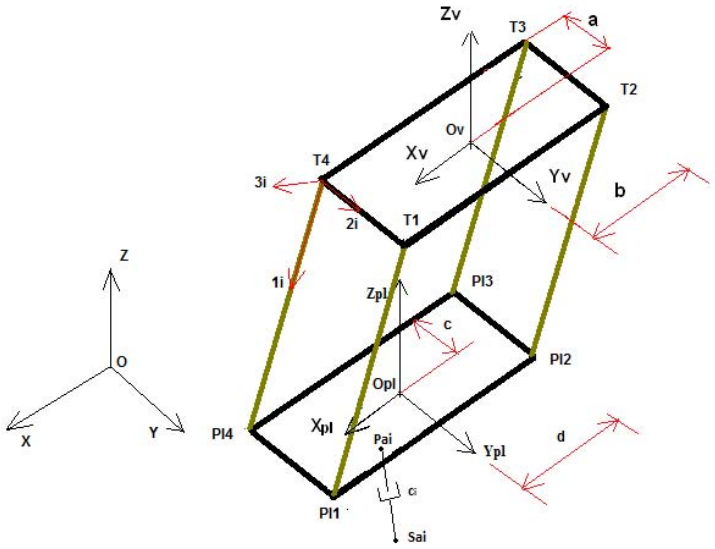

FIGURE 3.1: 3D multibody system

The equations of motion can be posed by mean of applying the Newtonian mechanics approach or the Lagrange mechanics, see [47, 48, 49] for instance. Different approaches have some advantages and disadvantages, in terms of easiness when posing the equations, and/or in terms of solving them. Here, the Newtonian mechanics approach was used in order to pose the equations in a more analytical way and to have an understanding of how different type of joints affect to the motion of the system, knowing (once the system of equations was solved) the reaction forces and torques applied to them in a more straightforward way than with the Lagrangian approach.

3.1.1 Equations of motion

Before posing the equations of motion through the two different approaches, some common aspects are going to be introduced.

3.1.1.1 Generalized coordinates

The position of each solid was defined through the position and orientation of a point that belonged to the solid. The absolute reference coincided with the ground, fixed horizontal plane algebraically depicted by an origin O and a vectorial base XYZ, of which Z axis had opposite direction to gravity. The solid, from which its 6 DOF were known, was associated to the local coordinate system (O_v,$X_vY_vZ_v$) and it was positioned through its origin O_v. Its orientation was defined by the sequence of the Euler angles (ψ_v, θ_v and φ_v), which orientated it with respect to XYZ. Each

bar $i,\ i = 1, \ldots, 4$, was positioned and orientated with respect to the local coordinate system (O_v,$X_vY_vZ_v$), through a point that coincided with their centre of mass $O_i,\ i = 1, \ldots, 4$, and the sequence of Euler angles (ψ_i, θ_i and φ_i, $i = 1, \ldots, 4$). The base was associated to the local coordinate system (O_{pl},$X_{pl}Y_{pl}Z_{pl}$) which was positioned and orientated with respect to the local coordinate system (O_v,$X_vY_vZ_v$), through a point that coincided with its centre of mass O_{pl} and the sequence of Euler angles (ψ_{pl}, θ_{pl} and φ_{pl}). So, the system generalized coordinates (q) were 18: ψ_i, θ_i and φ_i ($i = 1, \ldots, 4$), X_{pl}, Y_{pl}, Z_{pl}, ψ_{pl}, θ_{pl} and φ_{pl}.

3.1.1.2 Newtonian mechanics

The equations of motion of the system were obtained by posing the Momentum and the Kinematic Momentum Theorems applied to each one of the rigid solids (except to this one for which its 6 DOFs were known), defining the vectorial geometrical relationship between the solids (constraint equations). The Momentum Theorem applied in the centre of mass (c.m.) of each solid can be written in the form

$$\sum \overrightarrow{F_{ext}}(c.m) = m \cdot \overrightarrow{a}_{c.m}. \tag{3.1}$$

The Kinematic Momentum Theorems applied in the centre of mass (c.m.) of each solid can be written in the form

$$\sum M_{ext}(c.m) = \bar{\bar{I}}_G \cdot \overrightarrow{\alpha}^{solid} + \bar{\bar{\Omega^{solid}}} \cdot \left(\bar{\bar{I}}_G \cdot \vec{\Omega}^{solid}\right). \tag{3.2}$$

After applying the theorems to each solid, 30 equations and 48 additional unknowns referred to the Forces and Torques that act on each joint were obtained. Constraint conditions associated to the joints and to the geometrical relationships between the solids provided the remaining 36 equations (12 equations from geometrical constraints and 24 equations from joints constraints).

Geometrical relationships are independent of the type of joints with which the solids are linked to each other. They relates the position of the base centre of mass to the ground origin adopting the form of the following equation for each bar $i,\ i = 1, \ldots, 4$ (see Figure 3.1).

$$\overrightarrow{OO_v} + \overrightarrow{O_vT_i} + \overrightarrow{T_iPl_i} + \overrightarrow{Pl_iO_{pl}} - \overrightarrow{O_{pl}O} = 0. \tag{3.3}$$

The constraint equations related to the type of joints that bind the solids to each other were defined as equations (3.4) to (3.6) indicate, for configurations with spherical joints in all of their joints (equation (3.4)), cardan joints (equation (3.5)) and one revolute joint (equation (3.6)).

$$\begin{aligned} \overrightarrow{M_{T_i}} &= 0; 0; 0, \\ \overrightarrow{M_{Pl_i}} &= 0; 0; 0, \end{aligned} \tag{3.4}$$

$$\begin{aligned} \overrightarrow{M_{T_i z}}\}_{X_vY_vZ_v} &= 0, \\ \overrightarrow{M_{T_i y}}\}_{X_iY_iZ_i} &= 0, \\ \overrightarrow{\dot{\varphi}_i} &= 0, \end{aligned} \tag{3.5}$$

$$\begin{aligned} \overrightarrow{M_{T_i x}}\}_{X_v Y_v Z_v} &= 0, \\ \overrightarrow{\psi_i} &= 0, \\ \overrightarrow{\dot{\varphi}_i} &= 0. \end{aligned} \tag{3.6}$$

The resulting system of equations contained 66 second order algebraic differential equations of order 2. To reduce the order of the system, it was convenient to introduce 18 additional unknowns. Then, the first order system of algebraic differential equations could be solved by the BDF-Newton-Raphson numerical integration method.

3.1.1.3 Lagrangian mechanics

The equations of motion obtained by applying the Lagrangian mechanics theory [50] take the form

$$\frac{d}{dt} \cdot \left(\frac{\partial L}{\partial \dot{q}} \right) - \left(\frac{\partial L}{\partial q} \right) + (\Phi_q)^T \cdot \lambda = Q, \tag{3.7}$$

where Q is the vector that contains non-potential external forces applied to the system (in this case, the forces that dampers act on the centre of mass of the base), L is the Lagrangian (defined by equation (3.8)), $\Phi_q^T \cdot \lambda$ represents the constraint conditions and q the vector of generalized coordinates.

$$L = T - V, \tag{3.8}$$

where T represents the kinetic energy of the system and V its potential energy. The system of equations is formed by 30 equations (18 equations as a result of posing the Lagrangian equation of motion and 12 equations that come from the constraint conditions between the solids that form the system).

3.2 Methodology

Once the equations of motion of the system were posed, some changes had to be done in the system to reduce its order. We introduced 18 more equations so as to do the change of variable given by

$$\begin{aligned} u &= \dot{q}, \\ \ddot{q} &= \dot{u}. \end{aligned} \tag{3.9}$$

The system of equations was rewritten in compact form as follows

$$G(Y, \dot{Y}, t) = 0, \tag{3.10}$$

where G represents the column matrix of functions of the unknowns, Y is the column matrix of the unknowns and $\dot{Y}$ their first derivatives.

Once Y and $\dot{Y}$ were known at time t_{n-1}, the estimation of the solution at time t_n was obtained with a first order predictor polynomial, which took the form

$$y_n^{(0)} = y_{n-1} + \dot{y}_n \cdot h. \tag{3.11}$$

The Newton-Raphson numerical integration method linearized the nonlinear first order system by mean of transforming it in the form

$$J \cdot \Delta = -G(Y_n, \dot{Y}_n, t_n) = 0, \tag{3.12}$$

where J represents the jacobian matrix for the column matrix of functions G.

The Newton-Raphson algorithm evaluated Y_n of the column matrix Y at discrete times until the solution of (3.10) held within an acceptable tolerance error ε. The iterative process started supposing known the initial values of Y_{n-1} and then predicted the values for Y_n. When two consecutive approximations, Y_n^{m-1} and Y_n^m, that accomplish equation (3.12) agreed with the established tolerance error (equation (3.13)), the solution was taken as valid and the computation went forward.

$$\|\Delta\| < \varepsilon. \tag{3.13}$$

The expression $\|\Delta\|$ is the maximum norm of the corrections (Y_n^m - Y_n^{m-1}) to the solution of the linearized system (3.12).

3.2.1 Backward differentiation formula

As the system represented by (3.10) could not be transformed into an explicit system of ODE's, the first derivatives of $\dot{Y}$ were estimated by mean of a backward differentiation formula (BDF). Two different BDF were used, differing each other in their coefficients β, aY_n, aY_{n-1} and aY_{n-2} as equation (3.16) shows

$$\frac{aY_n \cdot f_i - aY_{n-1} \cdot f_{i-1} + aY_{n-2} \cdot f_{i-2}}{\beta \cdot h}, \tag{3.14}$$

where for a BDF method of order 1, $aY_n = 1$, $\beta = 1$, $aY_{n-1} = 1$ and $aY_{n-2} = 0$, and for a BDF method of order 2, $aY_n = 3$, $\beta = 2$, $aY_{n-1} = 4$ and $aY_{n-2} = 1$.

3.2.2 Variable step size

Different ways of defining the time step used during the integration method were chosen. We considered two types of steps: fixed and variable step size. In order to determine the variable step size, we used the following formula

$$C \cdot \|\varpi\| \cdot \left(\frac{h_n}{h_{n-1}}\right)^{k+1} < \varepsilon, \tag{3.15}$$

where $\|\varpi\|$ represents the normalized maximum integration error referred to the generalized coordinates. The step size obtained with this equation was kept within a predefined range that went between $0.1s$ to 0.01, 0.001 or $0.0001s$.

3.2.3 Cases of study

Three different configurations of the multibody system were analysed. They differed each other in the type of joints that disposed between their parts. The dimensions of the multibody system displayed in Figure 3.1 are listed in Table 3.1. They are referred to the nomenclature used previously in the figure.

Here Drb is the distance between the horizontal plane that contains the joints of the bars' upper ends and the base of the system, when it keeps static equilibrium. The position of the dampers' lower ends is defined by sa_i points. These points

TABLE 3.1: Multibody system dimensions

Name	Value	Units	Configuration (type of joints)
a	0.1	m	spherical and cardan
b	0.5	m	spherical and cardan
b	0.7	m	revolute
c	0.25	m	all
d	0.7	m	all
Drb	1.5	m	all
$c1 = c3$	500	$\frac{N \cdot s}{m}$	all
$c2 = c4$	1000	$\frac{N \cdot s}{m}$	all
$sa_{1x} = -sa_{3x}$	d	m	all
$sa_{2x} = sa_{4x}$	0	m	all
$sa_{1y} = sa_{3y}$	0	m	all
$sa_{2y} = -sa_{4y}$	c	m	all
sa_{iz}	-1.8	m	all

belong to the body in which the local coordinate system (O_v,$X_vY_vZ_v$) has been defined.

The system was exposed to a motion similar to which a vehicle can experience when it is driven on a highway. The inputs of the system of equations were the six degrees of freedom associated to the body to which were connected all the bars' upper ends of the multibody system. The duration of the motion was 40 seconds. It was the time that the "hypothetical" vehicle lasted to follow the path displayed in Figure 3.2.

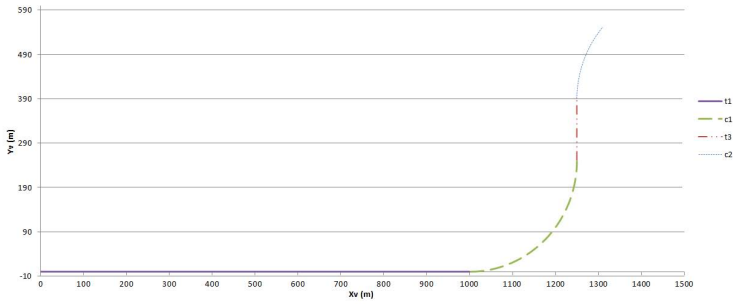

FIGURE 3.2: Path followed during simulation

For each configuration, its respective system of equations was solved applying:

- p1) A fixed step size and a BDF method of order 1.
- p2) A fixed step size and a BDF method of order 2.
- p3) A variable step size and a BDF method of order 1.
- p4) A variable step size and a BDF method of order 2.

Cases $p1$ and $p2$ were run for different step sizes and tolerance error ε. Cases $p3$ and $p4$ were run for different constants C, tolerance error ε and minimum step sizes. Cases $p3$ and $p4$ shared a maximum step size of 0.1 s. Figure 3.3 displays the map of the parameters used for all cases.

For each different configuration (with regards to the type of joint) the computational parameters that were considered were the followings:

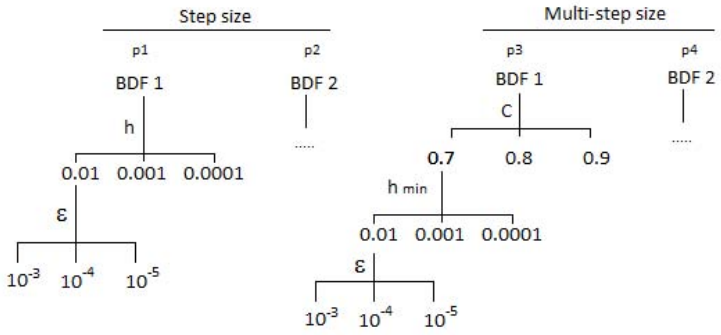

FIGURE 3.3: Cases map

- In cases $p1$ and $p2$, the step size, the order of the BDF and the tolerance of the error ε were the parameters to determine so as to minimize the absolute error and the computational time for the numerical integration method.
- In cases $p3$ and $p4$, the parameter C of equation (3.13), the order of the BDF and tolerance of the error ε were the parameters to determine so as to minimize the absolute error and the computational time for the numerical integration method.

The absolute error was analysed for the generalized coordinate φ_{pl} and θ_{pl}, which represented the roll and pitch angle of the base of the system with respect to the local coordinate system (O_v,$X_vY_vZ_v$). These generalized coordinates were chosen because when compensation of accelerations is analysed, the orientation of the body, to which compensation is applied, is directly related to the rate of compensation achieved (see [8]).

3.3 Numerical results

Accumulated error was calculated in the form

$$Error = |q_{calculated} - q_{reference}|. \tag{3.16}$$

In order to make comparable the results between different cases, the time series for the value of $q_{calculated}$ was normalised with respect to the time series of $q_{reference}$. The reference results were registered every 0.05 seconds. It might introduce an error in the cases where the step size was bigger than $0.05s$, but results were more precise when step size was smaller. As the generalized coordinate analysed could take values of zero radians, the error was not assessed in percentage terms.

Computation time was evaluated considering the original time series for each case. It represents the computational time that the computer took to solve the problem.

3.3.1 Step size

Both in cases $p1$ and $p2$ the accumulated error increased as the step size increased. However, the accumulated error remained in the same level for step sizes smaller than $0.001s$ when a BDF method of order 1 was used and smaller than $0.01s$ when the BDF was of order 2, as it can be seen in Figure 3.4.

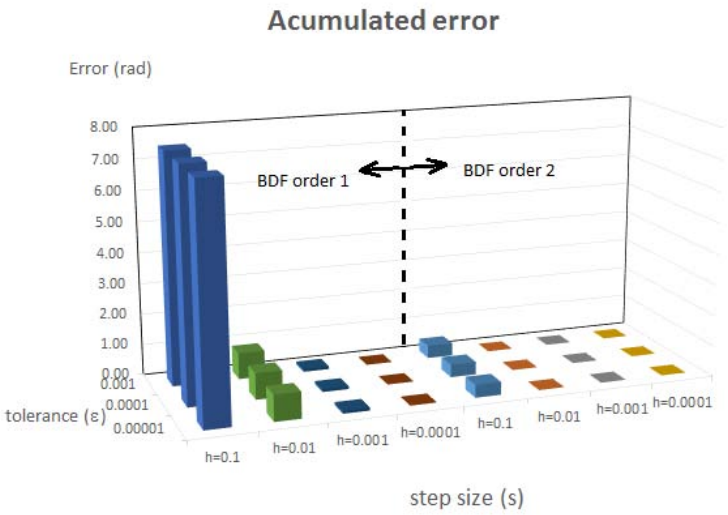

FIGURE 3.4: Accumulated error for φ_{pl} with BDF method of order 1 and 2

Independently of the order of the BDF method and the step size, the integration tolerance error did not seem to have influence in the accumulated error. The computational time increased as the step size decreased, as it was expected [51, 52]. It was not affected by the integration tolerance error and neither by the order of the BDF method. Table 3.2 contains the average of the total computational times for the generalized coordinate φ_{pl} at the step sizes considered in this study. The same results were found for the generalized coordinate θ_{pl}.

TABLE 3.2: Average of Total Computation times

Step size (s)	Total time (s)	
	Order 1	Order 2
0.1	41.76	50.65
0.01	284.99	271.58
0.001	2047.81	2140.08
0.0001	21444.89	20903.18

These findings were similar both for the generalized coordinates φ_{pl} and θ_{pl}. In order to determine the conditions where the computational cost was worth it in order to achieve an acceptable error in the solution, the product between the accumulated error and the averaged calculation time was used (average of the computational time taken between 0.01 seconds of simulation time). The conditions that minimize the product, were the ones that made the method more efficient. Figure 3.5 displays the efficiency levels for the generalized coordinate φ_{pl} solution considering all computational conditions in cases $p1$ and $p2$.

The use of a BDF method of order 2 at a fixed step size of $0.01s$ gave the most efficient solution independently of the tolerance error. Figure 3.6 displays a comparison between the best solutions achieved for the generalized coordinate φ_{pl} when the most efficient step size was used.

This Figure displays the variation of φ_{pl} as a consequence of the motion of a vehicle that follows the path displayed in Figure 3.2. From it, we see the small error in the solution that the model provided when the vehicle negotiated curves, because

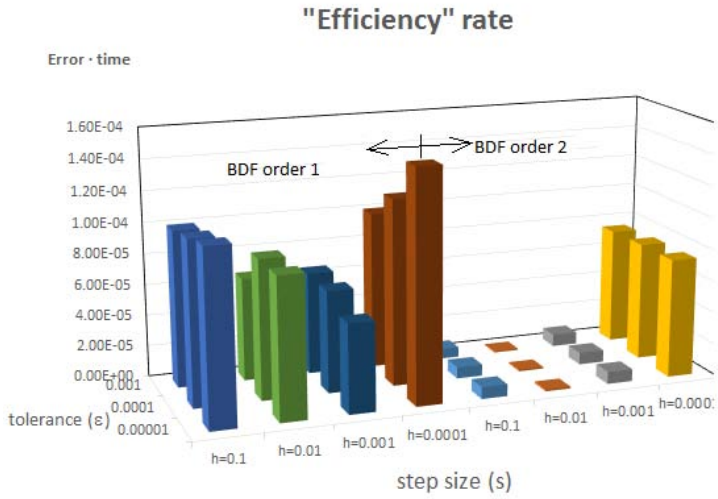

FIGURE 3.5: Efficiency levels for fixed step size cases

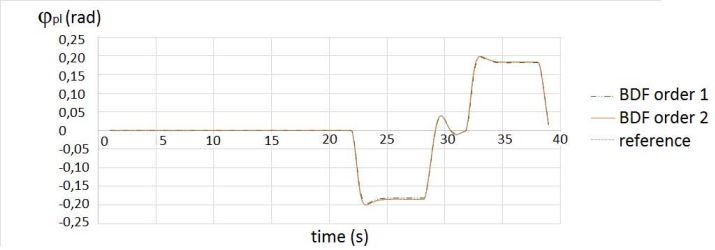

FIGURE 3.6: φ_{pl} with a BDF method of order 1 and 2 vs reference for the most efficient step size cases

it was then when the biggest changes in the values of the generalized coordinates occurred.

3.3.2 Variable step size

The limits for the lower value of the step size affected to the behavior of the solution respects to the accumulated error and the computational time. In case $p3$, the accumulated error remained very low (except when a tolerance error of 10^{-3} and the lower value of the step size was 10^{-4}); however, in case $p4$, the accumulated error increased as the lower value of the step size decreased. Tolerance error affected clearly to the accumulated error, decreasing the accumulated error as the tolerance decreased, as it occurred in cases $p1$ and $p2$.

High values of the constant C decreased the accumulated error $(C = 0.9)$ and also the computational time. The results obtained when a BDF method of order 1 was used, were much better than the ones obtained applying a BDF method of order 2. Accumulated error when a BDF method of order 2 was found to be in average up to 15 times higher than the same cases that use a BDF method of order 1. Figure 3.7 displays a comparison between the best results for the generalized coordinate φ_{pl} obtained with a BDF method of orders 1 and 2 when a variable step size approach was applied. They correspond to the case that had a constant C = 0.9 and a tolerance error ε of 10^{-5}.

FIGURE 3.7: φ_{pl} with BDF method of order 1 and 2 vs reference

This Figure displays also that the accumulated error decreased when the range between the minimum and maximum step size decreased. Similarly as it occurred with the fixed step size cases, computational time increased as the minimum step size decreased. Therefore, the order of the BDF method affected to the computational time, increasing considerably with a BDF method of order 2, especially when the lower value of the step size was far from the upper value.

Similarly as in the fixed step cases, efficiency levels for the generalized coordinate φ_{pl} solution considering all computational conditions in cases $p3$ and $p4$ were displayed in Figure 3.8.

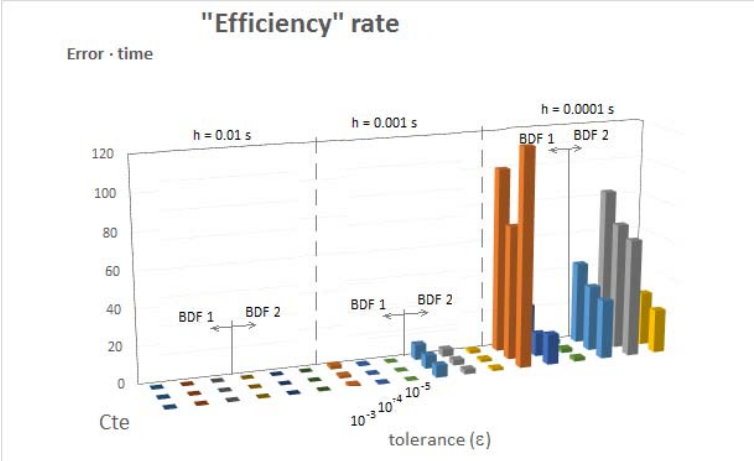

FIGURE 3.8: Efficiency levels for variable step size cases

The use of a BDF method of order 2 gave much worse results in terms of efficiency than a BDF method of order 1 when the step size could vary, and the step size was allowed to decrease to values smaller than $10^{-3}s$. If the step size was too small, with a BDF method of order 2 the convergence error increased and remained close to the tolerance error (what caused that equation (3.15) provided small step sizes all the time), increasing the number of iterations and then the computational time. These three factors worsen the efficiency of the method.

We must say that the numerical integration method did not converge in two cases where the minimum step size allowed was $0.01s$, the tolerance error $10^{-3}s$ and the values of constant $C = 0.7$ and $C = 0.8$.

3.3.3 Comparison between different step size approaches

There were some differences in the results when the order of the BDF method and the type of selection of step size were considered. Computational time was much

lower when a variable step approach with a BDF method of order 1 was chosen than when the step size was fixed for the same BDF method. However, when a BDF method of order 2 was used, variable step size cases took longer computation time than fixed step size cases, due to the small value that equation (3.15) gave to the step size, as it has been explained earlier.

Table 3.3 contains the average computational times for the step sizes of the BDF methods of order 1 and 2 cases more representatives. Variable step cases considered in this Table share constant $C = 0.9$ and a tolerance error of 10^{-5}. Fixed step cases have been averaged considering all tolerance error sub-cases, because this has been found not affect to the computational time.

TABLE 3.3: Comparison between all cases. Best average computation times

Step size (s)	Fixed step size		Variable step size	
	Order 1	Order 2	Order 1	Order 2
0.01	284.99	271.58	327.98	293.03
0.001	2047.81	2140.08	1241.37	2855.23
0.0001	21444.89	20903.18	1253.58	24699.80

The lowest accumulated error was obtained when the fixed step size approach was chosen along with a BDF of order 2. Figure 3.9 displays the accumulated errors for the same cases considered earlier. The accumulated error for any of the step sizes used was lower than 0.012 radians.

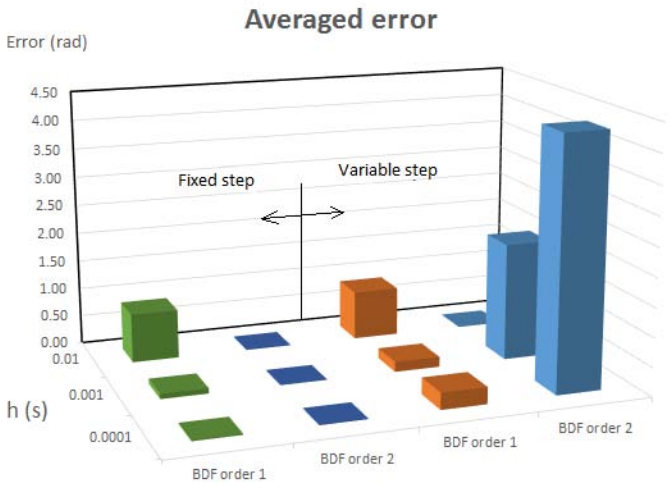

FIGURE 3.9: Averaged accumulated error. Step size vs Variable step

In terms of efficiency, Figure 3.10 displays the average values of efficiency both for the fixed and variable step cases. Variable step cases were averaged between all values of constant C, for cases that shared an error tolerance of 10^{-5}. As the efficiency of the case that shared a BDF method of order 2 with a variable step size was much worse than the others, Figure 3.10 has been duplicated to see at its right the rest of values without taking the bad result into account. It is clear that both, a low accumulated error and a low computational time, gave the best values of efficiency in the cases where a fixed step size was used along with a BDF method

of order 2. The reason why the same method did not provide such good results with a variable step size might be the way of calculating the size of the step (equation (3.15)), as it has been explained earlier.

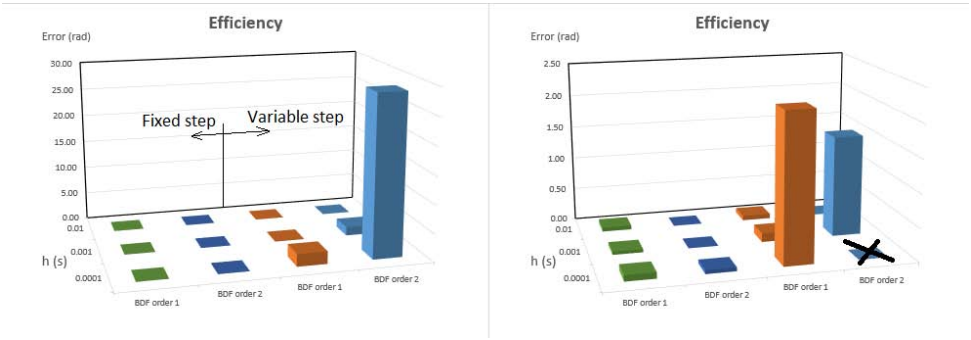

FIGURE 3.10: Efficiency levels. Step size vs Variable step

3.4 Discussion

In this work we have considered different ways of solving a system of nonlinear second order algebraic differential equations. We have used a backward differentiation formula to approximate the derivatives of the system, and we have analysed its implementation on fixed and variable step, to see the influence of its size. Among all possible combinations of computation cases, from the results obtained for the generalized coordinates most representative, we have seen that a BDF method of order 2 (see equation (3.16)), along with a step size of $0.01s$ solved the system of equations in the most efficient way for the cases where a fixed step size approach was used. However, when a variable step size approach was used, a BDF method of order 1 (see equation (3.16)) was the most efficient, avoiding the step size to reach values smaller than $0.001s$. The solutions achieved both with the step size approach and with the variable step size approach, in the cases mentioned earlier, provided high accurate results. Other ways of approximating the derivatives of the system and of calculating the size of the step may be used and compared with the ones analysed here, but that will be object of a future research.

Chapter 4

Kinematic and Dynamic analysis of a 3D multibody system applied to passively compensate horizontal accelerations in patient transportation

Abstract

The analysis of the kinematic and dynamic of a 3D multibody system that might act as support for the stretcher of a patient in an ambulance motivates this research. The system supports the stretcher and allows it to oscillate in a way that makes feasible to compensate passively the horizontal accelerations that act on the patient. The way in which the system oscillates influences the achievement of the rate of compensation of accelerations. It depends on the design of the system, which shares its kinematic with the articulated quadrilateral mechanism (AQM). Here, its design is analysed with regards to its kinematic and dynamic behaviour, considering how some of the parameters that form part of the system affect to the capabilities of the system to tilt the stretcher and also to its vibrational response. The analysis applies the Design of Experiments (DOEs) theory, in order to determine later the dimensions of the system more appropriate to achieve a specific rate of compensation of accelerations during its motion. Different designs of the system are obtained in order to achieve respectively a specific rate of compensation of accelerations under exposure to horizontal accelerations, in a range that can be experienced during driving conditions in an ambulance. The motion of the system is tested computationally with the software MSc Adams. The adequacy of the designs to be applied to transport patients is based on findings from previous researches focused on the effect that vibrations have on people who maintain seated postures, so further research is needed in order to test whether the motion achievable with this system is appropriate to people who maintain a recumbent supine posture.

4.1 Introduction

A 3D multibody system that shares its kinematic with an articulated quadrilateral mechanism (AQM) is designed with the aim of compensating horizontal accelerations passively. Passive systems used in railway transport [8] or road vehicles (see Robertson's or Parham's invents [16, 17]) share its kinematic with the (AQM). Here the design of the 3D multibody system is analysed for its particular

application to transport patients in a recumbent supine posture in ambulances. The system might be applied to compensate horizontal accelerations (measured in the plane of the stretcher) that acts on a patient who keeps a recumbent posture, when the vehicle negotiates curves (centripetal acceleration) or when it accelerates or brakes.

In an ambulance, the limited space available to install a stretcher and the required equipment that is needed for attending the patient, influence the way in which this multibody system can move the stretcher. European standards deals with the equipment and the design of the patient compartment of an ambulance and so with the supports of the stretcher [34, 35]. Hence, it is important to determine both the dimensions of the system and the design of the patient compartment in order to achieve an efficient behaviour of the system, accomplishing regulations. Here, the design of the patient compartment is not considered, it should be done once the system is completely defined following specific optimization techniques already used for these purposes [54, 55].

The dimensions of the system have been determined after applying the Design of Experiments (DOEs) theory to some of the parameters that form part of the model. The parameters considered have been the following: the distance between the horizontal plane that contains the joints of the bars' upper ends and the base of the system, when it keeps static equilibrium (Drb), the distance between the upper ends of the bars (contained in the plane where the width of the stretcher is measured) (p), the mass of the bars (m_b) and the mass of the assembly stretcher-person (m_s, it represents both the mass of the system and the patient).

The (DOEs) approach is often used by researchers when several parameters affect to the design and performance of a mechanical system (see [56, 57, 58, 59] for instance). The purpose of applying this approach is to guarantee that the system reaches a specific rate of compensation of accelerations during its motion (in terms of percentage with respect to the acceleration to be compensated). Results coming from these analysis have allowed to determine, from the parameters considered in the analysis, which parameters influence more the motion of the system.

For the designs obtained, the vibrational response of the system has been analysed considering its specific application to transport patients in road vehicles. It has been carried out computationally, with the software MSc Adams. The only external forces considered in this study are due to the lateral accelerations that appear during driving conditions through a conventional road as a consequence of the route followed by the vehicle (not to the irregularities of the terrain, it is considered that the road is flat and well maintained) and to gravity. The analysis and the computational simulations carried out with MSc Adams in this chapter have been focused on its lateral behaviour due to the limited space available in the interior compartment of the ambulance, but experimentation has been carried out with systems designed to compensate accelerations laterally and longitudinally (see annex A). Therefore, in chapter 3, which deals with the mathematical modelling of the equations of motion of the system, both directions have been considered).

Conclusions coming from these analysis along with the conclusions that come from previous researches focused on human vibrations (in what respect to motion sickness and discomfort), have allowed to hypothesise the specific geometry with which the system should be designed in order to be applied to transport patients. However, like the studies considered as a reference in the field of human vibrations are specifically focused on seated postures, further research must be carried out in order to determine whether the oscillatory motion achievable with this system is appropriate for transporting patients in a recumbent supine posture.

4.1.1 Multibody system

The system under study is formed by 6 rigid solids (a base, four bars and a supporting solid). All of them are linked to each other by mean of joints (ideally without friction and damping properties). One of the solids represents the vehicle where the system is installed, whose motion induces motion to the system (it is considered only as input of the motion for the system).

This study considers that the system achieves the desired rate of compensation of accelerations passively (no active systems intervene in its motion) and under steady conditions. To guarantee that the system does not vibrate indefinitely, two dampers are placed below the base of the system linking it with the floor of the vehicle. Their location is fixed there to allow ambulance staff walk around the stretcher without tripping on them.

Although the system is a 3D multibody mechanism (as it was considered in chapter 3 for the mathematical modelling of its equations of motion), due to limitations on the space available in the patient compartment of the ambulance and to limitations found during the experimentation stage related to this chapter with regards to the joints of type spherical (see annex A), its particular application to transport patients is restrained either to compensate lateral or longitudinal accelerations. Hence, one of the eight joints that link the bars with the base or with the roof of the vehicle must be a revolute joint aligned either laterally or longitudinally to allow the system to oscillate longitudinally or laterally, respectively. The rest of joints are either spherical joints or revolute joints equally aligned to the previous one. Figure 4.1 displays both configurations of the system.

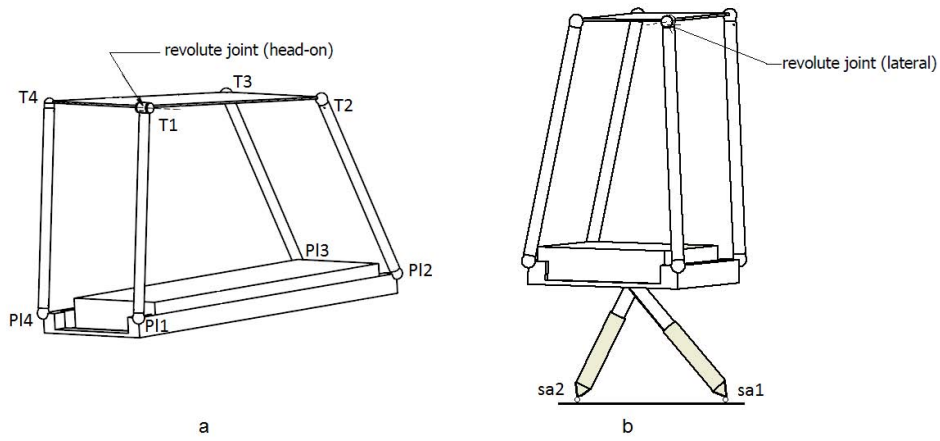

FIGURE 4.1: Longitudinal and lateral configurations

These configurations allow to reduce the motion of the spatial mechanism to the motion of a planar articulated quadrilateral mechanism (a double-crank four-bar mechanism), maintaining its properties and dimensions for some parts of the analysis considered here. It is a significative example useful to analyse and understand the effect that some parameters that belong to the design of the system have on its motion. Figure 4.2 displays the schematic parameterized design of the (AQM) that is going to be analysed here. For other applications, configurations equipped with spherical or cardan joints will require an additional analysis and experimentation.

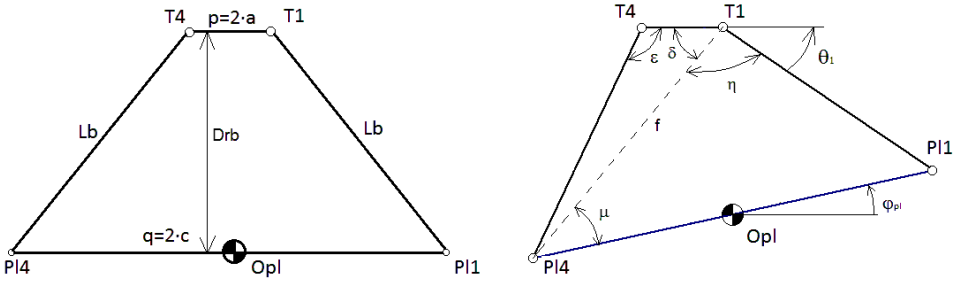

FIGURE 4.2: Reduced and parameterized system, lateral configuration (Figure 4.1.b)

The equations of motion of the (AQM) are:

$$p = 2 \cdot a \tag{4.1}$$

$$q = 2 \cdot c \tag{4.2}$$

$$f^2 = p^2 + Lb^2 - 2 \cdot p \cdot Lb \cdot \cos\varepsilon \tag{4.3}$$

$$Lb^2 = f^2 + q^2 - 2 \cdot f \cdot q \cdot \cos\mu \tag{4.4}$$

$$\delta = \arcsin \frac{Lb \cdot \sin\varepsilon}{f} \tag{4.5}$$

$$\mu = \pm \arccos \frac{Lb^2 - f^2 - q^2}{2 \cdot f \cdot q} \tag{4.6}$$

$$\theta = -\mu - \delta \tag{4.7}$$

where

- p represents the distance between the upper ends of the bars (contained in the plane where the width of the stretcher is measured)
- q represents the width of the stretcher
- Lb represents the length of the bars
- O_{pl} represents the centre of mass of the assembly stretcher-person
- Drb represents the height of the centre of mass O_{pl} with respect to the plane that contains the upper ends of the bars (measured when the system is in repose)
- θ_1 represents the tilting angle of the bar 1 (yaw)
- φ_{pl} represents the tilting angle of the base (roll)

The rest of parameters displayed in Figure 4.2 intervene in equations (4.3) - (4.8) for geometrical relationships. Figure 4.2 represents the configuration displayed in Figure 4.1.b. Equations (4.3) - (4.8) are referred to such configuration. For a longitudinal configuration parameters p and q are equal to $2 \cdot b$ and $2 \cdot d$, respectively and they represent the distance between the upper ends of the bars (contained in the plane where the length of the stretcher is measured) and the length of the

stretcher, respectively. What angle θ_1 represents does not change but the angle which represents the tilting angle of the base is θ_{pl} (yaw).

The width and length of the base of the system are fixed for the size of the stretcher so, the parameters to be determined are Drb and p, in order to allow the system to achieve a specific (selectable) rate of compensation of accelerations (RCA).

In this study the bodies that form part of the 3D multibody system are considered as rigid solids, their mass is concentrated in their centre of mass which coincides with its geometrical centre and their inertia tensors have values only in their principal axes. The inertia and mass of the solids that compound the system have been estimated taking into account the material of the solids (steel) and their geometry. Considerations with respect to friction between parts and transmission of vibrations between parts or the vehicle and the system are not considered. It requires further research and a more realistic approach in the design of the parts that make up the system including the vehicle. The focus of the research is on the capabilities of the system to compensate accelerations due to the oscillatory motion of its base, which depends on its design.

4.2 Methodology

4.2.1 Design of Experiments (DOEs)

The Design of Experiments (DOEs) approach allows to determine the behaviour model's sensitivity to variation of its dimensions. This technique avoids to carry out a big number of experimental tests with changes in the value of different parameters and it reduces simulation time [56, 57, 60].

Making use of the (DOEs) theory it was analysed the effect that parameters Drb, p, the mass of the bars m_b and the mass of the assembly stretcher-person m_s (it represents both the mass of the system and the patient) had on the tilting angle of the base φ_{pl} (θ_{pl} in the longitudinal configuration) and the displacement of the base Y_{pl} (both of interest for the study of its capabilities for compensating accelerations). Therefore, it was analysed the effect that these parameters had on the natural frequencies of the system f_n (of interest for the study of its vibrational response).

As it was introduced, the configuration analysed here was the lateral due to the limited space available in the interior of the patient compartment. Conclusions coming from the (DOEs) with regards to the effect that the variation on its dimensions and masses had on the tilting angle of its base, its displacement and on its natural frequency, are equally valid both for lateral and longitudinal designs .

A two factorial experiment 2^k type was chosen in order to understand the effect that variation in the parameters Drb and p (in the kinematic analysis) along with the mass of the assembly stretcher-person m_s and the mass of the bars m_b, had on the tilting angle of its base φ_{pl}, on its lateral displacement Y_{pl} and on its natural frequency f_n. Although the motion of the system is nonlinear, the range of variation of these parameters and the way in which its motion is tested, allows to use this type of DOEs. A higher factorial order (3^k, 4^k...) would have resulted in an increase of the number of experiments and in longer simulation time. This strategy consists of varying k factors together between two levels (one high and one low) in order to detect the effects that all possible combinations of the two levels of factors have on the variable objective. The estimation of their effect on the objectives is illustrated with the Pareto and/or normal probabilistic plots and the correlation between the factors and the objectives is measured through the Pearson coefficient [60].

The value of the parameters and their levels are listed in Table 4.1 both for the kinematic and dynamic analysis. In both cases, the width of the base of the system was fixed at 0.6 m and the weight of the assembly stretcher-person at 250 kg (both higher than the values considered in the standard, width = 0.55 ± 0.2 m, weight $\leq 150 + 51$ kg [61]). As the analysis of the effect that variation in the dimensions of the system had on the motion of the stretcher is equivalent for the lateral and longitudinal configuration (in terms of their effect), the dimensions listed in Table 4.1 correspond with the lateral configuration.

TABLE 4.1: Factors for the kinematic and dynamic analysis

Parameter	High level	Low level	Units	Analysis
p	0.595	0.02	m	Both
Drb	1.6	0.35	m	Both
m_s	250	0.1	kg	Dynamic
m_b	20	0.1	kg	Dynamic

Previously to introduce the methodology followed in both analysis, it is needed to clarify some reasoning followed in this study. When it is aimed to achieve a specific rate of compensation of a lateral acceleration a_H through roll oscillation, the relationship between the roll angle φ_{pl} and the rate of compensation RCA is:

$$RCA(\%) = 100 \cdot \frac{a_H - (a_H \cdot \cos\varphi_{pl} - g \cdot \sin\varphi_{pl})}{a_H} \tag{4.8}$$

Figure 4.3 displays a draft of this situation. equation (4.8) is used to calculate the theoretical angle with which the base of the system should be tilted in order to achieve a specific rate of compensation of accelerations RCA. Depending on the design of the system, the angle that the base adopts as it moves is either closer or further to the theoretical value given by this equation.

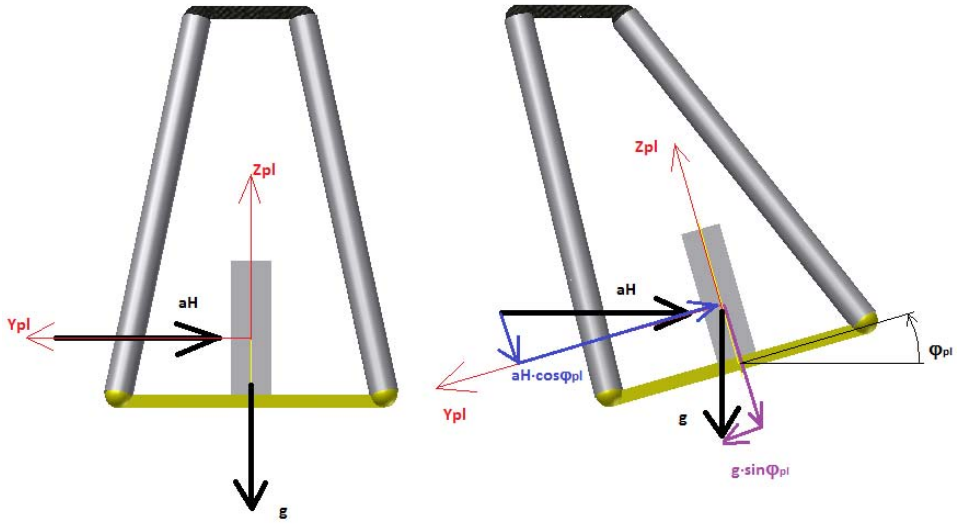

FIGURE 4.3: Diagram of forces during compensation of lateral acceleration

4.2.1.1 Kinematic analysis

The experiment consisted in evaluating equation (4.7) computationally having as inputs the parameters listed in Table 4.1 and angle ψ (see Figure 4.2). This (DOEs) approach analysed two factors (p and Drb) and two responses (φ_{pl} and Y_{pl}). The value of θ_1 varied so as to make the bar on the right side rotate in a counterclockwise sense until it was horizontal. Here was analysed the effect that variation of p and Drb have on φ_{pl} and Y_{pl}.

4.2.1.2 Dynamic analysis

From a simple one degree of freedom system formed by a hanging mass m attached to a cable of length L hanging like a pendulum, the influence on its natural frequency f_n of its mass m and the length of the cable L takes the form of equation (4.9) (considering that the amplitude of oscillation is small enough than $(\sin\phi \approx \phi)$, being ϕ the angle of oscillation).

$$\begin{aligned} \ddot{\phi} + \frac{g}{L}\phi = 0, \\ \phi = A\sin w_n t + B\cos w_n t, \\ f_n = \frac{1}{2\cdot\pi}\cdot\left(\frac{g}{L}\right)^{0.5} \end{aligned} \tag{4.9}$$

As the system can adopt configurations whose kinematic may differ from the kinematic of a pendulum, the (DOEs) approach was considered to detect how the variation in the dimensional parameters of the system along with in its mass and in the mass of its bars affected to its natural frequencies f_n. Specifically, a 2^4 factorial experiment was chosen. It analysed four factors (p, Drb, m_s and m_b) and one response f_n. MSc Adams calculates the modes of vibration of the system after linearizing its equation of motion [64]. The natural frequency of the system f_n considered here is the one obtained with MSc Adams.

4.2.2 Dimensional selection

Once that it has been analysed how the variation of the dimensions of the system affect to its motion, it is needed to choose a criterion on which the selection of the dimensions of the system is based.

- Achievement of a specific RCA
- Vibrational response appropriate for transporting people in a recumbent posture

On the one hand, its dimensions influence its kinematic and hence, the achievable rate of compensation of lateral accelerations. On the other hand, its dimensions along with the selection of its dampers influence its vibrational response.

The way in which the system oscillates is directly related to the discomfort experienced by the patient and to the likelihood of suffering motion sickness. Under the action of a force (during negotiation of a curve for example, the centrifugal force), ideally the system is going to oscillate until it achieves a steady equilibrium condition (situation in which it has been considered that the required RCA is achieved). However, like in reality there are more external forces (due to the irregularities of the terrain, aerodynamic forces...) that act on the vehicle, they are

going to excite the system making it to oscillate around its ideal dynamic equilibrium state (in which the (RCA) is achieved). Then the system is going to keep oscillating at a frequency very close to its damped natural frequency [53], so it should be desirable that this frequency was one at which the patient was less sensitive to the discomfort produced by horizontal oscillations.

Previous researches have found that when people are exposed to oscillatory motions at low frequencies and that the horizontal acceleration is compensated with roll oscillation, it is not recommended to achieve rates of compensation greater than 50% to avoid motion sickness [7] so, instead of designing a multibody system that shares its kinematic with a pendulum (where a rate of compensation of 100% might be achieved if it reaches its equilibrium position passively) the design proposed for the system should share its kinematic with an (AQM) (where rates of compensation are below 100%).

The motion achieved with an (AQM) combines roll and lateral oscillations. For seated postures, previous researches focused on the effect that pure roll, pure lateral and 100% roll-compensation of lateral oscillations have on passengers discomfort [4, 6] have concluded that the sensitiveness of the passenger to lateral accelerations is much lower when fully roll-compensation of lateral oscillations occurred at frequencies below about 0.63 Hz than under pure roll or lateral oscillations, and greater than under pure lateral oscillations at frequencies greater than about 0.63 Hz, increasing discomfort as frequency increases [4, 6]. It suggests that the system should dispose a natural frequency (a bit greater than the damped natural frequency of the system) less than this value in order to avoid that the system tends to oscillate at frequencies which may increase discomfort in patients. However, it may interfere with the likelihood of suffering motion sickness. When lateral accelerations are fully compensated through roll oscillation, the risk of suffering motion sickness increases with increasing frequency of oscillation in the range from 0.05 to 0.2 Hz and decreases with increasing frequency in the range from 0.315 to 0.8 Hz [70].

These findings come from studies focused on seated postures and have considered a rate of compensation of accelerations of 100%, but here they have been considered as a reference due to the lack of studies about compensation of lateral accelerations through roll oscillation at different rates for a recumbent supine posture.

4.2.2.1 Achievement of a specific RCA

The equilibrium position that the system has to reach coincides with the equilibrium position that the mass of the system concentrated in the middle point of its base would reach if it hung like a pendulum from the centre of rotation of the base CR at that instant. For a specific value of RCA and for a system with a base of width q, there are different configurations that satisfy equations (4.3) to (4.8), but once the length of the bars Lb are fixed, the value of p can be determined and vice versa. All configurations that can guarantee the achievement of a specific RCA have in common, at the moment of achieving their equilibrium position, that the centre of rotation of their base CR are aligned each other. Figure 4.4 displays two of them, obtained graphically. Configurations can be obtained also mathematically (from geometrical relationships between the coordinates of some characteristic points of the AQM and the centre of rotation of its base CR), but a graphic method is faster to solve the problem (mathematically some solutions have imaginary part and must be rejected).

Angle ϕ represents the angle that the pendulum has to rotate to reach its equilibrium position (where a rate of 100% compensation of acceleration exists). Angle φ_{pl} represents the required angle that the base has to be tilted to reach the specific RCA. Variation in parameters p and Drb are liable to the accomplishment of equations (4.3) to (4.8). As the system is configured with the kinematic of an (AQM) whose upper bar (p) is smaller than its lower bar q, for a value of p the value of Drb that satisfies these equations is unique (and vice versa).

Additionally to equations (4.1) to (4.8), to guarantee that the base of the system oscillates in the desired direction the conditions defined by equation (4.10) must be satisfied:

$$\begin{aligned} p &< q \\ 2\Delta Lb + p &> q \\ Lb &> \\ \sqrt{\left(\frac{q}{2}\right)^2 + \left(\frac{q}{2}\cdot\sin\varphi_{pl}\cos\phi\right)^2 - 2\cdot\frac{q}{2}\cdot\left(\frac{q}{2}\cdot\sin\varphi_{pl}\cos\phi\right)\cdot\cos\left(\frac{\pi}{2}-\phi+\varphi_{pl}\right)} & \end{aligned} \tag{4.10}$$

Equations (4.11) to (4.20) are used to find the configurations that have in common that the centre of rotation CR of their base are aligned each other, the width of their base q and the rate of compensation of accelerations RCA achieved when the system reaches its equilibrium position. These equations are referred to the position achieved by the system at the moment of reaching the specific RCA when it is in equilibrium, displayed in Figure 4.4.

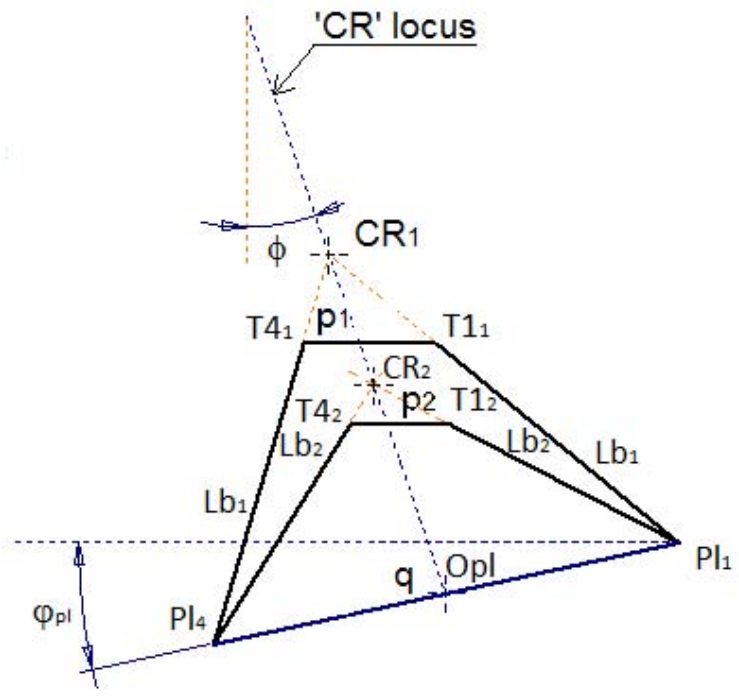

FIGURE 4.4: Different configurations that achieve a specific RCA

$$\frac{x - Pl4_x}{T4_x - Pl4_x} = \frac{y - Pl4_y}{T4_y - Pl4_y} \tag{4.11}$$

$$\frac{x - Pl1_x}{T1_x - Pl1_x} = \frac{y - Pl1_y}{T1_y - Pl1_y} \tag{4.12}$$

$$CR_x = \left(\frac{T1_x}{T4_y} \cdot \frac{(T4_y - Pl4_y) \cdot Pl4_x - Pl4_y \cdot (T4_x - Pl4_x)}{-(T4_x - Pl4_x) + \frac{(T4_y - Pl4_y) \cdot T1_x}{T4_y}} \right) \tag{4.13}$$

$$CR_y = \left(\frac{(T4_y - Pl4_y) \cdot Pl4_x - Pl4_y \cdot (T4_x - Pl4_x)}{-(T4_x - Pl4_x) + \frac{(T4_y - Pl4_y) \cdot T1_x}{T4_y}} \right) \tag{4.14}$$

$$\overrightarrow{v} = (0; 1) \tag{4.15}$$

$$\cos\varphi = \frac{\overrightarrow{CRO_{pl}} \cdot \overrightarrow{v}}{|\overrightarrow{CRO_{pl}}| \cdot |\overrightarrow{v}|} \tag{4.16}$$

$$d(Pl4T4) = t = \sqrt{((T4_x + q \cdot \cos\varphi_{pl})^2 + (T4_y + q \cdot \sin\varphi_{pl})^2)} \tag{4.17}$$

$$d(Pl1T1) = Lb = \sqrt{T1_x^2 + T1_y^2} \tag{4.18}$$

$$0 = T1_y - T4_y \tag{4.19}$$

Equations (4.11) to (4.12) are used to calculate the coordinates of the centre of rotation CR as equation (4.13) shows, and equations (4.15) - (4.19) serve to calculate the coordinates of point $T4$ and $T1$. After clearing $T4_y$ from equation (4.18) two solutions are obtained, but only one serves (4.20).

$$T4_y = \sqrt{-(T1_x - Lb) \cdot (T1_x + Lb)} \tag{4.20}$$

$$T4_y = -\sqrt{(-(T1_x - Lb) \cdot (T1_x + Lb)} \tag{4.21}$$

Substituting equation (4.20) in equations (4.15) and (4.17) and then, clearing $T4_x$ from equation (4.15) and substituting it in equation (4.17), the equation obtained relates the length of the bars Lb with $T1_y$, allowing to define accurately the geometry of the AQM. The new equation, (4.22), adopts a form that avoids $T1_y$ to be cleared directly, being needed iteration to find the value that accomplishes both the equation and the conditions that constraint the problem, equation (4.10).

$$T1_y = f(T1_y, Lb) \tag{4.22}$$

4.2.2.2 Vibrational response

Assessment of the dynamic behaviour of the system was carried out with the software MSc Adams, which formulates and solves the equations of motion of multibody systems through the Lagrangian Mechanics [62].

Simulation conditions

Three different conditions were tested in which the dimensions of the system were determined according to the results obtained previously with the (DOEs) approach (see section 4.2.2.1). The first condition was focused on the designs that guaranteed the achievement of a specific RCA. Three designs were obtained with which a RCA of 25%, 37.5% and 50% was respectively achieved. A system for achieving a greater RCA was not designed because of the problematic with the likelihood of suffering motion sickness. In the second and third condition the design

analysed was just the one with which a RCA of 25% was achievable, the mean value of the range of RCA below the limit in which the likelihood of suffering from motion sickness increases (50%).

The first condition analysed how the angle of the base of the system tilts in comparison with the theoretical angle that it should be tilted according to equation (4.8), when the lateral acceleration acts on it. A multi-run simulation was carried out in MSc Adams exposing the system in each run to a constant lateral acceleration (from 0 to 9.81 m/s^{-2}) in order to obtain, respectively, the angle tilted by the base of the system when it reaches its dynamical equilibrium position. This situation emulates the conditions to which the system would be exposed when the vehicle negotiates a curve with constant radius R_c at a constant velocity V_{veh} (after passing the transitory response). Under these conditions, the acceleration acting on the system is ($a_H = V_{veh}^2/R_c$).

The second condition analysed the transient oscillatory response of the system to the centripetal acceleration that appear when a vehicle negotiates a curve at constant velocity. Here different damping coefficients for its dampers were considered. The vehicle in which the system is installed followed the path displayed in Figure 4.5 at constant velocity, providing the system with a damping ratio of 0.2, 0.4, 0.6 and 0.8, respectively. Curves considered in this path were tangentially linked with straight sections without inserting transition curves among them, what resulted in exciting the system with a pure step-input signal of the centrifugal acceleration. Regulations consider that real road paths must contain transition curves avoiding such abrupt changes of centrifugal acceleration [65], so this simulation condition exposed the system to a situation sharper than it may experience in real roads.

During its transient response it was analysed how its damping ratio affected to its effectiveness for compensating accelerations (analysing the fastness with which the system reached the required tilting angle of its base for achieving the required RCA) and to its motion, with regards to the amplitude of its motion and some indicators of its damped response (peak time t_p, settlement time t_s and overshoot OS). The configuration of the 3D multibody system considered for the application to transport patients has four degrees of freedom (one associated to the spin on the longitudinal axis of the bars that own spherical joints in their ends and other associated to the oscillatory motion of the base, constrained by the revolute joint located at the upper end of one bar) but its response is dominated by the degree of freedom associated to the motion of its base. For a single-degree-of-freedom system with a transfer function like the one displayed in equation (4.23) these indicators are defined by equations (4.24) - (4.27) [63].

$$G(s) = \frac{K \cdot {w_n}^2}{s^2 + 2 \cdot \xi \cdot w_n \cdot s + {w_n}^2} \tag{4.23}$$

$$t_p = \frac{\Pi}{w_n \cdot \sqrt{1 - \zeta^2}} \tag{4.24}$$

$$t_s(2\%) \approx \frac{4}{w_n \zeta}, (\zeta \leq 0.88) \tag{4.25}$$

$$t_s(5\%) \approx \frac{3}{w_n \zeta}, (\zeta \leq 0.83), \tag{4.26}$$

$$\%OS = 100 \cdot e^{\frac{-\Pi\zeta}{\sqrt{1-\zeta^2}}} \tag{4.27}$$

The third condition considered low values of lateral accelerations experienced when a vehicle changes consecutively from on lane to another in a road. This motion is usually tested when studying the lateral stability control of a vehicle (see [66, 67] for instance). Like in previous conditions, it is analysed the relationship between RCA and a_H in time. The motion of the vehicle was simplified considering that it moved like a rigid solid. Simulations consisted on moving the solid that represents the hypothetical vehicle through a horizontal path as the one displayed in Figure 4.5, at different constant speeds (25 km/h, 45 km/h, 65 km/h and 100 km/h), without exceeding a yaw rate for the vehicle of 0.54 rad/s which is in the range of the ones analysed in previous research (see [66, 68]). Moving the vehicle in these conditions excited the system in a way that made it to oscillate at low frequencies (mainly at the frequency of its excitation force, because the irregularities of the terrain were not considered) and exposed it to low levels of lateral accelerations.

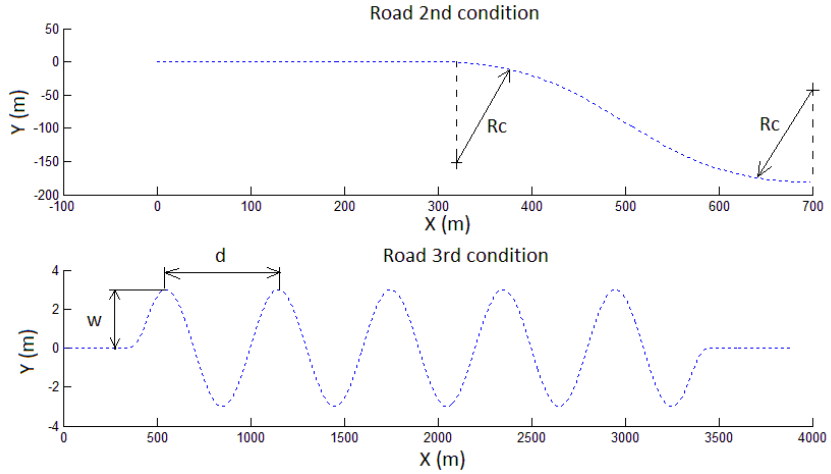

FIGURE 4.5: Paths followed by the vehicle in 2^{nd} and 3^{rd} simulation condition

Table 4.2 shows the value of the parameters of the last two simulation conditions.

TABLE 4.2: Parameters that define the simulations (referred to Figure 4.5)

Parameter	V_{veh}				Simulation condition
	25	45	65	100	
Rc (m)	-	-	-	250	2
w (m)	3	3	3	3	3
d (m)	177	232	285	350	3

where V_{veh} is the constant velocity of the vehicle, d is the distance driven by the vehicle in half manoeuvre of changing lane.

Transmissibility

Apart from these three conditions, it was analysed the effect of the damping ratio in the displacement transmissibility of the base of the system for this particular application to transport patients. The design of the system analysed here coincided with the RCA of 25%, like in the previous two simulation conditions. It was analysed in the range of frequencies between 0 - 10 Hz. The input displacement

was fixed at the geometrical centre of the roof of the vehicle, which coincides with the middle point between the upper ends of its bars, $T4_1$ and $T1_1$. The output analysed was the displacement of the centre of the base of the system, point O_{pl}. The transmissibility ratio (Tr) is defined by

$$Tr = \frac{Y_{pl}}{Y_v} \tag{4.28}$$

where Y_{pl} and Y_v are the displacement of the points O_{pl} and O_v, respectively. The assessment of the transmissibility has considered the input signal for the displacement of point Y_v defined by

$$Y_v(t) = Amp \cdot sin(2 \cdot \Pi \cdot freq \cdot t) \tag{4.29}$$

where Amp is the amplitude of the displacement, fixed at 50 mm, $freq$ is the frequency of the oscillation (between 0-10 Hz) and t is time.

The study of the displacement transmissibility allows to visualize the natural frequency of the system, in which the transmissibility of the displacement is maximized, determine the frequency from which the system reduces its oscillation and the effect of the damping ratio on the displacement transmissibility.

4.3 Results

4.3.1 DOES results

4.3.1.1 Kinematic analysis

The Pearson correlation coefficient obtained in the (DOEs) for φ_{pl} and p, ($\rho_{p,\varphi_{pl}} = -0.927$), indicates that parameter p has a clear effect on tilting the base whereas parameter Drb does not. Pearson coefficient sign indicates that its effect is opposite to the response, the bigger is p the less can tilt the base of the system. Figure 4.6 displays the main effects graph (left side) and the Pareto diagram (right side) for the tilting angle of the base, φ_{pl}.

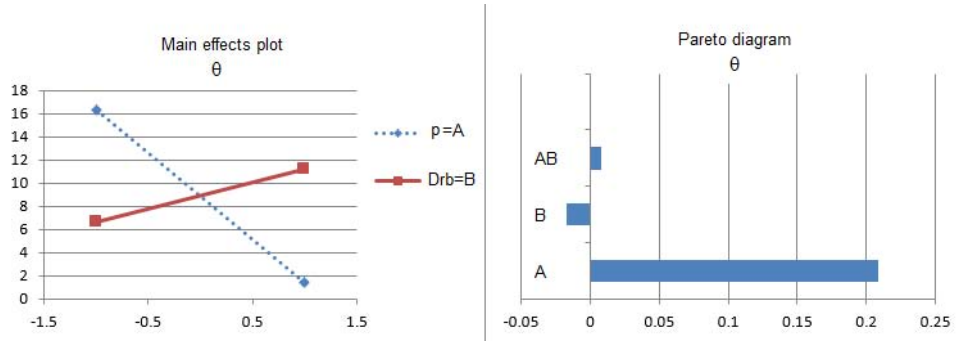

FIGURE 4.6: Effect of factors on φ_{pl}

Unlike that occurs with φ_{pl}, the factor that major effect has on the displacement of the base Ypl is parameter Drb, the bigger is Drb the bigger is the displacement ($\rho_{p,\varphi_{pl}} = 1$).

Parameters p and Drb affect directly to the capabilities of the system for compensating accelerations and also to the stability of the vehicle. Figure 4.7 displays the percentage of variation of the height of the centre of mass of the system

as φ_{pl} increases. It is desirable to obtain the required tilting angle of the base without lifting in excess its centre of mass, so as to avoid that the motion of the system overturns laterally the vehicle.

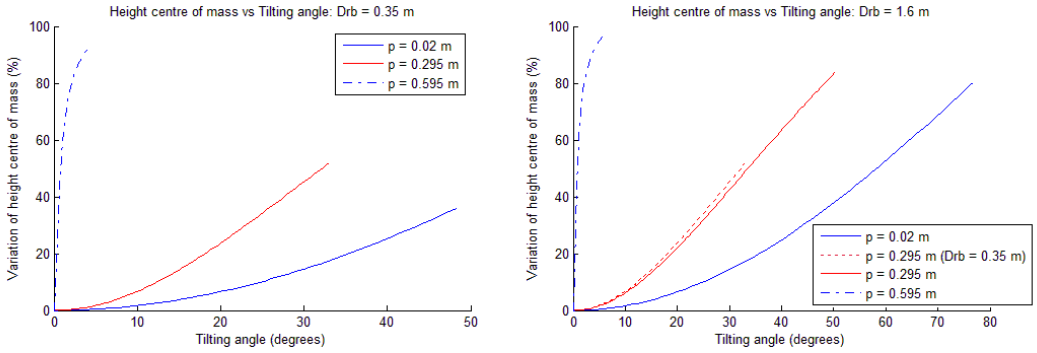

FIGURE 4.7: Variation of the height of the centre of mass of the system as φ_{pl} increases

Low values of p minimize Y_{pl} and maximize φ_{pl}, what results in a system with high capabilities of compensation of accelerations. Additionally, low values of p contribute to reduce the variation of the height of the centre of mass of the system, decreasing this variation slightly for high values of Drb. Both graphs include an intermediate condition for $p = 0.295m$.

4.3.1.2 Dynamic analysis

Findings from the (DOEs) corresponded with the behaviour of equation (4.9). Parameter Drb is the parameter that major effect has on f_n, followed by its interaction with p and then p. As Drb decreases, the natural frequency of the system increases, but natural frequencies are greater for greater values of p. The normal probabilistic graph displayed in Figure 4.8 displays the effects that are more significant, they are not aligned with the non significant effects.

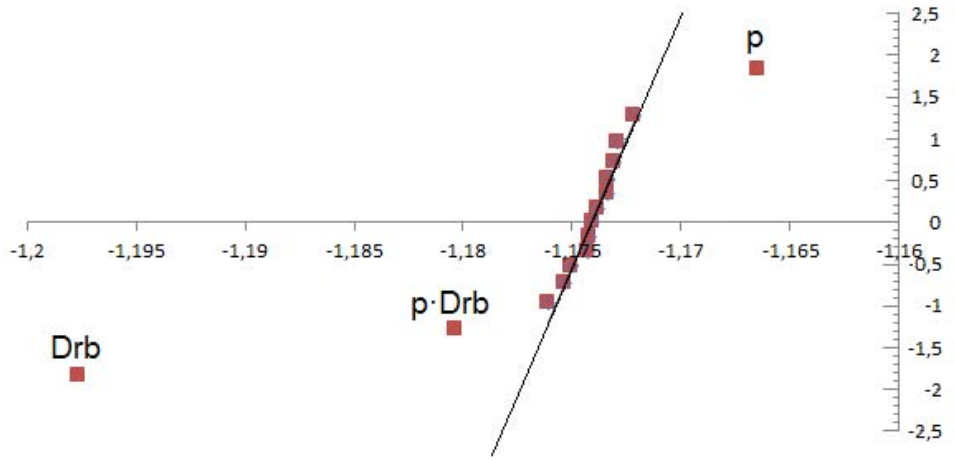

FIGURE 4.8: Normal probabilistic graph. Effect on the natural frequency of the system

The effect of both masses on the natural frequency of the system is not significant. Figures 4.9 and 4.10 display variation of the natural frequency as masses vary between the limits considered in the DOEs. Both figures support that the results coming from the (DOEs) are reliable.

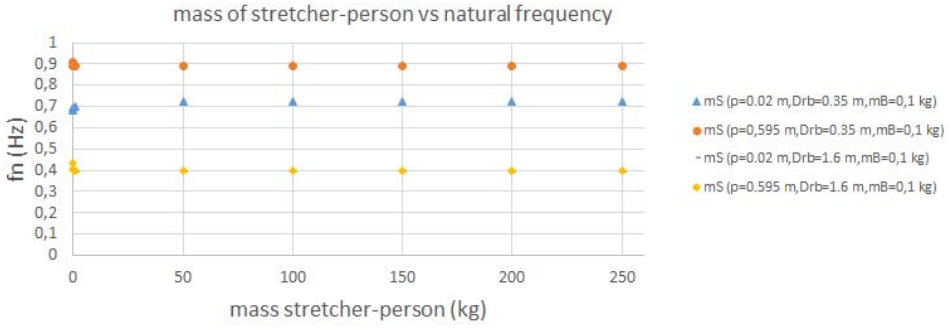

FIGURE 4.9: Natural frequency non-dependence from m_s

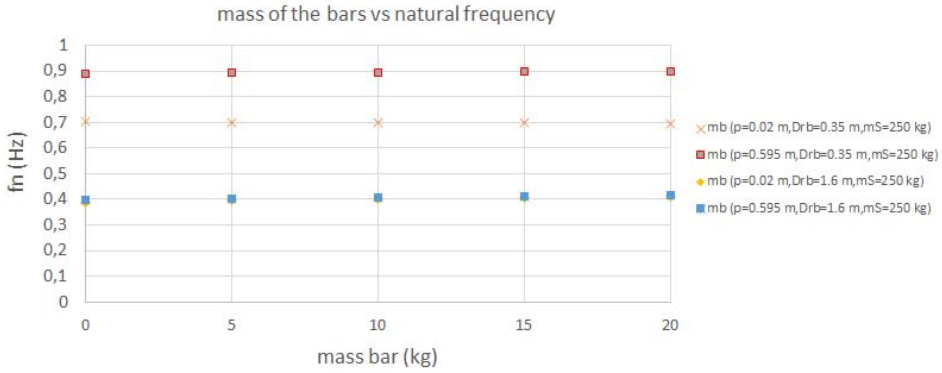

FIGURE 4.10: Natural frequency non-dependence from m_b

4.3.2 Dimensional selection

As it was introduced in section 4.2.2.1 there are multiple designs that allow to reach a specific (RCA) (see Figure 4.4), however it is required to fix either p or Drb in order to determine the complete design of the system (q is fixed by the width of the stretcher).

The parameter Drb represents the available space that the patient disposes above the plane of the stretcher for reclining his body. The value of Drb considered here for the design of the system should be of at least 0.7 m.

Increasing the value of Drb decreases the natural frequency of the system. With a value for Drb of 0.7 m, the natural frequency of the system is around 0.6 Hz, so greater values of Drb result in designs with a smaller natural frequency, what increases the likelihood of suffering motion sickness, apart from reducing the available space for the stretcher to oscillate. This frequency is below the frequency at which discomfort increases for fully compensation of lateral oscillations (0.63 Hz) and it is in the conservative side of the range of frequencies in which the likelihood of suffering motion sickness decreases.

4.3.2.1 Achievement of a specific RCA

Once that the value of Drb was fixed, the value of p was determined in order to achieve a specific rate of compensation of accelerations. Knowing that high values of p decrease the tilting capabilities of the base of the system, Table 4.3 contains the greatest values of p needed to achieve a specific rate of compensation of accelerations RCA under exposure to an acceleration $a_{max} = 3.08 m/s^2$ (i.e. achieved when cornering a curve of Radius of 250 m at constant speed of 100 km/h). They were obtained through iteration, accomplishing equations (4.1) to (4.22).

TABLE 4.3: Optimized dimensions for different RCA

RCA ($\%$)	p (m)	Drb (m)	fn (Hz)	φ_{pl} ($^\circ$)	Width (m)
50	0.29	0.7	0.6	8.83	1.02
37.5	0.37	0.7	0.6	6.65	1.01
25	0.45	0.7	0.6	4.46	1.01

Changes in p, coming from the requirement of achieving a specific RCA, does not alter significatively the natural frequency of the system.

4.3.2.2 Vibrational response

Variation of the tilting angle of the base with lateral acceleration. 1^{st} simulation condition

The three configurations designed to reach a specific RCA (see Table 4.3) were exposed to different accelerations until they reached a steady equilibrium state. The angle tilted by the base of the system was compared with the theoretical angle with which the base should be tilted to reach this RCA (see equation (4.8)). Figure 4.11 displays, for each configuration, the effectiveness of the system in reaching the angle required for achieving a specific RCA. A green dash-equipped vertical line marks the value of the lateral acceleration considered as reference during the design of the system (see section 4.3.2).

For all RCA conditions, the configurations tested reached very accurately the angle required to compensate lateral accelerations. At lateral accelerations greater than the reference value (green dash-equipped vertical line in Figure 4.11), the system under-compensated the lateral acceleration acting on it. This difference is mainly due to the value of Drb. Additionally, leaving apart the requirement of the available space above the stretcher ($Drb \geq 0.7$ m) and also under the criteria of achieving a specific RCA, different configurations were tested varying Drb. Figure 4.12 displays that for a fixed width of the base q, the smaller is Drb the bigger is the difference between the required angle and the angle reached by the base for accelerations greater than the reference value.

Selection of dampers. 2^{nd} and 3^{rd} simulation conditions

The transient response of the system was analysed exposing the system to a step-input lateral acceleration of 3.08 m/s^{-2}, equivalent to a situation in which a vehicle negotiates a curve of radius of 250 m at a constant speed of 100 km/h. Table 4.4 contains the parameters that characterize its response, presented previously in section 4.2.2.2. Figure 4.13 displays the tilting angle of the system for each simulation condition along with the lateral acceleration measured in the plane of the base of the system.

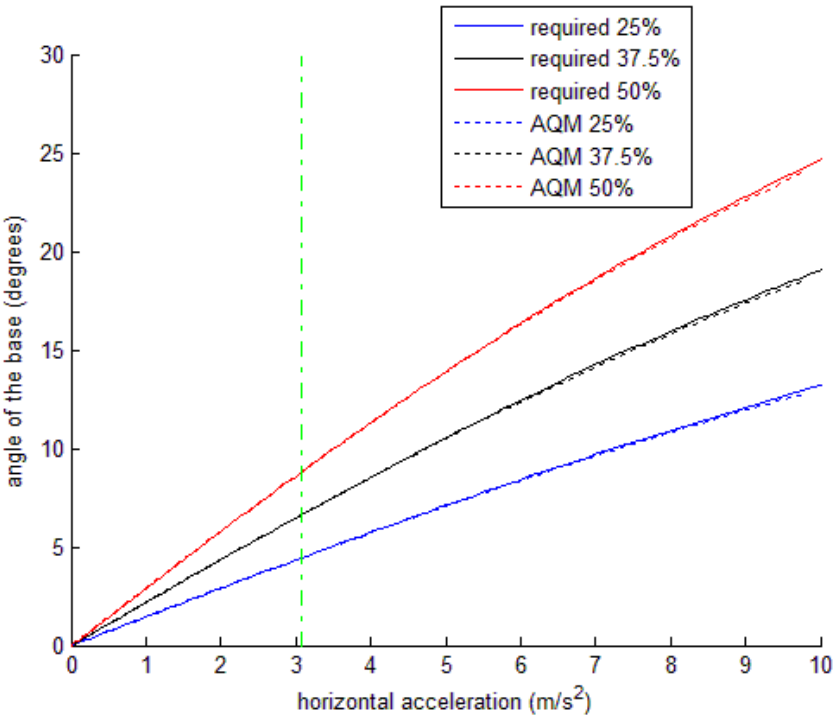

FIGURE 4.11: Tilting angle of the base vs Lateral acceleration for different RCA

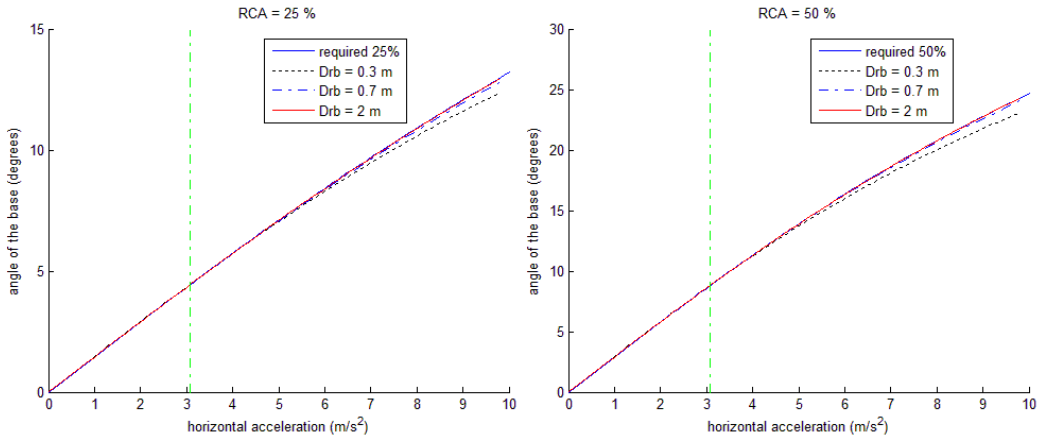

FIGURE 4.12: Differences in the achievement of the tilting angle required to compensate a specific RCA.

The smaller is the damping ratio the bigger is the overshoot of the response. On the contrary, the settlement time decreases as the damping ratio increases. The assessment of the vibrational response of the system under exposure to low frequencies lateral oscillations (third condition, as mentioned in section 4.2.2.2) revealed that the system is not capable of reaching the required angle for achieving fast enough the specific RCA for which it has been designed when it is configured with a high damping ratio. Figures 4.14 and 4.15 display how the tilting angle of the base varies as the centrifugal acceleration acts on it during the manoeuvres.

TABLE 4.4: Characteristics of the transient response when the system is exposed to a step-input acceleration

Damping ratio $-$	Damping coefficient (Ns/m)	Peak time (s)	Settlement time (s)	Overshoot $(\%)$	Amplitude $(degrees)$
0.2	530	0.82	5.22	51.28	8.15
0.4	1070	0.92	2.61	22.25	6.69
0.6	1600	1.02	1.74	7.26	5.68
0.8	2115	1.52	1.30	0.56	5.37

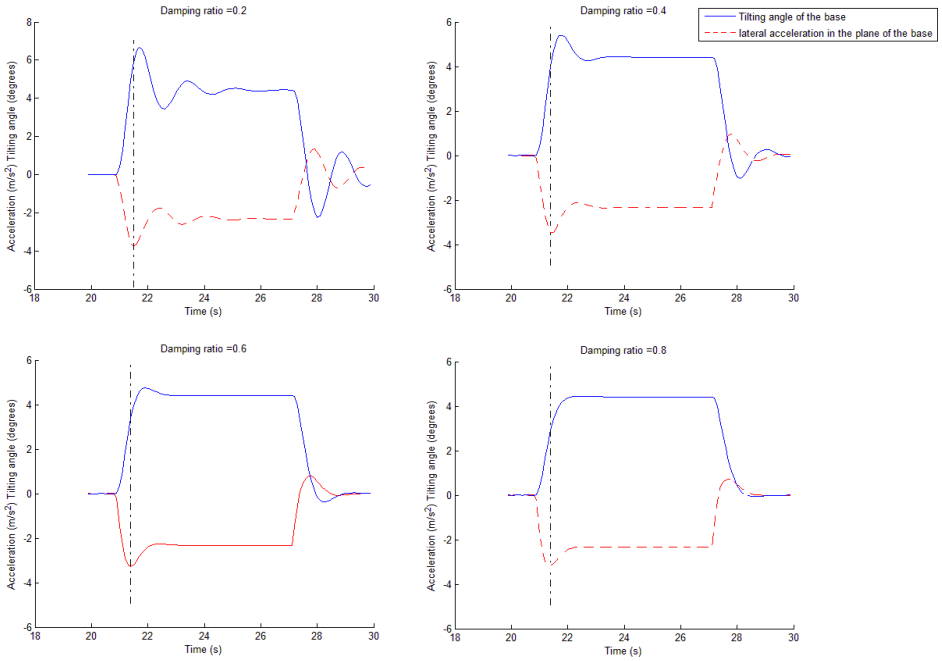

FIGURE 4.13: Transient oscillatory response of the system under a step-input lateral acceleration

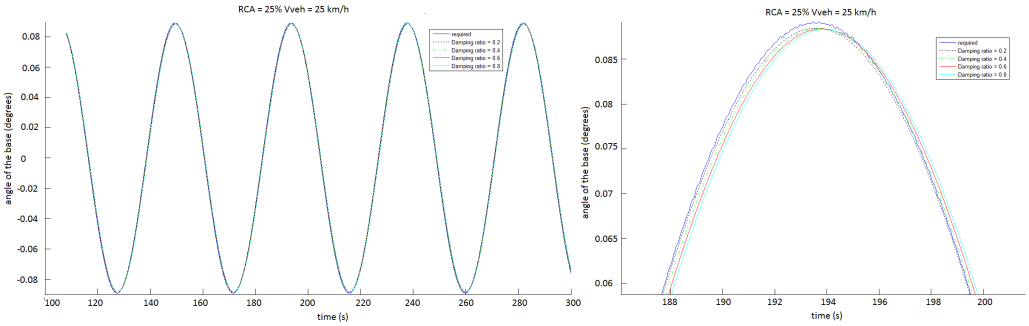

FIGURE 4.14: Transient oscillatory response of the system during the manoeuvre of changing consecutively from on lane to another in a road. Constant velocity of 25 km/h

At the beginning of the curve, the system has an under-compensator behaviour and over-compensator when the vehicle turns back to the original lane. Therefore, there is a lag between the response of the system and the input, as it occurred in

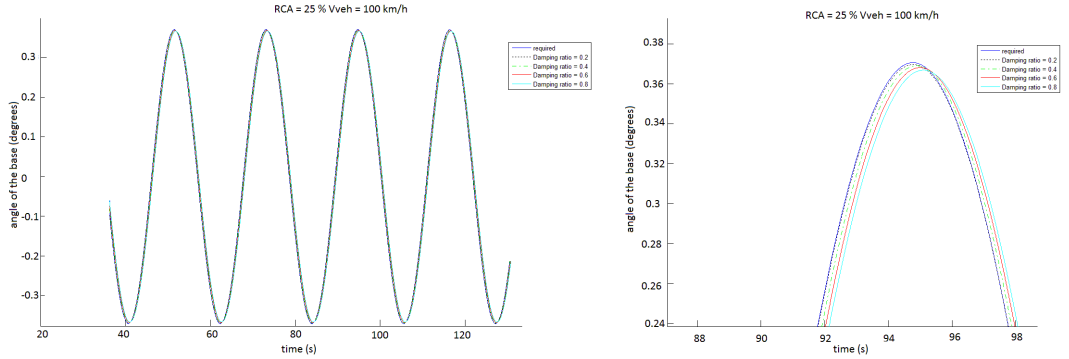

FIGURE 4.15: Transient oscillatory response of the system during the manoeuvre of changing consecutively from on lane to another in a road. Constant velocity of 100 km/h

passive systems used in rail transport [8], due to the inertia of the system and to the damped motion of its base. This lag is minimized for small values of damping ratios.

Transmissibility

The analysis carried out about how the displacement of the support of the system is transmitted to its oscillatory base shows that if the system is excited at frequencies greater than 0.85 Hz (this frequency is $\sqrt{2}$ times greater than the damped natural frequency of the system) the transmissibility of the displacement decreases. The peak of transmissibility appears at the natural frequency of the system for the case in which damping do not exist, as Figure 4.16 displays, and at the damped natural frequency of the system for the rest of cases.

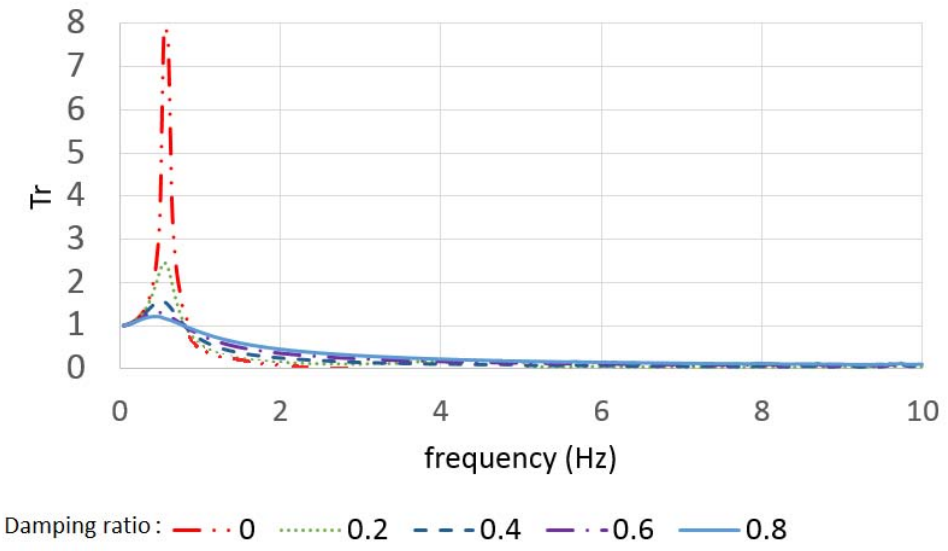

FIGURE 4.16: Displacement Transmissibility graph

The damping ratio of the system reduces the transmission of the displacement at frequencies less than 0.85 Hz, increasing transmissibility as the damping ratio is decreased, and it produces an opposite effect above such frequency. Nevertheless, at frequencies greater than 0.85 Hz the displacement transmissibility is less than 1 so

the system attenuates vibrations. The value of 0.85 Hz from which the displacement transmissibility of the system is attenuated is within the range of frequencies considered in the studies taken as a reference about the effect that different types of oscillations had on the discomfort of seated people.

4.4 Conclusions

This study has served to analyse how the motion of the system is affected by its dimensions and by the characteristics of its dampers. The design of the system has been particularly focused on its application to transport patients, and it has been influenced by conclusions coming from previous researches about motion sickness and discomfort experienced by people who maintain a seated posture.

The kinematic and dynamic of the system have been analysed theoretically and computationally, resulting in several findings that have influenced its design. As the rate of compensation of accelerations should remain below 50%, the system has been designed to move like an articulated quadrilateral mechanism. Keeping this particular geometry, the dimensional parameter that major effect has on the tilting capabilities of the base of the system is p whereas parameter Drb influences more the natural mode of vibration of the system.

In the range of accelerations for which the system is expected to work efficiently (up to $3.08\ m/s^2$), the system has obtained a good and accurate motion for its base, what has resulted in an achievement of the required rate of compensation of accelerations. The dimensions selected have resulted in a design that provides the system with a natural frequency that might be appropriate to transport patients, reducing the risk of suffering motion sickness and preventing discomfort. Under step-input excitations, the damping ratio that has provided a good vibrational response to the system is 0.6, allowing the system to achieve an intermediate behaviour in terms of lag in its response and in its effect for under/over compensate accelerations. Small damping ratios have been appropriate in low frequency oscillatory motions, however they have provided the system with high values of overshoot in its response when a step-input acceleration has excited it.

This analysis has not considered the effect that components of the system such as the foam of the stretcher, the links between the parts of the system and between the system and the vehicle or even the structure and stiffness of its components have on its vibrational response, including transmission of vibrations. This should be done building a prototype of the system, characterizing these new components and disposing of a vehicle similar to an ambulance in order to correlate the theoretical and computational results with the experimental ones.

Previous researches about motion sickness and discomfort have detected which motions are not appropriate for people in seated postures but not for people in recumbent postures. In order to verify that the motion achievable with this system is appropriate for people in a recumbent posture, experimentation in accord with the experiments carried out for seated postures should be done.

Chapter 5

Experimental analysis of the discomfort caused by lateral, roll and different rates of roll-compensation of lateral oscillations in recumbent people

Abstract

The study presented in this chapter intends to fulfill two goals: First, supplement previous studies that analysed the effect that fully roll-compensation of lateral oscillation, lateral oscillation and roll oscillation had on the discomfort of seated people, considering now a recumbent supine posture. Secondly, serve as an indicator for the design of a 3D multibody system focused on the passive compensation of horizontal accelerations that act on patients while they are transported in an ambulance. For the later, it has been added to the study a type of oscillation, 25% roll-compensation of lateral oscillations. The conclusions of the study are referred to the later goal, due to its relationship with chapter 4 of this thesis.

5.1 Introduction

5.1.1 Context

The experiment presented in this chapter was carried out at the Institute of Sound and Vibration Research at the University of Southampton, in the United Kingdom, in a research stay that lasted three months during the course of this thesis. In the previous chapter, the design of a 3D multibody system was analysed in order to reach a specific rate of compensation of horizontal lateral accelerations during its oscillatory motion. This system is aimed to be applied to transport patients in ambulances. Whether this design is appropriate for transporting patients in a recumbent supine posture was hypothesised on the basis of findings from previous researches that analysed the effect that different types of oscillations have on people who remain in seated postures. To supplement such findings, in this chapter it is analysed the effect that different types of oscillations have on the discomfort of people who maintain a recumbent supine posture.

5.1.2 Previous research

Low frequency lateral, roll and roll-compensated lateral oscillations can be experienced during road or rail transport and they can provoke discomfort and motion sickness on passengers [71]. Low frequency lateral oscillations can appear as a consequence of cornering in cars [72] and tilting in trains. In trains, roll-compensation of lateral oscillations is used to reduce the effect that lateral centripetal acceleration has on the dynamics of the coach. An increase of the speed of the vehicle increases the lateral acceleration during cornering. An appropriate tilt of the carriage can reduce the lateral acceleration measured in the plane of a passenger seat [8]. Recent studies have investigated the effect that low frequency lateral, roll and roll-compensated lateral oscillations have on the discomfort of seated passengers [4, 5], taking into account also the inclination and height of the seat backrest [6]. However, there are not yet studies that investigate the discomfort caused by lateral vibration of recumbent people, such as can occur when ambulances travel around bends.

Common systems used in Europe to transport patients in ambulances consider that the stretcher is fixed and completely restrained to the vehicle, avoiding it to move [34], however other countries like Japan have developed systems that allow patient stretchers to roll-compensate lateral accelerations that act on patients when the vehicle negotiates curves [36]. Roll compensation of lateral accelerations might benefit patients, especially those who have fractures in their limbs. A reduction of inertial forces has been proved to be beneficial for patients who suffered from cardiac or chest medical problems [30, 31, 32, 33], so it might be also for patients with injuries in their flanks, relieving them from some pain that can experience during transport.

Previous studies have found that fully roll-compensated lateral oscillations provoke less discomfort than pure lateral and roll oscillations at frequencies less than about 0.5 Hz in a sitting posture. However pure lateral oscillations cause less discomfort than fully roll-compensated at frequencies greater than about 0.5 Hz [4]. Backrest height also affects discomfort at low frequencies of oscillation, reducing discomfort caused by lateral oscillations at frequencies less than 1 Hz, less than 0.63 Hz for roll oscillations, and between 0.4 and 0.63 Hz when lateral oscillations are compensated with roll oscillations [6]. Additionally, in roll and fully roll-compensated lateral oscillation, the position of the centre of rotation affects the perception of discomfort because it alters the magnitude of acceleration perceived in different parts of the body [73].

The objectives of this experiment were to investigate the effect that frequency, magnitude and the rate of roll compensation of lateral oscillations have on physical discomfort caused by lateral oscillation, roll oscillation and roll-compensated lateral oscillation, for a person lying in a recumbent position. Therefore, there are other factors that influence motion sickness and discomfort (mentioned in chapter 2 [26, 27]) but here, like in the studies considered of reference, were considered only the type of oscillation, its frequency and the rate of compensation of accelerations. Additionally to investigate the discomfort caused by lateral vibration of recumbent people, this study has served as an indicator of reference in the design of a 3D multibody system focused on compensating accelerations passively, specifically for its possible application to transport patients in ambulances. With the results of this study it was intended to determine whether the motion of the 3D multibody system, capable of roll-compensating lateral oscillations at a different rates, could be beneficial for transporting patients in a recumbent posture. Here RCA values of 25% and 100% were tested. The value of 25% coincided with the mean value

of the range of RCA below the limit in which the likelihood of suffering from motion sickness increases (50%). The rate of 100% is the value analysed in previous researches mentioned previously. Other rates of compensation were not tested due to the work required to carry out the experiment and the limitation of the duration of the research stay.

5.1.3 Hypothesis

Considering the results found in previous researches focused on seated postures (Beard and Griffin, 2013 and 2016), the hypotheses of the experiment referred to the motion of the 3D multibody system were:

- At frequencies less than 0.5 Hz, with 25% roll-compensation of lateral oscillations, discomfort is less than with uncompensated lateral oscillation.
- At frequencies greater than 0.5 Hz, with 25% roll-compensation of lateral oscillations, discomfort is less than with fully-compensated lateral oscillation.

5.2 Method

5.2.1 Apparatus

Motions were produced by a six-axis motion simulator in the Human Factors Research Unit of the Institute of Sound and Vibration Research at the University of Southampton. The limits of motion for the simulator were: ± 0.5 m vertical motion, ± 0.25 m horizontal motion, and about $\pm 20^o$ of rotational motion. Subjects lay on a rigid stretcher positioned so that its half longitudinal plane was aligned with the half longitudinal plane of the motion platform (approximately 2.5 m by 3.0 m). The centre of rotation of the stretcher was located at 0.51 m above the platform and aligned with the half longitudinal plane of the stretcher. The stretcher consisted of a rigid flat horizontal surface (190 by 60 cm) located 50 cm above the platform surface. A rigid stretcher was used instead of cushioned stretcher so that the conditions could be repeated in other studies. Figure 5.1 displays the stretcher, its relative position with respect to the platform and the posture of one participant during the experiment.

Subjects were asked to maintain a comfortable supine recumbent posture ensuring full contact with the stretcher, with their eyes closed and with their hands on their tummy. Subjects wore three loose lap belts for safety, located at their chest, hip and ankle. During motion exposure, subjects wore headphones producing white noise at 65 dB (A) in order to mask the sounds of the simulator. The experimenter communicated with subjects through a microphone connected to the headphones by interrupting the white noise.

5.2.2 Experimental design

The experiment used a repeated measures (within-subjects) design to obtain ratings of discomfort. Subjects were exposed to a series of motion stimuli and used the method of magnitude estimation to rate discomfort produced by lateral oscillations, roll oscillations, fully roll-compensated lateral oscillations, and 25% roll-compensated lateral oscillations (i.e. the test stimuli) relative to the discomfort produced by a lateral oscillation (i.e. the reference stimulus).

FIGURE 5.1: Stretcher and its position with respect to the platform

5.2.3 Method of magnitude stimation

At the beginning of each session, subjects were instructed to rate the physical discomfort provoked by each stimulus with the method of absolute magnitude estimation using a set of practice motions (covering all three directions of oscillation at the lowest and highest magnitudes - see section 5.2.4). This method involves assigning a value to the test stimuli, in proportion to the magnitude of discomfort caused by the stimuli.

5.2.4 Motion stimuli

The motion stimuli consisted of seven frequencies at the preferred one-third octave centre frequencies from 0.25 to 1.0 Hz. The acceleration magnitude of the vibration to which subjects were exposed was expressed in terms of the root-mean-square (r.m.s.) value, as International Standards such as ISO 2631-1 recommend [69]. This represents the square root of the average value of the square of the acceleration record (Equation (5.1)). Each frequency was presented at, nominally, eight magnitudes in logarithmic series from 0.08 to $0.40\ ms^{-2}$ r.m.s. Due to simulator limitations, for all four types of oscillation only five magnitudes (0.08 - $0.20\ ms^{-2}$ r.m.s.) were presented at 0.25 Hz, seven magnitudes (0.08 - $0.315\ ms^{-2}$ r.m.s.) were presented at 0.315 Hz, and eight magnitudes (0.08 - $0.40\ ms^{-2}$ r.m.s.) were presented at all other frequencies (0.4 - 1 Hz).

$$a_{rms} = \sqrt{\frac{1}{T} \cdot \int_{T}^{0} a^2(t)dt} \tag{5.1}$$

For roll oscillation, the magnitude was defined by the acceleration in the plane of the stretcher (i.e., acceleration due to gravity g). For fully roll-compensated lateral oscillation, the lateral oscillation and the roll oscillation were combined in phase such that the resultant acceleration in the plane of the stretcher was zero, for 25% roll-compensated lateral oscillation, the lateral oscillation and the roll oscillation were combined in phase such that the resultant acceleration in the plane of the stretcher was 75% of the horizontal lateral acceleration acting on the stretcher. The directions of accelerations were displayed in Figure 5.2. All accelerations were in the YZ plane (reference system associated to the earth).

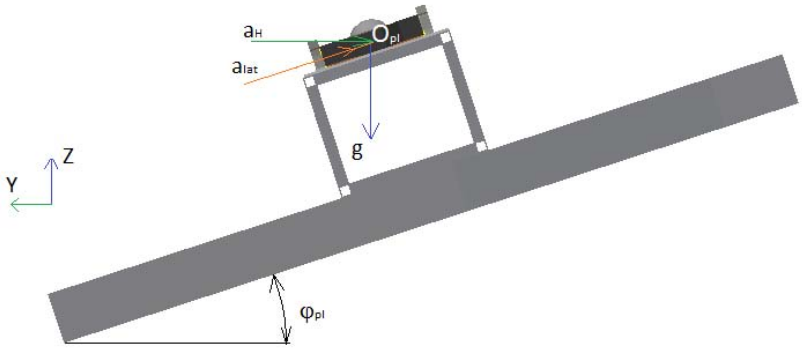

FIGURE 5.2: Direction of accelerations associated to motion stimuli

Roll oscillation, fully-compensated lateral oscillation, and 25% roll-compensated lateral oscillation were generated with respect to the lateral oscillation waveform. The lateral acceleration waveform was a transient waveform with a 3.5 cycle duration (as displayed in Figure 5.3) generated from the product of a sine wave of the desired frequency and a half-sine of the same duration. This motion was generated within MATLAB (version R2010a research) using the HVLab toolbox (version 1.0). This waveform represents the magnitude of the lateral acceleration measured in the plane of the stretcher that was experienced by subjects, in the time domain. For roll oscillation, the magnitude of the angle of roll (φ_{pl}) required so as that the motion of the simulator was capable of accomplishing the condition with the magnitude of lateral acceleration measured in the plane of the stretcher coinciding in time with the magnitude of lateral acceleration generated for lateral oscillation, is defined by

$$\varphi_{pl}(rad) = sin^{-1}\frac{a_{lat}}{g} \tag{5.2}$$

In Figure 5.2, the waveforms displayed for 0.5 Hz oscillation of the magnitude of acceleration measured in the plane of the stretcher (a_{lat}) for lateral oscillation and roll oscillation coincide in magnitude but differ in sign. For oscillations with a different rate of compensation of accelerations (RCA) such as fully roll-compensated and 25% roll-compensated lateral oscillations, the magnitude of the angle of roll required to compensate a specific magnitude of horizontal lateral acceleration (a_H) acting on the stretcher satisfied equation (5.3). The magnitude of horizontal lateral acceleration measured in the ground (a_H, absolute reference) coincided in time with the magnitude of lateral acceleration generated previously for lateral oscillation.

$$RCA(\%) = 100 \cdot \frac{a_H - (a_H \cdot \cos\varphi_{pl} - g \cdot \sin\varphi_{pl})}{a_H} \tag{5.3}$$

RCA represents the percentage of the horizontal lateral acceleration (a_H) that acted on the plane of the stretcher, considering that the magnitude of the lateral acceleration measured in the plane of the stretcher (a_{lat}) was composed by the acceleration due to gravity ($g \cdot \sin(\varphi_{pl})$) and the acceleration due to the horizontal motion of the simulator ($a_H \cdot \cos(\varphi_{pl})$). The magnitude of angle of roll (φ_{pl}) required so as that the motion of the simulator was capable of accomplishing the

condition defined by equation (5.3) was obtained through iteration. This procedure resulted in the waveforms illustrated in Figure 5.3. It displays the acceleration waveform measured in the plane of the stretcher (a_{lat}) for lateral oscillation, roll oscillation, fully roll-compensated lateral oscillation, and 25% roll-compensated lateral oscillation at 0.5 Hz and magnitude of $0.4\ ms_{-2}$ r.m.s.

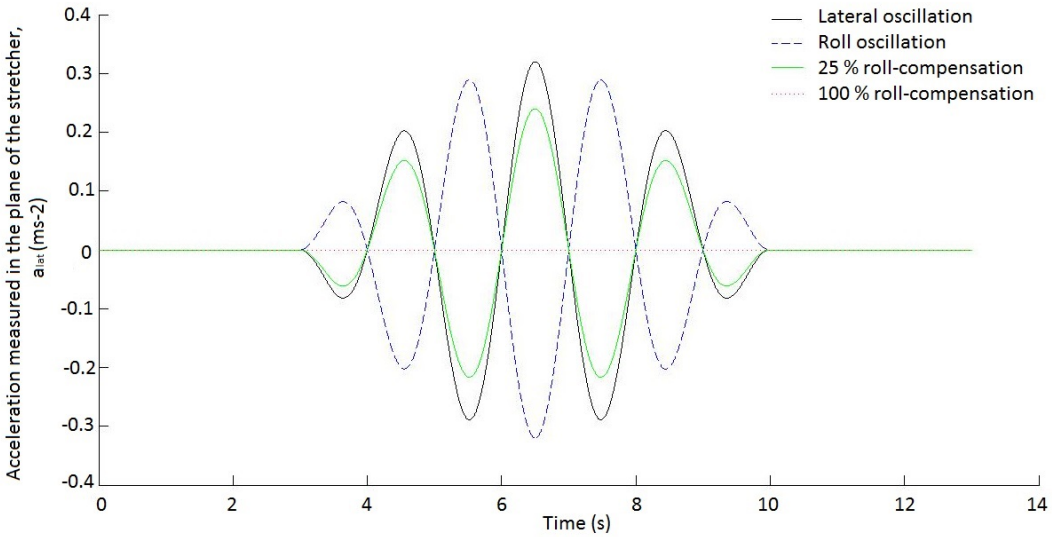

FIGURE 5.3: Example waveforms for 0.5 Hz oscillation showing the acceleration in the plane of the stretcher for lateral oscillation, roll oscillation, fully roll-compensated lateral oscillation and 25% roll-compensated lateral oscillation

5.2.5 Subjects

Subjects were recruited from the staff and student populations of the University of Southampton. Fourteen male volunteers aged between 23 and 40 years participated in the experiment, but the results from only twelve were taken into account (median age 27.5 years, inter-quartile range, IQR, 7.5 years; median weight 76.5 kg, IQR 22.5; median stature 1.79 m, IQR 0.09 m). The sample size was based on the sample size chosen in previous studies on horizontal vibration [74]. It has been displayed that 12 subjects is a reasonable number to perform statistical analysis and obtain significant results (see section 5.2.7). As the purpose of the experiment was to assess discomfort depending on the frequency of the stimuli, the direction of the stimuli and the magnitude of the stimuli only, the effect of other parameters had to be minimised. The gender can have a significant effect on discomfort [75] so this factor was removed from the experiment. In addition, due to low frequency motions the risk of occurrence of motion sickness existed and because female subjects are more susceptible to motion sickness than men [75] this risk can be reduced by selecting male subjects only. The ratings from two subjects were excluded because they were inconsistent with changes in the magnitudes of the stimuli throughout the experiment.

5.2.6 Analysis

The physical magnitudes, ϕ , of the motion stimuli were related to the subjective magnitude estimates, ζ, using Stevens' power law [76]:

$$\zeta = k \cdot \phi^n \tag{5.4}$$

The exponent, n, (i.e., the rate of growth of discomfort) and the constant, k, were determined by performing linear regression on the logarithmic transformation of equation (5.4):

$$log_{10}\zeta = log_{10}k + n \cdot log_{10}\phi \tag{5.5}$$

Lateral oscillation of the rigid stretcher at a frequency of 0.5 Hz and a magnitude of $0.2\ ms^{-2}$ r.m.s. was selected as a 'common reference' for constructing equivalent comfort contours. All subjects assigned a value of 100 to the reference stimulus, which served to normalise their subjective magnitudes, ζ. Equivalent comfort contours for subjective magnitudes, ζ, of 63, 80, 100, 125 and 160 were calculated for each subject and all four directions of oscillation using equation (5.4).

5.2.7 Statistical analysis

Non-parametric tests were used in the statistical analysis. The Friedman test was used to detect whether the acceleration required to cause a subjective magnitude, ζ, of 100 (i.e. the discomfort caused by the common reference stimuli) varied with the frequency of oscillation and also whether the rate of growth of discomfort varied with the frequency of oscillation, with each direction of motion. The Wilcoxon matched-pairs signed rank test was used to compare variations in the equivalent comfort contours and in the rate of growth of discomfort between directions. The Friedman test is a nonparametric test that examines whether the mean ranks of the data that belong to dependent groups differ. If the p-value obtained in the Friedman test is significant, a new test is required to compare differences among pairs of groups. In this case, the Wilcoxon test was used. The Wilcoxon matched-pairs signed rank test is a nonparametric test that serves to analyse differences between two dependent groups. It analyses whether the median value for the difference between the scores of each participant in the two groups is equal to zero. The results given by the tests are expressed in p-value terms [77]. The p-value indicates the probability that the results affirm that the hypothesis tested is true or not. Results were considered as statistically significant on the basis of a confidence level of 0.95 ($\alpha = 0.05$), which means that a p-value obtained in a test, had to be less than α to be statistically significant. In such cases, the decision adopted for accepting that there was a significant difference between the results, was right in the 95% of the times [77]. The questions to be solved with the Friedman test in this research were:

- Does the acceleration required to produce a subjective magnitude equal to that produced by the common reference stimulus vary with frequency?
- Does the acceleration required to produce a subjective magnitude equal to that produced by the common reference stimulus vary with the direction of oscillation?

- Does the rate of growth of subjective magnitude vary with frequency?
- Does the rate of growth of subjective magnitude vary with the direction of oscillation?

In the cases where the Friedman test found significant differences, the Wilcoxon test was used to test:

- Among directions of oscillation, at which frequencies is the acceleration required to produce a subjective magnitude of 100 greater.
- Among directions of oscillation, at which frequencies is the rate of growth greater.

5.3 Results

The physical magnitudes, ϕ, of the motion stimuli considered for each type of oscillation were the acceleration (ms^{-2} r.m.s.) measured in the plane of the stretcher (a_{lat}) for lateral and roll oscillation and the horizontal lateral acceleration (a_H) measured in the plane with respect to which the platform moved (absolute reference) for fully-compensated lateral oscillation and 25% roll-compensated lateral oscillation (see Figure 5.2).

5.3.1 Rate of growth of discomfort

Median rates of growth of discomfort for all directions of oscillation (lateral, roll, 25% and fully roll-compensated lateral oscillation) are displayed in Figure 5.4.

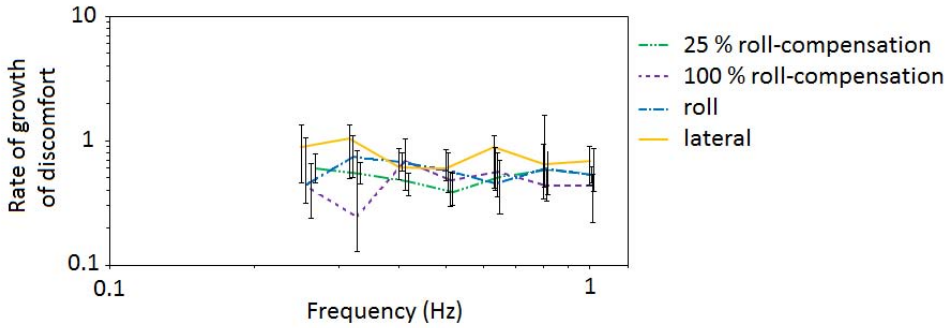

FIGURE 5.4: Median rates of growth of discomfort for lateral, roll, fully and 25% roll-compensated lateral oscillation. Upper and lower error bars show 75^{th} and 25^{th} percentiles, respectively.

The rate of growth, n, did not vary with frequency of oscillation in any direction ($p > 0.339$; Friedman), but depended on direction at frequencies of 0.25 Hz ($p < 0.042$; Friedman), 0.4 Hz ($p < 0.028$; Friedman) and 0.8 Hz ($p < 0.034$; Friedman). For 25% roll-compensated lateral oscillation, the rate of growth was less than for roll at 0.4 Hz ($p < 0.028$; Wilcoxon) but greater than for 100% roll-compensated lateral oscillation at 0.8 Hz ($p < 0.034$; Wilcoxon). The rate of growth of discomfort was less for 100% roll-compensated lateral oscillation than for roll oscillation at 0.8 Hz ($p < 0.023$; Wilcoxon) and less than for lateral oscillation at 0.25 Hz ($p < 0.034$; Wilcoxon).

5.3.2 Effect of frequency of oscillation on discomfort

For lateral oscillation, roll oscillation, and for 100% roll-compensated lateral oscillation, the acceleration required to produce a subjective magnitude of 100 (the same as the common reference selected in this study: the discomfort caused by 0.5 Hz lateral oscillation at 0.20 ms^{-2} r.m.s.) varied with the frequency of oscillation ($p < 0.019$; Friedman). For 25% roll-compensated lateral oscillation, variation with frequency of the acceleration required to produce a subjective magnitude of 100 was not statistically significant ($p > 0.168$; Friedman). Whereas for seated postures with roll oscillation the acceleration required to produce a subjective magnitude of 100 was almost constant between 0.25 Hz and 0.4 Hz [4], for a recumbent supine posture the range of frequencies in which the rate remained constant changed to 0.315 – 0.5 Hz. From these limits up to 1 Hz respectively, the acceleration required to produce a subjective magnitude of 100 declined at approximately 5 dB per octave for a recumbent supine posture and at a rate greater for seated postures (12 dB per octave) [4]. For lateral oscillation, the variation of acceleration required to produce a subjective magnitude of 100 for a recumbent supine posture differed from seated postures. Whereas for seated postures, the acceleration required to produce a subjective magnitude of 100 decreased at a rate of 5 dB per octave in the range of frequencies between 0.4 – 1 Hz [4], for a recumbent supine posture it increased at a rate of 5.21 dB per octave between 0.4 – 0.63 Hz and then it decreased at a rate of 3.7 dB per octave for frequencies greater than 0.63 Hz. For 100% roll-compensated lateral oscillation, the acceleration required to produce a subjective magnitude of 100 declined at approximately 17 dB per octave from 0.25 Hz to 0.315 Hz, increased at a rate of 2.4 dB per octave to 0.5 Hz and declined at approximately 12 dB per octave to 1.0 Hz.

5.3.3 Effect of direction of oscillation on discomfort

Except for 0.5 Hz and 0.63 Hz oscillation, the acceleration required to produce a subjective magnitude of 100 differed between the four types of oscillation ($p < 0.027$; Friedman). Figure 5.5 displays the median equivalent comfort contours for all four types of oscillation that produce similar discomfort to the reference stimulus.

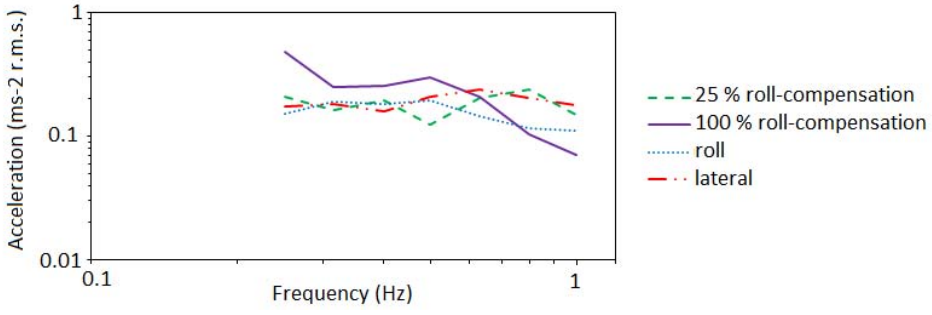

FIGURE 5.5: Median equivalent comfort contours for lateral, roll, 100% and 25% roll-compensated lateral oscillation, each producing the same discomfort as produced by a 0.5 Hz lateral oscillation at 0.20 ms^{-2} r.m.s.

Table 5.1 summarizes the statistically significant results found with the Wilcoxon test.

TABLE 5.1: Statistical significances for the effect of frequency in the Equivalent comfort contours

Greater magnitude required to produce the same discomfort for	Frequencies Hz	Statistical significance ($p - value$)
100% than 25%	< 0.5	0.034
25% than 100%	> 0.63	0.002
25% than roll	> 0.63	0.019
100% than roll	0.4	0.015
Roll than 100%	0.25	0.003
Roll than 25%	0.25	0.015
Roll than lateral	0.25	0.034
Lateral than roll	> 0.63	0.019
100% than lateral	0.25 and 0.4	0.012 and 0.005
Lateral than 100%	> 0.63	0.015

The equivalent comfort contours show that subjects were more sensitive to oscillations with 100% compensation or to pure roll oscillations at frequencies greater than 0.63 Hz than to oscillations with 25% compensation or pure lateral oscillation. As expected, at frequencies less than 0.5 Hz, a greater magnitude of oscillation was required to produce the same discomfort with 100% compensation than with 25% compensation.

5.3.4 Effect of magnitude on the frequency-dependence of equivalent comfort contours

Median equivalent comfort contours were calculated for subjective magnitudes between 63 and 160 (Figure 5.6)

Unlike with seating postures [4], the rate of growth did not change with frequency, so equivalent comfort contours were similar at all magnitudes.

5.4 Discussion

5.4.1 Rate of growth of vibration discomfort

The rate of growth did not vary significantly with frequency at any direction. Previous studies for seated postures found a decrease in the rate of growth with increasing frequency [4, 5, 6]. This indicates that in a recumbent posture over the range of frequencies studied here, sensitivity to changes in the magnitude of the oscillation was not significantly affected by the frequency of the oscillation. Consequently, the shapes of the equivalent comfort contours were not affected by the magnitude of oscillation.

5.4.2 Effect of frequency of oscillation on discomfort

The frequency of oscillation had a statistically significant effect on discomfort caused by sensitivity to acceleration for all types of oscillation, except for 25% roll-compensated lateral oscillation ($p > 0.168$; Friedman). For roll oscillation, sensitivity to lateral acceleration increased with increasing frequency, at frequencies greater than 0.5 Hz, at a rate less than with seated postures (5 dB per octave against 12 dB per octave for seated postures) [4]. For 100% roll-compensated lateral oscillation, sensitivity to lateral acceleration was low at low frequencies, increasing as frequency increased, especially at frequencies greater than 0.63 Hz. Sensitivity to

lateral oscillation differed from that for seated postures. Whereas for seated postures sensitivity to lateral acceleration increased with increasing frequency at a rate of 5 dB per octave from 0.4 Hz [4], for the recumbent supine posture sensitivity to lateral acceleration decreased at a rate of 5.21 dB per octave in the range of frequencies between 0.4-0.63 Hz and increased at a rate of 3.7 dB per octave for frequencies up to 1 Hz.

5.4.3 Effect of direction of oscillation on discomfort

At frequencies greater than 0.63 Hz, subjects were more sensitive to lateral acceleration when they were exposed to oscillatory motions in which the component of roll was high, like pure roll oscillation or 100% roll-compensated lateral oscillation. At frequencies less than 0.63 Hz, subjects were more sensitive to lateral oscillations or to 25% roll-compensated lateral oscillations (with a small component of roll) than to pure roll or 100% roll-compensated lateral oscillations.

5.4.4 Effect of magnitude on the frequency-dependence of equivalent comfort contours

Because the rate of growth of discomfort with increasing magnitude of acceleration did not vary with the frequency of oscillation in any direction, the equivalent comfort contours calculated for different magnitudes did not vary with frequency.

5.5 Conclusions

Contrary to the hypothesis, 25% roll-compensation of lateral oscillation was neither more comfortable nor less comfortable than pure lateral oscillation at frequencies less than 0.5 Hz or at frequencies greater than 0.5 Hz. Apart from that, it was found that 25% roll-compensation of lateral oscillation only produced less discomfort than roll oscillations at frequencies greater than 0.63 Hz, and not in the entire range of frequencies studied here as it was hypothesised. In accord with the hypothesis, pure lateral oscillation and 25% roll-compensation of lateral oscillation were less uncomfortable than 100% roll-compensation of lateral oscillation at frequencies greater than 0.63 Hz, because under both types of oscillation the acceleration required to produce the same discomfort than that caused by the reference stimulus was more than with 100% roll-compensation.

This experiment has not found statistically significant evidence to conclude that a design of the 3D multibody system that provides it with the capacity of roll-compensating a rate of 25% of lateral accelerations is better or worse than a design where no compensation exists. Results confirm, like for seated postures, that at low frequencies (less than 0.5 Hz) a rate of 100% roll-compensation of lateral oscillation is less uncomfortable than no compensation, although it interferes with the likelihood of suffering motion sickness like previous studies focused on motion sickness for seated postures concluded [7] (reason why a lower rate than 100% had been proposed). Therefore, they confirm that at frequencies greater than 0.63 Hz a rate of 25% is less detrimental than a rate of 100%. To find out whether a lower rate than 100% of roll-compensation of lateral oscillations is less detrimental for a person in a recumbent supine posture than no compensation or 25% compensation at frequencies less than 0.5 Hz, further research is needed.

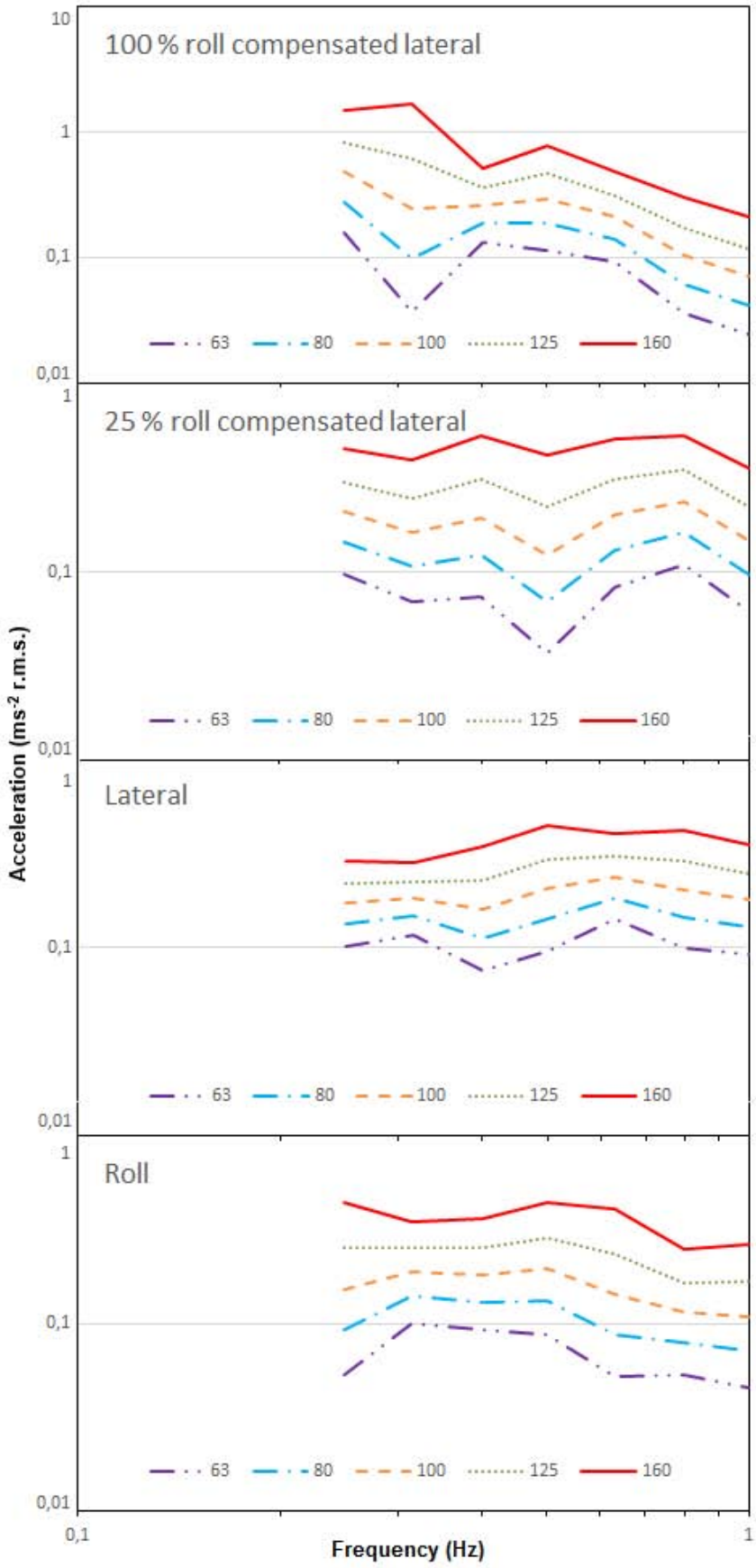

FIGURE 5.6: The effect of acceleration magnitude on median equivalent comfort contours caused by lateral, roll, 100% and 25% roll-compensated lateral oscillation. Contours represent discomfort equal to subjective magnitudes of 63, 80, 100, 125 and 160

Chapter 6

Discusión

6.1 Conclusiones

Los capítulos anteriores han tratado con los objetivos de esta tesis mencionados en el capítulo 1.

6.1.1 Desarrollo de un sistema multicuerpo 3D capaz de compensar pasivamente las aceleraciones horizontales que actúan en él

El objetivo principal que se pretendía conseguir con esta investigación, el desarrollo del sistema multicuerpo 3D capaz de compensar en diferentes porcentajes y de forma pasiva las aceleraciones horizontales que actúan sobre él, ha quedado justificado a lo largo de los capítulos de la tesis.

- Durante la revisión de la literatura referida a sistemas pasivos compensadores de aceleraciones, en la que se han considerado tanto patentes como publicaciones cienífica, no se ha encontrado un sistema pasivo aplicable al transporte de cargas delicadas o al de pacientes con las capacidades de este sistema para compensar de manera pasiva aceleraciones horizontales. Este sistema puede ser instalado en vehículos aéreos, terrestres o marítimos, su diseño permite compensar aceleraciones en diferentes direcciones y en diferentes porcentajes. Los sistemas encontrados han sido limitados a ser instalados en un determinado vehículo, han formado parte del chasis del vehículo, han compensado sólo aceleraciones horizontales en una dirección en particular y/o han tenido limitado el porcentaje de compensación de aceleraciones. El hecho de que en el transporte de cargas o pacientes se hayan encontrado sistemas que, aunque en un modo diferente, intenten compensar aceleraciones de forma pasiva, pone de manifiesto que existe un interés en alcanzar una compensación de aceleraciones para reducir la aceleración a la que las cargas o las personas están expuestas durante su transporte.

- El modelo matemático general que se ha desarrollado permite llevar a cabo el análisis cinemático y dinámico del sistema sin importar el vehículo en el que se instala el sistema ni el tipo de carga transportada.

- El análisis específico llevado a cabo para su aplicación en el transporte de pacientes, ha permitido definir las dimensiones más apropiadas del sistema para que durante su movimiento se alcance el porcentaje de compensación de aceleraciones deseado así como analizar su comportamiento dinámico a través de la simulación por ordenador.

- La parte experimental centrada en el movimiento del sistema, ha servido para construir dos prototipos con los que se ha podido analizar experimentalmente el

comportamiento lateral y longitudinal del sistema. Se ha podido verificar que el movimiento de la base del sistema permite que la aceleración medida en su plano sea menor que la que actúa horizontalmente y en esa misma dirección sobre el sistema, como se esperaba, y se ha permitido detectar limitaciones en su uso y durante su ensamblaje.

- La parte experimental centrada en el efecto que diferentes oscilaciones tienen sobre el malestar que pueden experimentar las personas que mantienen una postura de decúbito supino, ha permitido detectar para el tipo de movimiento que se puede experimentar con el sistema desarrollado, bajo qué condiciones las personas son más o menos sensibles a las aceleraciones laterales.

6.1.2 Modelo matemático y validación

El segundo y tercer objetivos han estado centrados en el desarrollo de un modelo matemático de las ecuaciones de movimiento del sistema y en su validación. El planteamiento de las ecuaciones de movimiento se ha llevado a cabo empleando la formulación de la mecánica newtoniana. El modelo ha considerado que todos los sólidos tienen un comportamiento como sólido rígido, pueden moverse en un espacio tridimensional, tienen su masa concentrada en su centro geométrico y sus tensores de inercia sólo tienen valores en la diagonal principal. Los amortiguadores han sido modelados caracterizando únicamente su comportamiento viscoso, sin tener en cuenta el fenómeno de fricción en estos ni en las uniones entre los sólidos. El modelo matemático ha contemplado cuatro variantes en lo que a las uniones entre los sólidos que lo constituyen se refiere, considerando uniones de tipo esférico, bisagra lateral, bisagra frontal y cardan, respectivamente.

La resolución del sistema de ecuaciones de movimiento del sistema multicuerpo se ha llevado a cabo con Matlab, a través de un método de resolución basado en el método de integración numérica de Newton-Raphson, programado manualmente. El método de integración utilizado para resolver el modelo está formado por diferentes parámetros que tienen influencia sobre la eficiencia del método (tipo de paso, tamaño de paso, constante C influyente en el tamaño de paso variable, orden de la fórmula de diferenciación hacia atrás y tolerancia del error de integración ε). Las combinaciones de todos estos parámetros han dado lugar al análisis de 288 casos diferentes. Los resultados obtenidos se han validado computacionalmente, contrastando estos con los obtenidos con el programa MSc Adams, pudiendo determinar así el valor de los parámetros influyentes en el método de integración numérico con el que su eficiencia se optimiza.

- Cuando se adoptó un tamaño de paso fijo, una fórmula de diferenciación hacia atrás de orden 2, junto con un tamaño de paso de 0.01 s, resolvió el sistema de ecuaciones de la manera más eficiente, independientemente del valor escogido para la tolerancia del error de integración.

- Cuando se adoptó un tamaño de paso variable, una fórmula de diferenciación hacia atrás de orden 1 fue la más eficiente, evitando que el tamaño de paso alcanzase valores menores que 0.001 s.

- Cuando se seleccionó un tamaño de paso variable, la tolerancia del error de integración afectó claramente al error acumulado, reduciéndose éste conforme la tolorancia se reducía.

- El menor error acumulado en la solución proporcionada por el método propuesto se obtuvo cuando se eligió un tamaño de paso fijo y una fórmula de diferenciación hacia atrás de orden 2.

- El tiempo de cálculo fue mucho menor cuando se selccionó un tamaño de paso variable y una fórmula de diferenciación hacia atrás de orden 1.

- En la selección de un tamaño de paso variable, valores elevados de la constante C ($C = 0.9$), redujeron el error acumulado y el tiempo de cálculo.

6.1.3 Aplicación del sistema al transporte de pacientes

El sistema multicuerpo analizado ha sido parametrizado teniendo en cuenta las dimensiones de sus componentes, sus masas, inercias y los coeficientes de amortiguamiento de los amortiguadores. Con el propósito de cumplir el cuarto objetivo de definir un diseño del sistema para su uso específico en el transporte de pacientes, se ha analizado una configuración de éste que comparte un comportamiento cinemático con el del mecanismo de cuadrilatero articulado, por tratarse de un ejemplo significativo que facilita el análisis del movimiento del sistema.

El diseño del sistema se ha realizado para que con su movimiento se alcance un porcentaje de compensación específico. Para esto, mediante la aplicación de la teoría del Diseño de Experimentos, se ha analizado la influencia que la distancia entre la base del sistema y el plano en el que se encuentran los extremos superiores de las barras (Drb) y la distancia entre los extremos superiores de las barras (p) tienen sobre el movimiento de la base del sistema. Asimismo, se ha analizado la influencia de estos parámetros junto con la masa transportada y con la masa de las barras sobre el modo de vibración natural del sistema. Se han considerado estos parámetros y no otros, por ser los parámetros más fácilmente modificables en la fase experimental.

Este análisis ha permitido identificar **de entre los parámetros considerados y para esta configuración** que:

- El parámetro dimensional que mayor efecto tiene sobre la capacidad de inclinación de la base del sistema es la distancia entre los extremos superiores de las barras.

- El parámetro dimensional que mayor efecto tiene sobre el desplazamiento de su base es la distancia entre la base del sistema y el plano en el que se encuentran los extremos superiores de las barras.

- El parámetro dimensional que mayor efecto tiene sobre el modo natural de vibración del sistema es el desplazamiento de su base es la distancia entre la base del sistema y el plano en el que se encuentran los extremos superiores de las barras.

En base a los resultados hallados con la teoría del Diseño de Experimentos, se ha definido el diseño del sistema para alcanzar en su movimiento un porcentaje de compensación de aceleraciones específico y su movimiento ha sido comprobado computacionalmente.

- En el intervalo de aceleraciones para el que el sistema se espera que trabaje de manera eficiente (hasta $3.08\ m/s^2$), con los tres diseños que se han obtenido (uno por cada porcentaje de compensación considerado en el análisis), se ha alcanzado con precisión el porcentaje de compensación de aceleraciones para el que fueron diseñados.

- Un factor de amortiguamiento del sistema de 0.6 se ha considerado el más apropiado para dotarlo de un comportamiento vibratorio intermedio en términos de retraso en su respuesta y en su efecto para compensar aceleraciones por encima o por debajo del valor requerido.

Teniendo en cuenta lo que previas investigaciones han concluido al analizar el efecto que diferentes tipos de oscilaciones tienen sobre el malestar y el mareo de personas sentadas, el diseño propuesto para transportar pacientes en una posición tumbada puede ser apropiado porque:

- Al analizar la transmisión de los desplazamientos desde el soporte del sistema hasta la base del sistema, se ha visto que la oscilación de la base del sistema se atenúa en el intervalo de frecuencias desde la que el malestar crece.

- Las dimensiones y la configuración del sistema (cuya cinemática es similar a la del cuadrilátero articulado) que se ha contemplado para esta aplicación hacen que su frecuencia natural esté cercana a 0.6 Hz, por debajo de la frecuencia en la que el malestar aumenta cuando se produce la compensación total de aceleraciones laterales y en el lado conservador del intervalo de frecuencias en el que la probabilidad de experimentar el mareo disminuye.

Como se ha mencionado, estas últimas conclusiones se han obtenido en base a los resultados de estudios llevados a cabo con personas que mantenían una posición sentada y en los que la compensación de aceleraciones se llevó a cabo al 100%.

6.1.4 Experimentación con personas

La estancia de tres meses llevada a cabo en un centro de investigación de referencia en lo que se refiere a la investigación en vibraciones humanas, en el Instituto de Investigación de Sonido y Vibraciones de la Universidad de Southampton, ha servido para cumplir con el quinto objetivo. Debido a la intención de utilizar el sistema para el transporte de pacientes, para confirmar que el tipo de movimiento que se consigue con el sistema puede ser apropiado para transportar personas que mantienen una postura de tumbado supino, se ha llevado a cabo un experimento en el que se analizó el efecto que la compensación de la aceleración lateral a través del giro (a diferentes porcentajes, 25% y 100%) tiene sobre el malestar de las personas que están tumbadas en una postura de decúbito supino.

Los hallazgos más relevantes, con respecto al diseño del sistema son:

- La compensación de aceleraciones laterales con el giro en un porcentaje del 100% es mejor que en un porcentaje del 25% para oscilaciones a frecuencias menores de 0.63 Hz.

- La compensación de aceleraciones laterales con el giro en un porcentaje del 25% es mejor que un porcentaje del 100% a frecuencias mayores.

- Se supuso que un porcentaje del 25% de compensación de la aceleración lateral a través del giro sería mejor que oscilaciones puramente laterales a frecuencias menores a 0.5 Hz, pero los resultados han indicado que en este porcentaje, las oscilaciones puramente laterales no son ni mejor ni peor que con una compensación del 25%.

- Transfiriendo estos resultados al diseño del sistema multicuerpo 3D y considerando sólo el malestar experimentado por las personas (no el mareo), tras esta experimentación parece razonable pensar que un diseño que permite compensar un porcentaje cercano al 25% es menos perjudicial que un diseño configurado para alcanzar un porcentaje de compensación del 100%, pero sólo cuando el sistema oscila a frecuencias mayores de 0.63 Hz.

Aunque la experimentación no pudo probar que un porcentaje de compensación del 25% era mejor que la ausencia de compensación, éste fue mejor que un porcentaje del 100% a frecuencias mayores del 0.63 Hz. Posiblemente, diferentes porcentajes de compensación den como resultado diferentes resultados, pero para confirmar esto sería necesario continuar investigando.

6.1.5 Experimentación con prototipos

El sexto objetivo, centrado en la validación experimental del modelo matemático de las ecuaciones de movimiento del sistema, fue reorientado para validar la teoría sobre la que se ha basado el diseño del sistema detallado en el capítulo 4.

- Ante la acción sobre el sistema de una aceleración horizontal (experimentada como consecuencia del movimiento del vehículo en el que se encuentra instalado), el movimiento oscilatorio de su base ha sido acorde al que se esperaba, comprobando que la aceleración medida en el plano de la base es inferior que la que actúa sobre el sistema en la misma dirección (lateral o longitudinal).

- Para poder llevar a cabo una validación experimental completa del modelo matemático desarrollado en el capítulo 3, es necesario disponer de un vehículo dotado de un sistema de suspensión que evite una transmisión directa de las vibraciones hacia el sistema oscilante, realizar un prototipo robusto que permita llevar a cabo ensayos en diferentes condiciones, que el ensamblaje entre las partes del sistema esté perfectamente ajustado y disponer de una pista de pruebas que no suponga una limitación al movimiento del vehículo. En estas condiciones, el diseño del sistema deberá realizarse atendiendo al razonamiento considerado en el capítulo 4.

6.2 Aportaciones científicas

Esta tesis ha dado como resultado las siguientes aportaciones científicas.

- Desarrollo de un sistema mecánico 3D que, aunque comparte elementos en común con otros sistemas pasivos previamente mencionados, sus capacidades para poderse instalar en diferentes tipos de vehículos, para compensar de forma pasiva un porcentaje específico de aceleraciones, para poder compensar aceleraciones en diferentes direcciones y para poder transportar sobre él diferentes tipos y tamaños de cargas lo hace diferente del resto.

- Desarrollo de un modelo matemático general que permite analizar la dinámica del sistema mecánico 3D, pudiendo ser configurado con diferentes tipos de uniones entre sus partes.

- Propuesta y validación del método de resolución del sistema no lineal de ecuaciones diferenciales algebráicas de segundo orden (que constituyen las

ecuaciones de movimiento del sistema) en el que se han determinado: el tipo de paso (fijo o variable), su tamaño, la tolerancia del error de integración ε, la constante C interviniente en el tamaño de paso variable y el orden de la fórmula de diferenciación hacia atrás empleados durante su resolución para que ésta sea lo más eficiente posible.

- Desarrollo de la metodología para definir el diseño del sistema para garantizar que la compensación de aceleraciones se consigue durante todo su movimiento.

- Un diseño del sistema específico para transportar pacientes en una posición tumbada capaz de mantener un porcentaje de compensación de aceleraciones durante todo su movimiento, que atenúa la oscilación de la base del sistema en el intervalo de frecuencias desde la que el malestar crece y que dispone de una frecuencia natural que está por debajo de la frecuencia en la que el malestar aumenta cuando se produce la compensación total de aceleraciones laterales y en el lado conservador del intervalo de frecuencias en el que la probabilidad de experimentar el mareo disminuye.

- Complementar los estudios llevados a cabo con personas sentadas sobre el efecto que las vibraciones tienen sobre el malestar, considerando una postura de decúbito supino y una condición de compensación de aceleraciones no analizada anteriormente. No se ha podido probar que un porcentaje de compensación del 25% es mejor que la ausencia de compensación, pero sí es mejor que un porcentaje del 100% a frecuencias mayores de 0.63 Hz.

- Presentación de una alternativa fundamentada razonadamente al transporte de pacientes en ambulancias que podría ser beneficioso para el paciente, debido a la reducción de las aceleraciones horizontales medidas en el plano de la base del sistema, y por lo tanto, de la camilla del paciente, lo que podría contribuir a una reducción del dolor que éstas puedan ocasionarle.

6.3 Trabajo futuro

Posibilidad de patentar el sistema

Durante esta investigación, se ha intentado patentar este nuevo sistema como fue hecho con su predecesor [1], pero la Universidad de Zaragoza ha requerido para ello que se construyese un prototipo de dimensiones reales y que se ensayase en una ambulancia con personas. Como se ha mencionado en el anexo A, el presupuesto limitado disponible para ello ha condicionado la fase experimental de esta investigación. Como la Universidad de Zaragoza ha desestimado tomar parte en este proceso, si una empresa estuviera interesada en este sistema, sería una gran oportunidad para ellos para patentar el sistema, construyendo un nuevo prototipo más robusto y llevando a cabo pruebas con un vehículo apropiado.

Validación experimental del modelo matemático

Aunque el modelo matemático de las ecuaciones de movimiento del sistema ha considerado que todos los cuerpos que integran el sistema se comportan como sólidos rígidos, investigaciones futuras pueden considerar analizar su comportamiento lineal. Asimismo, otras formas de aproximar las derivadas del sistema y de calcular el tamaño del paso utilizado en el método de integración pueden utilizarse y compararse con los analizados aquí.

Factores no considerados

El sistema presentado aquí pretende aplicarse para el transporte de cargas delicadas y/o pacientes, sin embargo aquí su aplicación para transportar cargas delicadas no ha sido analizada. Hay una gran variedad de tipos de cargas, diferenciándose entre ellas en su tamaño, peso, forma y en otros muchos factores. Analizar la efectividad del sistema y su diseño requiere continuar investigando, definiendo con precisión las cargas y el tipo de vehículo en el que van a transportarse, lo que puede ser de interés para fabricantes de productos de vidrio o cerámica, por ejemplo.

En esta línea, investigaciones futuras pueden considerar el efecto que otros componentes del sistema, tales como el acolchado de la camilla, las uniones entre las partes del sistema y también entre éstas y el vehículo o la estructura soporte y la rigidez de sus componentes, tienen en su respuesta vibratoria, incluyendo la transmisión de las vibraciones. Adicionalmente, como se ha mencionado anteriormente, un prototipo de dimensiones reales debería ser construido e instalado en una ambulancia (o en un vehículo similar) para verificar la correlación entre los resultados obtenidos teórica y computacionalmente y los obtenidos experimentalmente.

Aplicabilidad en el transporte de personas tumbadas

La experimentación llevada a cabo con personas ha estado centrada en el malestar y ha considerado sólo dos porcentajes de compensación de aceleraciones. Esto fue debido al limitado tiempo disponible para llevar a cabo las pruebas en la Universidad de Southampton. Como los trabajos llevados a cabo en investigaciones anteriores han analizado tanto la probabilidad de sufrir mareo como la percepción del malestar para personas que mantienen una postura sentada, sería recomendable que se complementase el experimento llevado a cabo con experimentos que considerasen para una postura tumbada la problemática del mareo. Asimismo, sería recomendable que tanto para el mareo como para el malestar se tuvieran en cuenta dos porcentajes más de compensación de aceleraciones (50% y 75%). Ello puede ayudar a encontrar el punto en el que el porcentaje de compensación de aceleraciones laterales comience a ser significativamente mejor que la ausencia de compensación en lo que respecta al malestar.

6.4 Publicaciones

6.4.1 Conferencias

P. J. Fernández; S. Baselga, Passive compensation of accelerations applied to transport patients in emergency vehicles. 51^{st} Conference on Human Responses to Vibration. (2016) Gosport, United Kingdom.

P. J. Fernández; S. Baselga, Passive mechanical system, compensator of accelerations, for transporting delicate loads in road vehicles. XII Conference on Transport Engineering. (2016) Valencia, Spain.

P. J. Fernández; S. Baselga; J. Lladó, An alternative system and way of transport patients in an emergency vehicle. Speaker in the I Forum of Transportation Engineering. (2015) Cercedilla, (Madrid), Spain.

6.4.2 Artículos

P. J. Fernández; S. Baselga, Passive systems applied to compensate accelerations. Review of the literature and presentation of a new approach for transporting patients. (2017) submitted to Journal of Modern Transportation.

C. Clavero; P. J. Fernández, Efficiency of a BDF-Newton-Raphson numerical integration method applied to solve a system of nonlinear differential equations modeling a mechanical multibody system. (2017) submitted to the journal Multibody System Dynamics.

S. Baselga; C. Clavero; P. J. Fernández, Kinematic and Dynamic Analysis of a 3D multibody system applied to passively compensate horizontal accelerations in patient transportation. (2017) submitted to the journal Multibody System Dynamics.

Chapter 7

Discussion

7.1 Conclusions

The previous chapters have dealt with the objectives of this thesis mentioned in chapter 1.

7.1.1 Development of a general 3D multibody system capable of compensating passively the horizontal accelerations that act on it at different rates

The main objective that was intended to fulfill with this research, the development of a general 3D multibody system capable of compensating passively the horizontal accelerations that act on it at different rates, has been justified throughout the chapters of this thesis.

- During the review of the literature referred to passive systems applied to compensate accelerations, in which both patents and scientific papers have been considered, have not been found a passive system applicable to transport delicate loads or people with the capabilities of this system to compensate passively horizontal accelerations. This system can be installed into aerial, ground, or maritime vehicles, its design allows to compensate accelerations in different directions and also at different rates. The systems found have been limited to be installed in a particular type of vehicle, have formed part of the frame of the vehicle, have compensated only horizontal accelerations in one direction and /or have had limited its rate of compensation of accelerations. The fact that in transportation of loads or patients have been found systems which, although in a different way, have tried to compensate accelerations passively, highlights that there is an interest of achieving compensation of accelerations in order to reduce the acceleration to which loads and people are exposed during their transport.

- The general mathematical model that has been developed allows to carry out the kinematic and dynamic analysis of the system irrespectively of the type of vehicle in which the system is installed neither the type of load transported.

- The specific analysis carried out for its application to transport patients has allowed to define the dimensions more appropriate for the system so as to achieve during its motion the desired rate of compensation of accelerations in addition to analyse its dynamic behaviour through computational simulation.

- The experimental part focused on the motion of the system has served to build two prototypes of the system with which it has been able to analyse experimentally the lateral and longitudinal behaviour of the system. It has been able to verify that

the motion of the base of the system allows that the acceleration measured in the plane of the base is less than the horizontal acceleration that acts on it in the same direction (laterally or longitudinally), like it was expected, and it has been detected some limitations in its use and during its assembly.

- The experimental part focused on the effect that different types of oscillation have on the discomfort of people who maintain a recumbent supine posture, has allowed to detect for the type of motion that can be experienced with the system, under which conditions people are more or less sensitive to lateral accelerations.

7.1.2 Mathematical model and its validation

The second and third objectives have been focused on the development of a mathematical model of the equations of motion of the system and on its validation. The pose of the equations of motion of the system has been carried out by mean of applying the Newtonian mechanics approach. The model has considered that all solids have a behaviour like rigid solid, they can move in a tri-dimensional space, they have their mass concentrated in their geometrical centre and their inertia tensors have values only in their principal axes. The dampers have been modelled characterizing only their viscous behaviour, without considering the phenomena of friction between them neither in the links between the solids. The mathematical model has considered four cases in what the links between their parts is referred, considering spherical joints, lateral revolute joints, longitudinal revolute joints and cardan joints.

The solution to the system of equations of motion of the 3D multibody system has been carried out with Matlab, by mean of applying a solving method based on the Newton-Raphson numerical integration method manually programmed. The method used to solve the model is formed by different parameters that have influence in the efficiency of the method (type of step, size of step, constant C influencing the size of the variable step, order of the backward differentiation formulae (BDF) and the integration tolerance error ε), the combinations among them have resulted in analysing 288 cases. The results obtained have been validated computationally against the results obtained with the software MSc Adams, determining then the value of the parameters influencing the numerical integration method with which its efficiency is maximized.

- When a fixed step size approach was used, a BDF method of order 2, along with a step size of 0.01 s solved the system of equations in the most efficient way, independently of the value of the integration tolerance error.

- When a variable step size approach was used, a BDF method of order 1 was the most efficient avoiding the step size to reach values smaller than 0.001 s.

- When a variable step size approach was used, the integration tolerance error affected clearly to the accumulated error, decreasing as the integration tolerance decreased.

- The least accumulated error was obtained when a fixed step size approach and a BDF method of order 2 were used.

- The computational time was much less when a variable step size approach a BDF method of order 1 were used.

- For a variable step size approach, high values of the constant C ($C = 0.9$), reduced the accumulated error and the computational time.

7.1.3 Application of the system to transport patients

The multibody system analysed here has been parameterized having into account the dimensions of its components, their masses, inertias and the damping coefficients of the dampers. With the purpose of fulfil the fourth objective of defining a design of the system for its specific application to transport patients, it has been analysed a configuration which shares its kinematic behaviour with the articulated quadrilateral mechanism, because it is a significative example that eases the analysis of the motion of the system.

The design of the system has been carried out in order to achieve with its motion a specific rate of compensation of accelerations. For it, through applying the Design of Experiments theory it has been analysed the influence that the distance between the distance between the horizontal plane that contains the joints of the bars' upper ends and the base of the system, when it keeps static equilibrium (Drb) and the distance between the upper ends of the bars (contained in the plane where the width of the stretcher is measured, p) have in the motion of the base of the system. Therefore, it has been analysed the influence that these parameters along with the mass of the bars (m_b) and the mass of the assembly stretcher-person (m_s, it represents both the mass of the system and the patient)have in the natural mode of vibration of the system. These parameters have been considered and no others because they are the parameters most easily modifiable during the experimental stage.

This analysis has allowed to identify **among the parameters considered and for this configuration** that:

- The dimensional parameter that a major effect has on the tilting capabilities of the base of the system is the distance between the upper ends of the bars.

- The dimensional parameter that a major effect has on the displacement of the base of the system is the distance between the horizontal plane containing the joints of the bars' upper ends and the base of the system.

- The dimensional parameter that a major effect has on the natural mode of vibration of the system is the displacement of the base of the system is the distance between the horizontal plane containing the joints of the bars' upper ends and the base of the system.

On the basis of the results found after applying the Design of Experiments theory, the design of the system has been defined in order to achieve a specific rate of compensation of accelreations during its motion and its motion has been verified computationally.

- In the range of accelerations for which the system is expected to work efficiently (up to $3.08\ m/s^2$), with the three designs obtained (one for each rate of compensation of acceleration considered in the analysis) the system has obtained a good and accurate motion for its base, what has resulted in an achievement of the required rate of compensation of accelerations.

- A damping ratio for the system of 0.6 has been considered to be the most appropriate, in order to provide the system with an intermediate behaviour in terms of lag in its response and in its effect for under/over compensate accelerations.

Having into account what previous researches have concluded after analysing the effect that different types of oscillations have on the discomfort and on the likelihood of suffering motion sickness for people who maintain a seated posture, the design proposed for the system for its application to transport patients in a recumbent supine posture might be appropriate because:

- When analysing the transmission of the displacements from the support of the system to its base, the oscillation of the base has been attenuated in the range of frequencies from which discomfort increases.

- The dimensions and the configuration of the system (whose kinematic is similar to the kinematic of the articulated quadrilateral mechanism) that has been considered for this application result in a natural frequency for the system close to 0.6 Hz, below the frequency at which discomfort increases for fully compensation of lateral oscillations (0.63 Hz) and in the conservative side of the range of frequencies in which the likelihood of suffering motion sickness decreases.

As mentioned previously, these last conclusions are based on results obtained in previous studies carried out for people who maintain a seated posture and in which the rate of compensation of accelerations was 100%.

7.1.4 Experimentation with people

The research stay of three months carried out in a centre of reference in what Human Vibration Research refers, at the Institute of Sound and Vibration Research at the University of Southampton, has served to accomplish the fifth objective. Due to the aim of applying the system to transport patients, in order to confirm that the type of motion achievable with the system may be appropriate for transporting people who maintain a recumbent supine posture, an experiment has been carried out in which was analysed the effect that roll-compensation of lateral oscillation (at different rates, 25% and 100%) have on the discomfort of people who lie in a recumbent supine posture.

The most relevant findings with regards to the design of the system are:

- A rate of 100% of roll-compensation of lateral oscillation is better than a rate of 25% for oscillations at frequencies less than 0.63 Hz.

- A rate of 25% of roll-compensation of lateral oscillation is better than a rate of 100% at greater frequencies.

- It was hypothesised that a rate of 25% of roll-compensation of lateral oscillation would be better than pure lateral oscillation at frequencies less than 0.5 Hz but the results have indicated that at this rate, pure lateral oscillation is no better and no worse than a rate of 25%.

- Transferring these findings to the design of the 3D multibody system and considering just the discomfort experienced by people (no motion sickness), after this experimentation it seems reasonable to think that a design that allows to compensate a rate closer to 25% is less detrimental than a design configured to achieve a rate of 100%, but only when the system oscillates at frequencies greater than 0.63 Hz.

Although the experimentation could not prove that a rate of compensation of accelerations of 25% was better than no compensation, it was better than 100% at frequencies greater than 0.63 Hz. Possibly different rates of compensation result in different findings, but for confirming that, further research would be needed.

7.1.5 Experimentation with prototypes

The sixth objective, focused on the experimental validation of the mathematical model of the equations of motion of the system was reoriented in order to validate the theory on which the design of the system is based, detailed in chapter 4.

- Under the exposure of the system to a horizontal acceleration (experienced as a consequence of the motion of the vehicle in which it is installed), the oscillatory motion of its base has been in accord with the motion expected, verifying that the acceleration measured in the plane of its base is less than the acceleration that acts on the system in the same direction (laterally or longitudinally).

- In order to carry out a complete experimental validation of the mathematical model developed in chapter 3 is needed to: dispose of a vehicle equipped with a suspension system that avoids a direct transmission of the vibrations towards the oscillatory system, build a robust prototype that allows to carry out different tests in different load conditions, that the assembly of the parts of the system is perfectly adjusted (without looseness) and sispose of a test-track which does not limit the motion of the vehicle. In these conditions, the design of the system should be defined attending to the reasoning and methodology followed in chapter 4.

7.2 Scientific contributions

This thesis has resulted in the following scientific contributions:

- Development of a general 3D multibody system that, although it shares common characteristics with other passive systems previously mentioned, has the capacity of being installed into different types of vehicles, can compensate passively a specific rate of the horizontal acceleration that acts on it and in different directions and can transport on it different loads of different types and sizes, what makes it different from the rest of systems.

- Development of a general mathematical model of the equations of motion of the system that allows to analyse the dynamic behaviour of the system, being able to be configured with different types of joints between its parts.

- Proposal and validation of a solving method for the nonlinear system of second order differential algebraic equations (which constitute the equations of motion of the system) in which have been determined: the type of size (fixed or variable), its size, the integration tolerance error ε, the constant C influencing the size of the variable step, order of the backward differentiation formulae (BDF) used during its resolution in order to make its solution as efficient as possible.

- Development of a methodology to define the design of the system in order to guarantee that a specific rate of compensation of accelerations is achieved during the motion of the system.

- A specific design of the system to transport patients in a recumbent supine posture that achieves a specific rate of compensation of accelerations during its motion, that attenuates the oscillation of the base of the system in the range of frequencies in which discomfort increases and that disposes of a natural frequency that is below the frequency at which discomfort increases for fully compensation of lateral oscillations and in the conservative side of the range of frequencies in which the likelihood of suffering motion sickness decreases.

- Supplement the studies carried out with people who maintain a seated posture about the discomfort that they experienced under the exposure to different types of oscillations, considering a recumbent supine posture and the condition of roll-compensation of lateral oscillation not analysed previously. It has not been able to be proved that a rate of 25% of roll compensation of lateral accelerations is better or worse than no compensation but it has been proved that a rate of 25% is better than a rate of 100% at frequencies greater than 0.63 Hz.

- Presentation of a substantiated and reasoned alternative to the way of transporting patients in ambulances that might be beneficial for the patient, due to the reduction of the horizontal accelerations measured in the plane of the base of the system, and hence, in the stretcher, what might contribute to a reduction of the pain that these people can experience during transport.

7.3 Future lines of work

Posibility for patenting the system

During this research it has been intended to patent this new system like it was done with its predecessor [1] but the University of Zaragoza has required that for it a prototype of real dimensions is built and tested in an ambulance with people. As it has been mentioned in the annex A, the limited budget available for it has influenced the experimentation stage of this research. As the University of Zaragoza has declined to take part of it, if a company was interested in this system, it would be a great opportunity for them to contribute to patent the system, building a new prototype more robust and carrying out tests with an appropriate vehicle.

Experimental validation of the mathematical model

Although the mathematical model of the equations of motion of the system has considered that all bodies integrating the system behave as rigid solids, further research may consider to analyse their linear behaviour. Therefore, other ways of approximating the derivatives of the system and of calculating the size of the step used in the integration method may be used and compared with the ones analysed here.

Factors not considered

It is aimed to applied the system presented here to transport delicate loads and/or patients, however here its used for transport delicate loads has not been analysed. There are a great variety of types of loads, differing each other in their size, weight, shape and in other factors. Analyze the effectiveness of the system and its design requires future research defining accurately the loads and the type of vehicle in which they are going to be transported, what might be of interest for example for manufacturers of glass or ceramic products.

In this basis, further research may consider the effect that components of the system such as the foam of the stretcher, the links among the parts of the system and also the vehicle and the supporting structure and the stiffness of its components have on its vibrational response, including the transmission of vibrations. Additionally, like it has been mentioned previously, a prototype of real dimensions should be built and installed in an ambulance (or in a similar vehicle) in order to correlate the theoretical and computational results with the experimental ones.

Applicability for transporting people who maintain a recumbent posture

The experimentation carried out with people has been focused on the discomfort and it has considered only two rates of compensation of accelerations. It was due to the limited time available for carrying out tests at the University of Southampton. As the work carried out in previous researches have analysed both the likelihood of suffering motion sickness and the perception of discomfort for people who maintain a seated posture, it would be recommended to supplement these studies with experiments that consider, for a recumbent supine posture, the problematic of motion sickness. Therefore, it would be recommended that both for the motion sickness and for the discomfort two more rates of compensation of accelerations (50% and 75%) were considered. It may help to find when the rate of compensation of lateral oscillations starts to be significantly better than no compensation in what respect to discomfort.

7.4 Publications

7.4.1 Conferences

P. J. Fernández; S. Baselga, Passive compensation of accelerations applied to transport patients in emergency vehicles. 51^{st} Conference on Human Responses to Vibration. (2016) Gosport, United Kingdom.

P. J. Fernández; S. Baselga, Passive mechanical system, compensator of accelerations, for transporting delicate loads in road vehicles. XII Conference on Transport Engineering. (2016) Valencia, Spain.

P. J. Fernández; S. Baselga; J. Lladó, An alternative system and way of transport patients in an emergency vehicle. Speaker in the I Forum of Transportation Engineering. (2015) Cercedilla, (Madrid), Spain.

7.4.2 Papers

P. J. Fernández; S. Baselga, Passive systems applied to compensate accelerations. Review of the literature and presentation of a new approach for transporting patients. (2017) submitted to Journal of Modern Transportation.

C. Clavero; P. J. Fernández, Efficiency of a BDF-Newton-Raphson numerical integration method applied to solve a system of nonlinear differential equations modeling a mechanical multibody system. (2017) submitted to the journal Multibody System Dynamics.

S. Baselga; C. Clavero; P. J. Fernández, Kinematic and Dynamic Analysis of a 3D multibody system applied to passively compensate horizontal accelerations in patient transportation. (2017) submitted to the journal Multibody System Dynamics.

Appendix A

Experimentation with prototypes

A.1 Introduction

This annex describes the experimentation carried out with two prototypes at the University of Zaragoza. The purpose of these experiments was to supplement the computational validation of the mathematical model of the equations of motion of the 3D multibody system that was done previously (see chapter 3) and validate the theory that supports the definition of the design of the system (see chapter 4). For it, two different prototypes of the 3D multibody system were built and tested. The methodology followed during this experiments is explained below and also the results obtained with them. Some problems experienced during the tests influenced the experimental validation.

A.1.1 Limitations found during the design of the prototypes

In order to carry out tests with a prototype of real dimensions in a vehicle it is needed first, to dispose of a vehicle in which the prototype can be installed and secondly, to accomplish traffic and vehicle regulations (in this case, Spanish regulations) [78]. In what respect to experimentation with people, it is necessary that once the vehicle receives authorization to be driven on roads after being modified, authorities allow that a person can be transported in a recumbent supine posture on the base of the prototype (securely attached) during driving conditions. In addition to traffic and vehicle regulations, experimentation with people requires the approval of the Ethic Committee of the University in which this research is being carried out.

Although in theory and mathematically the 3D multibody system can be configured with spherical or cardan joints in all ends of its bars, the configuration of the prototypes corresponded with those that provided them either with a lateral oscillatory behaviour or with a longitudinal oscillatory behaviour. Two prototypes were built, one with real dimensions configured to compensate longitudinal accelerations and other scaled ($1:30$), configured to compensate lateral accelerations. The scaled-prototype was used to test the lateral behaviour of the system in order to avoid experiencing instability problems that might appear with the light trailer.

A limited budget constrained the manufacturing of the prototypes. Funds came from the Automotive Laboratory of the University of Zaragoza (Zaragoza, Spain). They were allocated to buy the materials needed for building the structure and bars of the prototypes and their supporting structure. The prototype with real dimensions was formed by steel L-shape beams perforated along their entire length (the cheapest metallic beam found taking into account its load capacity) whereas the scaled-prototype was built with wood panels.

Due to the difficulties found in getting an automobile in which the prototypes were installed, a light trailer towed by a real vehicle was used for carrying on the prototype with real dimensions. The scaled-prototype constituted a trailer by itself and a radio-control vehicle was used to tow it. Both the vehicle, the light trailer and the radio-control vehicle were lent selflessly. Figure A.1 displays both prototypes. Approval for driving the light trailer with a vehicle in conventional roads was not obtained. It required that the supporting structure and the prototype remained permanently installed in it (even when experimentation finishes) [78] and it was not accepted by the owner of the trailer. Hence, experimentation was carried out in a straight track, with a length of 230 m, at the University of Zaragoza close to the traffic.

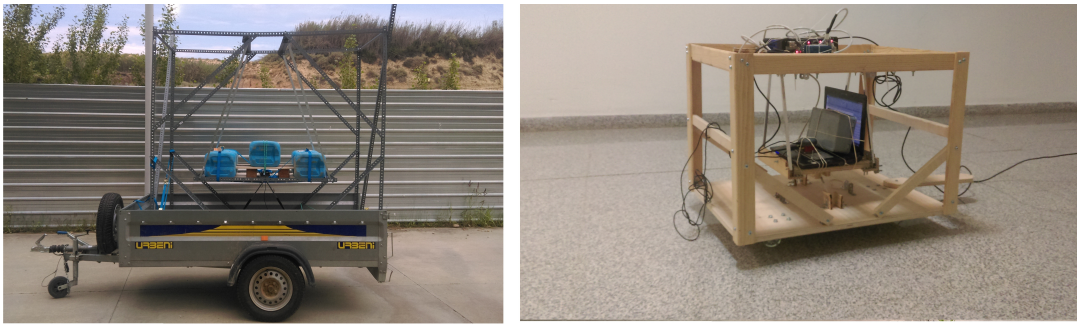

a b

FIGURE A.1: Prototypes used during experimentation

Dampers for the prototype with real dimensions (A.1.a) were provided by the company Alontec SL. Their damping properties were unknown and they were not pure dampers but gas dampers, like those used for a car boot or in windows. It added an external force acting on the base of the system due to the internal pressure of the gas of the dampers. To counter this force, the weight placed on the base of the prototype had to be increased. In the scaled-prototype (A.1.b) dampers were substituted by air syringes and their properties were unknown.

A.1.2 Limitations coming from the measurement equipment

The equipment used to record and measure the motion of the prototype was formed by an inertial measurement unit (IMU) formed by a gyroscope and a tri-axial accelerometer; a tri-axial accelerometer; a data acquisition unit (DAQ); a laptop and a portable power supply. Their characteristics are listed in Table A.1.

TABLE A.1: Characteristics of the equipment

Equipment	Full scale	Sampling rate	Channels	Voltage
IMU	8 g	3 kHz	-	5-36 V
tri-axial accelerometer	$\pm 2/\pm 2$ g	1kHz	-	3.7 - 10 V
DAQ	-	-	8	10 V

To validate entirely the mathematical model (see chapter 3) is needed to measure the 6 degrees of freedom of the vehicle in which the prototype is installed and at least one generalized variable associated either to the motion of the base or to the motion of one bar (parameter to compare with the results obtained with the mathematical

model). As it was not possible to capture these 6 degrees of freedom with enough accuracy and concordance in time to guarantee the convergence with the integration method used to solve the equations of motion of the system, the validation of the mathematical model was done just computationally, comparing the results obtained with the model against the results obtained with MSc Adams (see chapter 3). For this reason, the tests were focused on validating the theory behind the definition of the design of the prototype, which related the horizontal acceleration that acted on the system, the tilting angle of the base and the acceleration measured in the plane of the base (see section 4.2.2). Hence, under the action on the system of a horizontal lateral and longitudinal acceleration, the acceleration measured in the plane of the base of the system was compared against the theoretical acceleration that should be measured in accord with the tilting angle of the base and the input acceleration.

A.2 Methodology

A.2.1 Instrumentation

The portable power supply and the laptop were installed in the trailer in both prototypes. In the prototype of real dimensions the locations of the portable power supply, the laptop and the DAQ were not relevant, but in the scaled-prototype they were, due to the reduced space available in it. The laptop was located on the oscillatory base of the prototype, acting as the mass to which acceleration was compensated. The tri-axial accelerometer was firmly attached to the laptop, in the geometrical centre of the base, and the DAQ was located on the roof of the prototype along with the IMU.

In the scaled-prototype the IMU was located on its base to measure the acceleration in the plane of the base and its tilting angle and the tri-axial accelerometer was located on the roof of the trailer, to measure the input acceleration to the system (the horizontal acceleration, in the lateral direction of the prototype). Therefore, in the light trailer the IMU was located at the geometrical centre of its oscillatory base to measure its tilting angle (its angle of pitch, θ_{pl}) and the acceleration in its base, and the tri-axial accelerometer was located on the floor of the trailer to measure the horizontal acceleration that acted on its longitudinal direction.

In the prototype of real dimensions the mass transported on the oscillatory base of the prototype was 100 kg. This value was needed to counter the force of the gas dampers in static conditions, whereas in the scaled-prototype a mass of 1.8 kg (mass of the laptop) was located on its oscillatory base.

As it was not possible to transport people with the system, the dimensions of the prototype of real size were adjusted to take advantage of the available space in the trailer. Table A.2 shows the dimensions of the prototype, they are referred to the parameterized model of Figures 4.2 and 3.1. The dimensions of the scaled prototype were proportionally scaled $(1/30)$.

TABLE A.2: Dimensions of the real-size prototype

Parameter	(m)
Drb	1.3
p = $2 \cdot b$	0.35
length of the base ($q = 2 \cdot d$)	1.2
width of the base	0.75

A.2.2 Tests

The path that the scaled-prototype followed was random, it varied depending on the skills of the radio-control driver. The prototype of real dimensions followed a straight track of length of 230 m.

Tests of the scaled-prototype were influenced by the mass of the prototype and the mass of the radio-control vehicle. Although the high mass of the prototype was not a problem for the traction capacity of the radio-control vehicle to which it was coupled, it provoked that the light radio-control vehicle negotiated incorrectly curves and experienced the effect of jackknifing (during negotiation of a curve the trailer pushed too much force against the tractor vehicle what provoked that the tractor vehicle lost the control of its rear wheels and turned around its front axle hitting the trailer). The weight of the trailer could not be reduced and neither increased the weight of the radio-control vehicle, so different trials were carried out in order to obtain data that allowed to analyse the motion of the system during the negotiation of a curve or at least until the jackknifing effect occurs. However, with the light trailer it did not occur because the size of the vehicle and the trailer accomplished what regulations require to this respect (mainly and for this type of trailers, that the permissible towable mass must not exceed half of the mass in running order of the towing vehicle and never be greater than 750 kg)[79].

Different tests had to be carried out with both prototypes until the measuring process was adjusted.

For validating the theory behind the definition of the design of the system, the situation of dynamic equilibrium displayed in Figure 4.3 was analysed (like in chapter 4. The horizontal acceleration captured with the tri-axial accelerometer located at the vehicle (or at the structure that supports the system) (a_H) and the tilting angle of the base (φ_{pl}) of the system were used as input parameters of equation (A.1). With it, the acceleration that should be measured in the plane of the base of the system (a_{lat}) was calculated.

$$a_{lat} = a_H \cdot \cos\varphi_{pl} - g \cdot \sin\varphi_{pl} \tag{A.1}$$

A.3 Results

In both cases, results allowed to compare the acceleration measured in the plane of the base of the system with the theoretical value calculated with equation (A.1). They served to validate the theory applied in section 4.2.2 with which the design of the system was determined in order to achieve a specific rate of compensation of accelerations. A low pass filter with a cut-off frequency of 10 Hz was used to filter the data captured by the sensors during the tests. The data captured by the sensors are displayed in Figures A.2 and A.3, for the scaled-prototype and the real-size prototype respectively.

The lateral acceleration measured at the plane of the base of the prototype when it oscillated was lower than the lateral acceleration measured at the roof of the prototype, as a consequence of the change of orientation of the base with respect to the roof. The effect of the dampers (in this case, substituted by air syringes) was appreciated only because the system did not oscillate permanently as if they did not exist. On the contrary, with the prototype of real dimensions the effect of dampers was more clear than in Figure A.2.

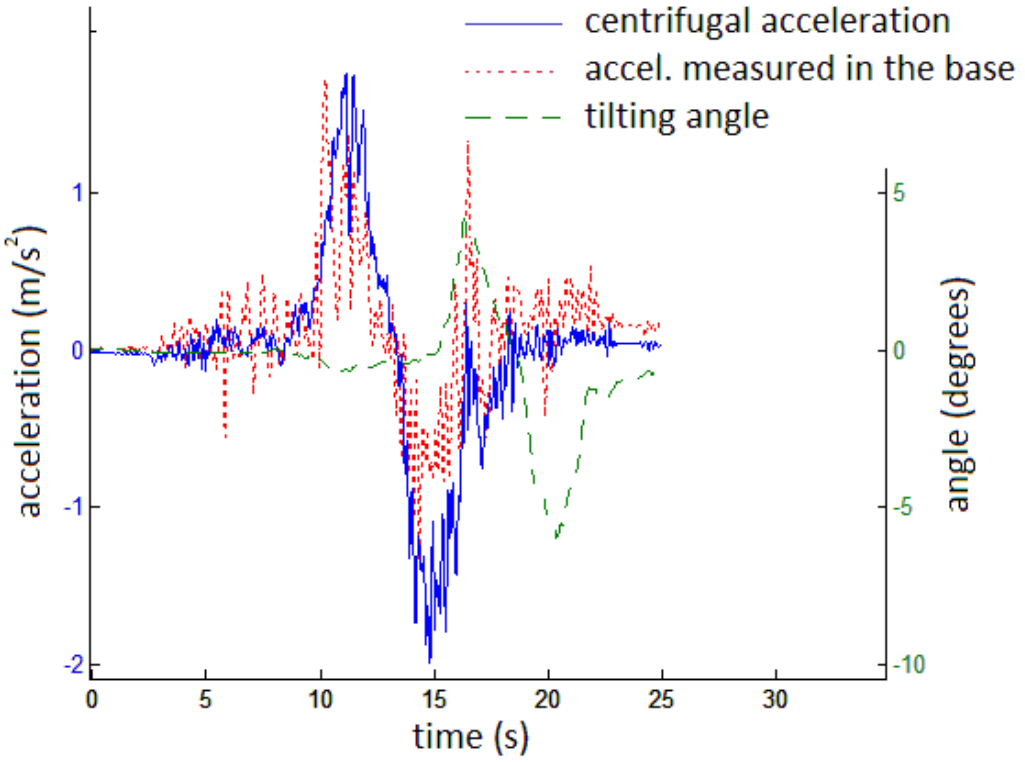

FIGURE A.2: Measures of the oscillatory motion of the base of the scaled-prototype

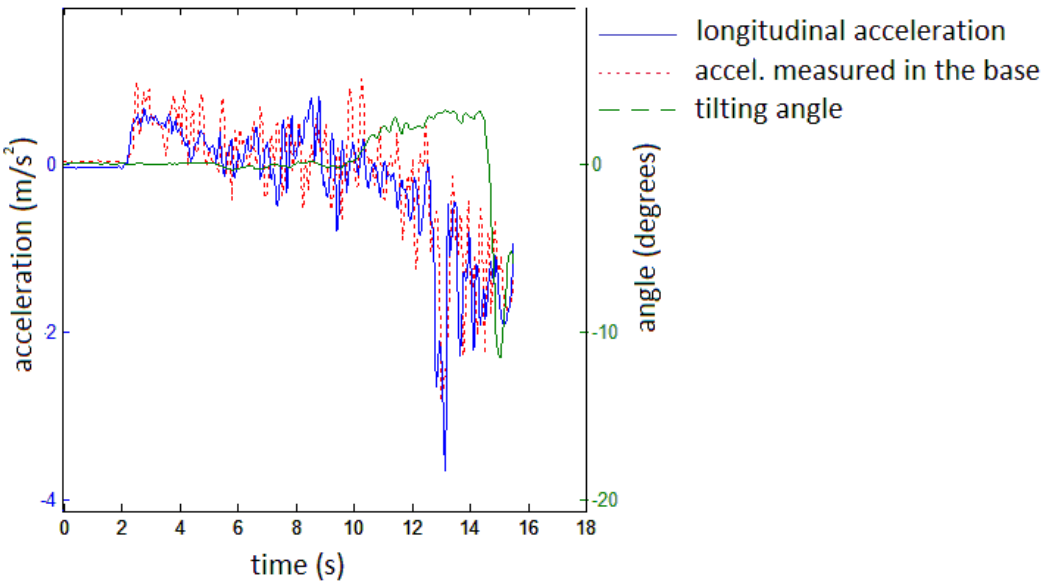

FIGURE A.3: Measures of the oscillatory motion of the base of the prototype of real dimensions

The theoretical values of the acceleration measured in the plane of the base calculated for both prototypes respectively, were compared against the data captured by the sensors located on the base of the prototypes, respectively.

Figure A.4 displays the results obtained for the scaled-prototype and Figure A.5 the results obtained for the real-size prototype.

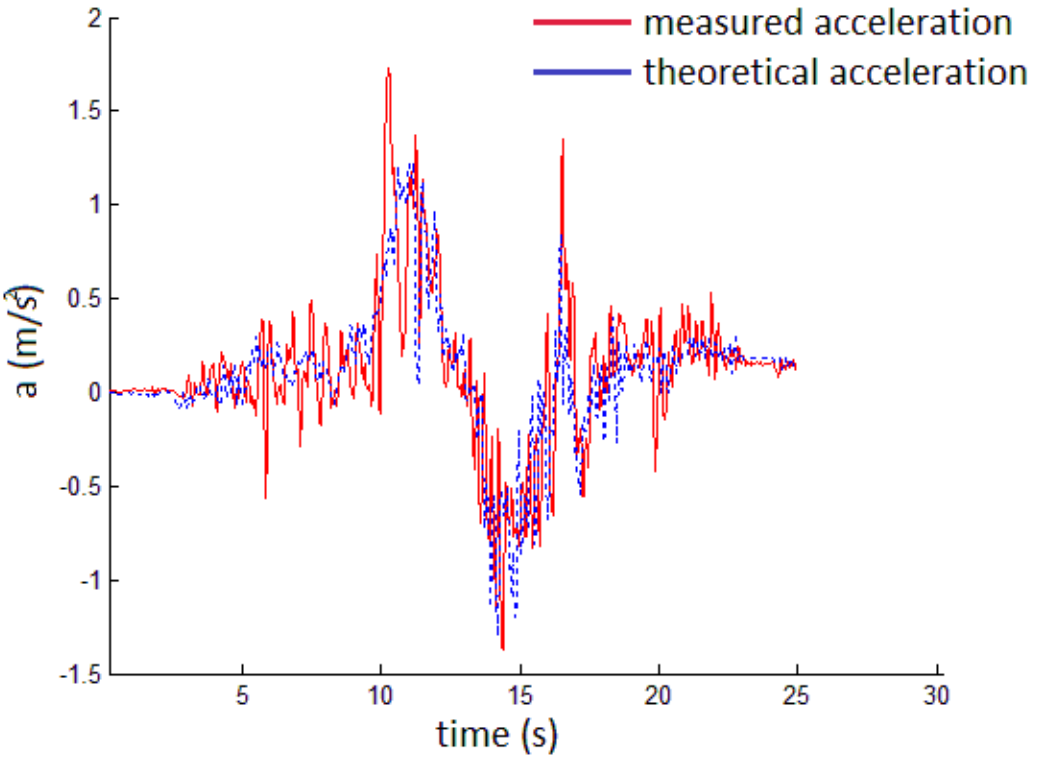

FIGURE A.4: Acceleration measured in the plane of the base of the scaled-prototype

As it can be appreciated in Figures A.4 and A.5 the theoretical values were very similar in both situations. Differences between the them were due to different reasons. The assembly of parts for both prototypes lacked of accuracy due to looseness problems, especially in the prototype of real dimensions. The holes of its perforated L-shaped beams served to connect more easily the bars of the oscillatory base to the roof of the supporting base and also to connect the dampers between the base and the floor of the supporting structure. However, the geometry of the holes was not exactly circular what resulted in the existence of looseness in the pinned connections of the assembly. These problems of looseness along with a no exactly lateral flatness of the track used for experimentation (in average a slope of 3%) resulted in the existence of an additional torque (around the longitudinal axle of the vehicle, X_v) that the joints of the system (and the supporting structure) had to absorb.

Apart from the lack of accuracy in the assembly of its parts, the measurement process was influenced by the type of vehicle used and by its structure. In the case of the real-size prototype, its wheels and the damper that formed part of its inertial brake system were the only damping elements capable of filtering vertical and longitudinal vibrations. The trailer disposed of a rigid axle directly linked to the lower part of its floor. The supporting structure of the oscillatory base was directly linked to this floor, so vibrations that appeared as a consequence of the irregularities in the pavement and the ones transmitted by the coupling device coming from the vehicle were transmitted directly to the supporting structure. As

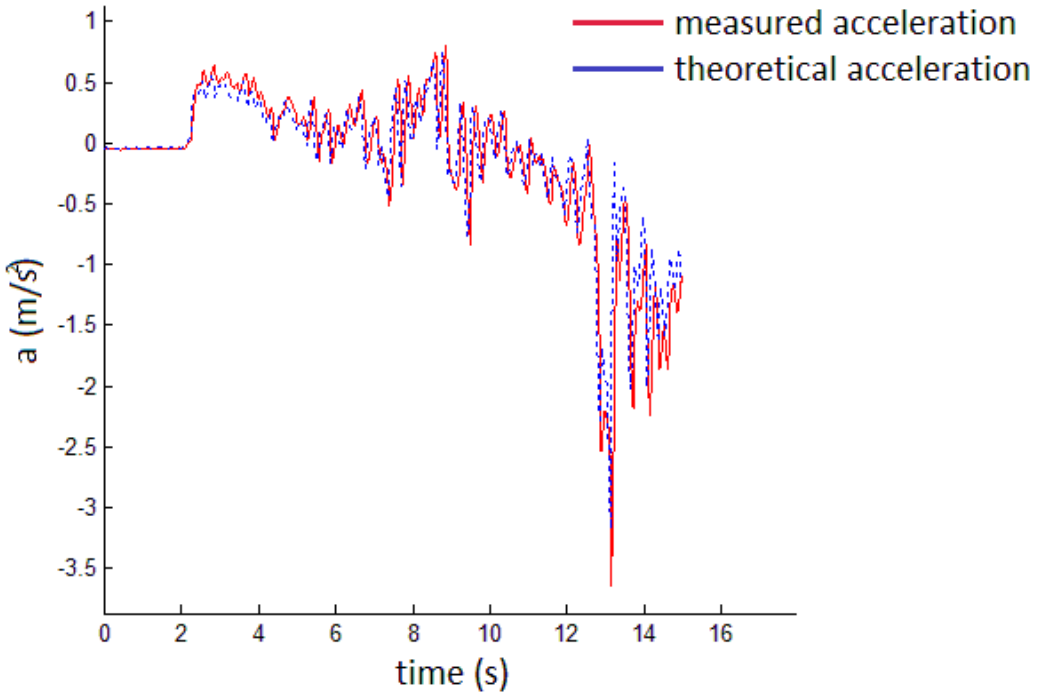

FIGURE A.5: Acceleration measured in the plane of the base of the prototype of real dimensions

the supporting structure was only fixed to the floor of the trailer in just four points, it resulted in capturing data with a relevant component of high frequencies during the measurement process.

With the scaled-prototype the existence of high frequency components in the data captured by the sensors increased. It was due mainly to the high stiffness of the prototype and to its low mass. In this prototype all components of the assembly can be considered as rigid solids, so the irregularities of the pavement were not filtered by any element. Like with the prototype of real dimensions, the pinned connections between parts suffered from looseness problems.

With these fluctuations in the captured data was not possible to obtain the 6 degrees of freedom correspondent to the motion of the vehicle with enough accuracy to be able to be used as input parameters in the numerical integration method employed to solve the equations of motion of the system. This is why the validation of the mathematical model was carried out just computationally. Instead of that, like it has been mentioned previously, it was analysed the correspondence between the acceleration measured in the plane of the oscillatory base and its theoretical value calculated with equation (A.1).

A.4 Conclusions

In spite of all problems faced in experimentation, the validation of the theory behind the definition of the design of the system was carried out successfully. Looking at the behaviour of the system during the tests carried out with the prototype of real dimensions it was concluded that the use of this system might be

more appropriate to compensate just lateral accelerations. When the trailer in which the prototype was installed started its motion, until it reached a stable velocity, the base of the oscillatory system oscillated constantly back and forward due to the changes of acceleration experienced during the shift of gears of the vehicle. In this case it was amplified due to the existence of an inertial brake connected between the vehicle and the trailer. A bad adjustment of the dampers resulted in a negative effect on the oscillatory motion of the base of the system, what was experienced with both prototypes. Therefore, the vehicle in which the 3D multibody system is installed must dispose of an appropriate damping system that reduces the effect that the irregularities in the pavement may have on the system. Both prototypes lacked of it and vertical vibrations affected to the data measured during the tests.

As it was introduced previously in this annex, to obtain data that allow validating the dynamics of the 3D multibody system and its equations of motion it is needed to dispose of the equipment appropriate that allow to capture with enough reliability and accuracy the 6 degrees of freedom associated to the vehicle in which the system is installed along with a vehicle that disposes of a suspension system that filters the external vibrations to the motion of the oscillatory system.

That the experimental validation of the mathematical model could not be accomplished with this experimentation is not negative, having into account the conditions available to do it and mainly, because the mathematical model of the equations of motion of the system was entirely validated computationally, as it was detailed in chapter 3. Therefore, that this experimentation could not be carried out with people it was not a limit for this research because the main experimental part to this respect was carried out at the Institute of Sound and Vibration at the University of Southampton, a research centre of reference in what Human Vibration refers (see chapter 5).

Bibliography

[1] S. Baselga; P. J. Fernández, Sistema de compensación pendular, ES 2333925 B1, España, 2010.

[2] World Intellectual Property Organization, http://www.wipo.int/

[3] Alcorze, EBSCO Industries, Inc., http://blog.biblioteca.unizar.es/tag/alcorze/

[4] G. F. Beard; M. J. Griffin, Discomfort caused by low-frequency lateral oscillation, roll oscillation and roll-compensated lateral oscillation, Ergonomics, 56, (2013), 103–114.

[5] G. F. Beard; M. J. Griffin, Discomfort of seated persons exposed to low frequency lateral and roll oscillation: Effect of seat cushion, Applied Ergonomics, 45, (2014a), 1547–1557.

[6] G. F. Beard; M. J. Griffin, Discomfort of seated persons exposed to low frequency lateral and roll oscillation: Effect of backrest height, Applied Ergonomics, 54, (2016), 51–61.

[7] J. A. Joseph; M. J. Griffin, Motion sickness: Effect of changes in magnitude of combined lateral and roll oscillation, Aviation, Space and Environmental Medicine, 79, (2008), 1019–1027.

[8] R. Persson, R. M. Goodall, K. Sasaki, Carbody tilting - technologies and benefits, Vehicle System Dynamics 47 (8) (2009) 949-981.

[9] L. Chung, Y. A. Lai, C.-S. Walter, K.-H. Lien, L.-Y. Wu, Semi-active tuned mass dampers with phase control, Journal of Sound and Vibration 332 (2013) 3610-3625.

[10] A. Toran, Speed and track curvature suspension control system (1977).

[11] A. Toran, T. Toran, Pendular suspension system (1979).

[12] A. Furukawa, Track management for curve passing speed improvement., Railway Technical Research Institute 66 (2009) 13-16.

[13] J. Candlin, Lansing, R. W. Lanman, H. Ind., W. Sluys, Suspension system (1956).

[14] R. M. G. J. Z. Jiang, A. Z. Matamoros-Sanchez, M. C. Smith, Passive suspensions incorporating inerters for railway vehicles, Vehicle System Dynamics 50 (sup1) (2012) 263-276.

[15] K. Guenther, W. P. Sergeant, Overhead suspended transportation system and method (2007).

[16] P. Robertson, Trailer structure for transporting sheet glass and frangible material (1986).

[17] H. D. Parham, Three-wheel motorcycle (1977).

[18] W. Trautwein, Stabilized three-wheeled vehicle (1977).

[19] S. F. Coil, Tiltable three-wheeled vehicle (1984).

[20] F. J. Winchell, K. O. Winkelmann, Three-track motorcycle with cambering main frame (1984).

[21] J. E. Gribble, Self-leveling, gravity-stabilized (10 2012).

[22] S.-G. Luca, C. Pastia, Passive tuned mass damper for seismic protection, Bulletin of the Polytechnic Institute of Iasi Construction and Architecture section 63 (6) (2013) 9-17.

[23] Y. Bigdeli, D. Kim, Damping effects of the passive control devices on structural vibration control: Tmd, TLC and TLCD for varying total masses, Bulletin of the Polytechnic Institute of Iasi - Construction and Architecture section 20 (1) (2016) 301-308.

[24] L. Chung, L.-Y. Wu, H. H. Huang, C.-H. Chang, K.-H. Lien, Optimal design theories of tuned mass dampers with nonlinear viscous damping, Earthquake engineering and engineering vibration 8 (2009) 547-560.

[25] J. Grinberg, S. Skikne, A. Deardorff, B. Deardorff, Weight-stabilizing stretcher (2014).

[26] M. Turner, M. J. Griffin, Motion sickness in public road transport: The relative importance of motion, vision and individual differences, British Journal of Psychology 90 (1999) 519-530.

[27] C. Butler, M. J. Griffin, Motion sickness with combined fore-aft and pitch oscillation: Effect of phase and the visual scene, Aviation, Space and Environmental Medicine 80 (2009) 946-954.

[28] A. Lawther, M. J. Griffin, The motion of a ship at sea and the consequent motion sickness amongst passengers, Ergonomics 29 (4) (1986) 535-552.

[29] J. A. Joseph, M. J. Griffin, Motion sickness from combined lateral and roll oscillation: Effect of varying phase relationships, Aviation, Space and Environmental Medicine 78 (2007) 944-950.

[30] T. N. Chung, S. W. Kim, Y. S. Cho, S. P. Chung, I. Park, S. H. Kim, Effect of vehicle speed on the quality of closed-chest compression during ambulance transport, Resuscitation 81 (2010) 841-847.

[31] M. C. Kurz, S. A. Dante, B. J. Puckett, Estimating the impact of off-balancing forces upon cardiopulmonary resuscitation during ambulance transport, Resuscitation 83 (2012) 1085-1089.

[32] E. L. Lee, W. C. Hayes, Occupant accelerations and injury potential during an ambulance-to-curb impact, Forensic Science International 237 (2014) e6-e10.

[33] W. S. Tucker, E. E. Swartz, S. D. Hornor, Head and trunk acceleration during intermediate transport on medical utility vehicles, Clinical Journal of Sport Medicine 26 (2016) 53-58.

[34] E. C. for Standardization, EN 1789:2007+a2:2014 medical vehicles and their equipment road ambulances (2014).

[35] E. C. for Standardization, EN 1865-5:2012 patient handling equipment used in road ambulances. part 5: Stretcher support. (2012).

[36] T. Ono, H. I. H, Actively-controlled beds for ambulances, International Journal of Automation and Computing 06 (1) (2009) 1-6.

[37] M. V. Zeebroeck, V. V. Linden, H. Ramon, J. D. Baerdemaeker, B. Nicola, E. Tijskens, Impact damage of apples during transport and handling, Postharvest Biology and Technology 45 (2007) 157-167.

[38] G. Wu, C. Wang, Investigating the effects of simulated transport vibration on tomato tissue damage based on vis/nir spectroscopy, Postharvest biology and technology 98 (2014) 41-47.

[39] Y. Ishikawa, H. Kitazawa, T. Shiina, Vibration and shock analysis of fruit and vegetables transport cherry transport from Yamagata to Taipei, Japan International Research Center for agricultural Sciences 43 (2009) 129-135.

[40] C. J. Pretorius, W. Steyn, Investigating the effects of simulated transport vibration on tomato tissue damage based on visnir spectroscopy, Abstracts of the 31st Southern African Transport Conference (SATC 2012).

[41] P. Amodio; F. Mazzia, Numerical solution of differential algebraic equations and computation of consistent initial/boundary conditions, Computational and Applied Mathematics, Vol. 87, pp. 135-146, 1997.

[42] K. Brenan; S. Campbell; L. Petzold, Numerical Solution of Initial Value Problems in Differential-Algebraic Equations, North-Holland, 1989.

[43] J. Yen, Constrained equations of motion in multibody dynamics as ODEs on manifolds, SIAM Journal on Numerical Analysis, Vol. 30, pp. 553-568, 1993.

[44] K. Alloulaa; F. Monfreda; R. T. Hetreuxa; J-P. Belaud, Converting DAE Models to ODE Models: Application to Reactive Rayleigh Distillation, Chemical Engineering Transactions, AIDIC, 2013, vol. 32 doi: 10.3303/CET1332220.

[45] W. D. Iwan, A generalization of the concept of equivalent linearization. International Journal of Non-linear mechanics, 8, 3, p. 279–287, 1973.

[46] S.R.K. Iyengar; R. K. Jain, Numerical methods, New Age International, 2009.

[47] V. I. Arnold, Mathematical methods of classical mechanics, Springer-Verlag, 1989.

[48] C. F*ü*hrer; R. Schwertassek, Generation and solution of multibody system equations. International Journal of Non-Linear Mechanics, 25(2-3), 127–141, 1990.

[49] F. E. Udwadia; R. E. Kalaba, A new perspective on constrained motion, Proceedings: Mathematical and Physical Sciences, Vol. 439, pp. 407-410, 1992.

[50] J. Agullo, Mecánica de la partícula y del sólido rígido. Publicaciones OK Punt, Gran Vía Carles, 3(55), 08028.

[51] R. Militaru, An adaptative stepsize algorithm for the numerical solving of initial-value problems, ANALELE STIINTIFICE ALE UNIVERSITATII OVIDIUS CONSTANTA-SERIA MATEMATICA, 23(1), 185–198, 2015.

[52] L. F. Shampine; A. Witt, A simple step-size algorithm for ODE codes, Journal of Computational and Applied Mathematics, 58, pp. 345–354, 1995.

[53] F. Fahy; D. Thompson, Fundamentals of Sound and Vibration, CRC Press, 2015.

[54] E. Byran; I. Gilad, Design Considerations to Enhance the Safety of Patient Compartments in Ambulance Transporters, International Journal of Occupational Safety and Ergonomics, (2012), 18:2, 221-231.

[55] F.J. Sánchez-Alejo; J.M. López-Martínez, J.L. Fernández-Sánchez. Design of the internal space of an ambulance through linear programming, DYNA, (2008), 83, 5, p.313–320.

[56] B.M. Kim; J.W. Kim; I.D. Moon; Journal of Mecheanical Science and Technology, (2014), 28, 963–969, doi:10.1007/s12206-013-1167-7.

[57] M. M. Topaç; U. Deryal; E. Bahar; G. Yavuz, Optimal kinematic design of a multi-link steering system for a bus independent suspension: An application of response surface methodology, Mechanics, (2015), 21, 5, 404–413.

[58] Y. Wu; A. Klimchik; S. Caro; B. Furet; A. Pashkevich, Geometric calibration of industrial robots using enhanced partial pose measurements and design of experiments, Robotics and Computer-Integrated Manufacturing, (2015), 35, 151–168.

[59] B. K. Rout; R. K. Mittal, Parametric design optimization of 2-DOF R–R planar manipulator—A design of experiment approach, Robotics and Computer-Integrated Manufacturing, (2008), 24(2), 239–248.

[60] D. Montgomery, Design and analysis of experiments, 5th ed. Ed. John Wiley and Sons, Inc. New York, USA, (2001).

[61] E. C. for Standardization, EN 1865-1:2010+A1:2015 Patient handling equipment used in road ambulances. Part 1: General stretcher systems and patient handling equipment. (2015).

[62] J. B. McConville; J. F. McGrath, Introduction to ADAMS Theory, Mechanical Dynamics, Inc., 1998.

[63] P. H. Lewis; C. Yang, (1999). Sistemas de control en Ingeniería. Madrid: PRENTICE HALL IBERIA S.R.L.

[64] MSC Software Corporation, Introduction to ADAMS/Vibration theory, 2013.

[65] España. Ministerio de Fomento (2000). ORDEN de 27 de diciembre de 1999 por la que se aprueba la Norma 3.1-IC. Trazado, de la Instrucción de Carreteras. Madrid. BOE

[66] B. Li; F. Yu, Design of a vehicle lateral stability control system via a fuzzy logic control approach, Proceedings of the Institution of Mechanical Engineers, Part D: Journal of Automobile Engineering, (2010), 224(3), 313-326.

[67] F. You; R. Zhang; G. Lie; H. Wang; H. Wen; J. Xu, Trajectory planning and tracking control for autonomous lane change maneuver based on the cooperative vehicle infrastructure system, Expert Systems with Applications, (2015), 42(14), 5932-5946.

[68] C. Sierra; E. Tseng; A. Jain; H. Peng, Cornering stiffness estimation based on vehicle lateral dynamics, Vehicle System Dynamics, (2006), 44(1), 24–38, DOI:10.1080/00423110600867259.

[69] International Organization for Standardization (1997). Evaluation of human exposure to whole-body vibration. Part 1: General requirements. ISO 2631-1-1997. International Organization for Standardization, Geneva.

[70] J. A. Joseph, M. J. Griffin, Motion sickness with fully roll-compensated lateral oscillation: effect of oscillation frequency, Aviation, Space and Environmental Medicine, (2009), 80, 94-101.

[71] M. J. Griffin, Discomfort from feeling vehicle vibration. Vehicle System Dynamics, (2007), 45 (7), 679–698.

[72] M. J. Griffin, M. M. Newman, An experimental study of low-frequency motion in cars. Proceedings of the Institution of Mechanical Engineers, Part D: Journal of Automobile Engineering, (2004), 218(11), 1231-1238.

[73] G. F. Beard, M. J. Griffin, Motion sickness caused by roll-compensated lateral acceleration: Effects of centre-of-rotation and subject demographics, Journal of Rail and Rapid Transit, 228, (2014b), 16–24.

[74] I. H. Wyllie; M. J. Griffin, Discomfort from sinusoidal oscillation in the pitch and fore-and-aft axes at frequencies between 0.2 and 1.6 Hz. Journal of Sound and Vibration, 324(1), (2009), 453-467.

[75] Griffin, M. J. (2012). Handbook of human vibration. Academic press

[76] S.S. Stevens, (1975). Psychophysics: introduction to its Perceptual, Neural, and Social Prospects. Transaction Publishers, Oxford.

[77] S. Siegel; N.J. Castellan, Nonparametric Statistics for the Behavioral Sciences, McGraw-Hill international editions. Statistics series, (1988), McGraw-Hill.

[78] Ministerio de Industria, Energía y Turismo, Manual de Reformas de Vehículos, Revisión 3,(2016)

[79] European Commission, COMMISSION REGULATION (EU) No 1230/2012, Official Journal of the European Union, (2012).